INTRA-CHAMBER PROCESSES, COMBUSTION AND GAS DYNAMICS OF DISPERSED SYSTEMS

Second International Seminar
June 30 - July 5, 1997
Saint Petersburg
RUSSIA

Proceedings

Saint Petersburg
1997

REPORT DOCUMENTATION PAGE

Form Approved OMB No. 0704-0188

1. AGENCY USE ONLY (Leave blank)	2. REPORT DATE	3. REPORT TYPE AND DATES COVERED
	19 August 1997	Conference Proceedings

4. TITLE AND SUBTITLE

Intra-Chamber Processes, Combustion and Gas Dynamics of Dispersed Systems
Second International Seminar

5. FUNDING NUMBERS

F6170897W0069

6. AUTHOR(S)

Conference Committee

7. PERFORMING ORGANIZATION NAME(S) AND ADDRESS(ES)

Baltic State Technical University
1st Krasnoarmeyskaya Str 1
St. Petersburg 198005
Russia

8. PERFORMING ORGANIZATION REPORT NUMBER

N/A

9. SPONSORING/MONITORING AGENCY NAME(S) AND ADDRESS(ES)

EOARD
PSC 802 BOX 14
FPO 09499-0200

10. SPONSORING/MONITORING AGENCY REPORT NUMBER

CSP 97-1018

11. SUPPLEMENTARY NOTES

12a. DISTRIBUTION/AVAILABILITY STATEMENT

Approved for public release; distribution is unlimited.

12b. DISTRIBUTION CODE

A

13. ABSTRACT (Maximum 200 words)

The Final Proceedings for 2nd International Seminar on Intra-Chamber Processes, Combustion & Gas Dynamics, 30 June 1997 - 5 July 1997

The Topics covered include: Interior ballistics; heat & mass transfer, heat protection of channels; combustion of metal droplets in active media; spray combustion and two-phase flows.

14. SUBJECT TERMS

Chemical Propulsion

15. NUMBER OF PAGES

118

16. PRICE CODE

N/A

17. SECURITY CLASSIFICATION OF REPORT	18. SECURITY CLASSIFICATION OF THIS PAGE	19. SECURITY CLASSIFICATION OF ABSTRACT	20. LIMITATION OF ABSTRACT
UNCLASSIFIED	UNCLASSIFIED	UNCLASSIFIED	UL

State Committee for Science and Education of Russia
Russian Academy of Sciences
Russian Academy of Rocket and Artillery Sciences
Baltic State Technical University
Institute of Applied Mechanics
Institute of Chemical Physics

INTRA-CHAMBER PROCESSES, COMBUSTION AND GAS DYNAMICS OF DISPERSED SYSTEMS

Second International Seminar
June 30- July 5, 1997
Saint Petersburg
RUSSIA

Proceedings

Saint Petersburg
1997

SECOND INTERNATIONAL SEMINAR ON INTRA-CHAMBER PROCESSES, COMBUSTION AND GAS DYNAMICS OF DISPERSED SYSTEMS

Saint Petersburg, Russia
June 30- July 5, 1997

Scientific Advisory Committee

F.E.C.Culick (USA), P.Clavin (FR) V.K.Donchenko (RU), B.T.Erokhin (RU), N.K.Egorov (RU), G.P.Gardymov (RU), A.M.Gubertov(RU), A.M.Lipanov (RU), B.I.Larionov (RU), N.A.Makarovets(RU), B.V.Novozhilov (RU), Ju.V.Polezhaev (RU), V.I.Pepekin (RU), O.Ya.Romanov (RU), V.S.Solovyov (RU), A.A.Shraiber (Ukraine), V.E.Zarko(RU), A.N.Zolotko (Ukraine), A.A.Zenin (RU).

Organizing Committee

Co-Chairmen: A.M.Lipanov, V.I.Pepekin, O.Ya Romanov.

I.G.Assovskii, A.V.Aliev, G.T.Aldoshin, V.A.Babuk, M.S.Malakhov, G.T.Potekhin, Yu.N.Philimonov, V.V.Sviridov, V.A.Vasilyev, M.Ya.Vodopyanov, V.N.Uskov, V.E.Zakharenkov.

Organizing committee wishes to thank the following for their contribution to the success of this seminar:

UNITED STATES AIR FORCE EUROPEAN OFFICE OF AEROSPACE RESEARCH AND DEVELOPMENT

PRESIDIUM OF THE RUSSIAN ACADEMY OF ROCKET AND ARTILLERY SCIENCES

SPC "SPLAV"

PC "SEVERNY ZAVOD"

Abstracts are reproduced with original copies.

Section 1
INTERIOR BALLISTICS

4

INTERIOR BALLISTICS OF FORCEMENT PERIOD

EVGENY V. CHURBANOV
Doctor of Technical Sciencies,
Professor,
State Baltic Technical University,
St. Petersburg

The onward movement of projectile inside the barrel takes place due to pressure force coursed by powder gas towards the bottom of the projectile, and the drag forces caused by interconnection between the projectile and the barrel, i.e. drag force caused by gripping of projectile by rifling, by driving band sliding along the rifles, by resistance that appears in course of interaction between positioning band and the barrel.

A special ballistic parameter - engraved pressure - is used in interior ballistics for indirect consideration of the process of gripping of projectile by rifling. In this case the gripping drag force is not considered in the projectile onward movement equation. At the same time at the beginning period of the projectile movement, which is called the period of forcement, when driving band grips into rifles, the drag force is comparable to powder gas pressure force. The period of forcement is the most complicated stage of the shot due to the fact that besides the main processes, i.e. powder burning, powder gas formation, projectile onward movement, gripping of projectiles by rifles, additional processes are to be also considered, i.e. ignition of explosive propellant, powder gas heat emission, outflowing of powder gas.

The process of gripping of projectile by rifles to a large extent depends on the gun loading method. In case of separate loading, the gripping process starts at the beginning of the onward movement of projectile, and the process itself is relatively slow. In case of unitary loading the projectile gets out of the projectile case before the gripping process begins, so the gripping process starts under dynamic conditions, and it is fast.

In the process of gripping there appears contact surface between driving band and inner wall of the barrel. This contact surface is characterized by development of normal tension and tangent tension. As the result the gripping resistant force becomes a factor. This force can be determined by experiment and by calculation.

Without simplification the main task of forcement period interior ballistics can only be solved numerically. One will need to integrate the system of equations that includes 9 simple differential equations and 18 algebraic equations containing 28 variables and more than 100 ballistic parameters. For engineering purpose the system of equations can be simplified, and analytic dependencies of different phases of projectile onward movement on time within the period of forcement can be determined.

The period of forcement can be considered indirectly with accuracy needed with the use of three forcement parameters, not one parameter as is usually done. Investigation of those parameters leads to understanding the physical essence of engraved pressure, and helps in finding methods of its theoretical and experimental determination.

In the author's book "Interior Ballistics of Forcement Period" issued in 1997 in State Baltic Technical University one can find detailed description of the theory, experiments and methods of consideration of period of forcement in solving ballistic problems.

ESTIMATION OF INFLUENCE INPUT PARAMETERS ON SERVICEABILITY OF BALLISTIC SYSTEMS

ZAKHARENKOV V.F., MOROZ S. A., Baltic State Technical University, 198005, Saint-Petersburg, Russia

The estimation of serviceability of ballistics launchers demands to take into account the influence of input random information at output characteristics such as maximal or muzzle gas pressure, the muzzle projectile velocity, position of the powder burning end and so on. All that demand the modernization of existing methods of ballistic calculations and design of sets in the direction of researching the random relationships, escorting the shot phenomena. Random spread of output parameters (the response functions) is wholly and fully determines by relationships of input parameters spreads.

The response functions can be install as theoretically so experimentally. The using of the models with that or other accuracy degree describing real ballistic processes are demand at theoretical solution. The connection between probability values of input and output data may be ascertain or on the basis of extreming deviation method, or by the Monte-Carlo statistical tests' method. The first method is a more simple, but he does not reflect actual relationships of random deviations of output parameters, and mostly base on their apriori assumption on the normal (Gauss) law of distribution. The more reliability results give the Monte-Carlo statistical test method that has not limitations on complexity systems but demand's availability of great statistical sampling.

Table 1

Characteristics	Symbol	Distribution law
Burning rate	U_1	Gauss
Covolume	α	Uniform
Charge density	Δ	Gauss
Energy of powder	f	Gauss
Initial pressure	p_o	Uniform
Ignition pressure	$p_в$	Uniform
Powder density	δ	Uniform
Projectile mass	q	Gauss
Charge mass	ω	Gauss
Initial chamber volume	W_0	Gauss
Bore cross-section area	S	Gauss
Flame temperature	T_1	Uniform
Caliber	d	Gauss

The module kla.exe of the block ballistic calculations KOBRA of Baltic State Technical University (BSTU) was chose as a working program for ballistic calculations in the frames of present paper. These program modules were modify in direction of inclusion in it the procedures for forming random pseudonumbers generator RAV and NORM for modeling random input parameters distributed on uniform Gauss and laws (Table 1). The choice of distribution laws was base on analysis the statistical information of a number ballistic systems. The extreme deviations of parameters (constructive, physical and of load conditions) chosen out from condition $\delta p = \pm 5\%$ from nominal values and corresponded to 3σ-rule for the level of confidence probability as 0, 997. The

integral function of distribution F(x) calculated as: $F(x)=\int_a^x \frac{1}{b-a}dx=\frac{1}{b-a}(x-a)$ - for uniform distribution law; $F(x)=\int_{-\infty}^{x}\varphi(z)dz=0.5+0.5\Phi(x)$ - for normal (Gauss) distribution law, where $\Phi(x)=\int_{-x}^{x}\frac{1}{\sqrt{2\pi}}e^{-\frac{z^2}{2}}dz$.

The calculation procedure for random-numbers generation for making input random information given on Fig.1. The system of serviceability conditions may be write as: $[V_0]_{min} \le V_0 \le [V_0]_{max}$; $P_3 \rangle P_S$; $\bar{N} \ge n$; $P_S \langle [P_S]$; $P_3 \langle [P_3]$; $d_K \langle [d_K]$.

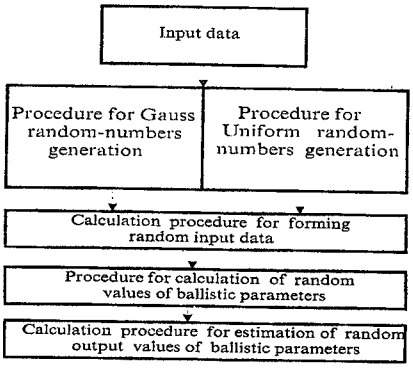

Fig.1 Block -scheme for forming of random values of ballistic parameters

The restrictions on values of parameters must be give. The probability estimation demands the knowledge distribution of reliability density f(n), which for scheme with accumulation of faults (for example, decreasing ballistics due to erosion wear) have view [5] $f(n)=[\Gamma(\bar{N})]^{-1}\lambda^{\bar{N}}n^{\bar{N}-1}\exp(-\lambda n)$, if $n \ge 1$, where $\Gamma(\bar{N})$ - gamma-function. If the level of the aimfunction is know that probability $P(\bar{N} \ge n)$ may be calculates as $P(\bar{N} \ge n)=1-F(n)$. The calculation of the total probability with allowance of other serviceability conditions may be carry out in compliance with relation, which takes into account interaction effects and three-parametrical conditions of serviceability [5,6]: $P_{y_1y_2y_3}(\sum n)=\prod_{j=1}^{n}(P_{y_1y_2y_3})j$; $(P_{y_1y_2y_3})j=\sum_{i=1}^{m}P_{y_1i}P_{y_2i}/Y_{1i}(\sum_{i=1}^{m}\sum_{j=1}^{n}P_{y_3i}/Y_{1i,y_2j})+...$,

where:

$(P_{y_1y_2y_3})j$ - total probability of serviceability conditions for j-loading; m- number of intervals; i- elementary interval of serviceability; y_{1i} - probability Y_1 (V-velocity) realizing inside i-interval; P_{y_2i} - conditional probability Y_2 (P_m), realizing inside i-interval; $P_{y_3i}/Y_{1i,y_2j}$ - condition of probability Y_3 ($P_д$), realizing inside i and j-intervals.

The calculation of distribution character parameters characterizing serviceability and stability of ballistic set (gas pressure and projectile velocities), in characteristic time moments corresponding to achievement of initial pressure (t_o), maximal pressure (t_m), finish time of powder burning ($t_к$) and muzzle time

($t_д$) at the example of repeated many times random shot-loading of 122 mm caliber gun system reflected on Fig. 2.

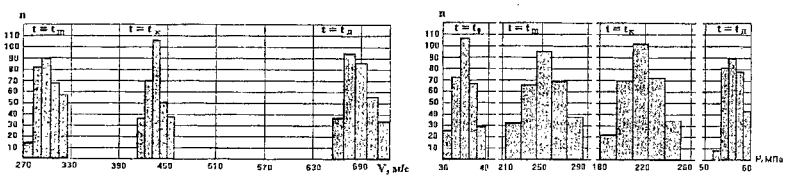

Fig.2 Histograms of pressure and projectile velocity's distributions in characteristic moments of time

Given graphs allow to speak about the character of variation not only of output values of ballistic parameters v and p, but about their dynamics of changing in different moments of the shot period. The treatment of got results have let to build the variation field of velocity and pressure. The results of calculation represented on Fig. 3.

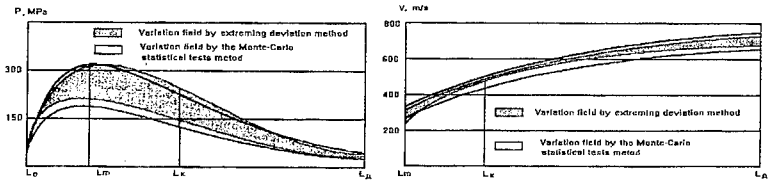

Fig. 3 Variation fields of gas pressure and projectile velocities

The values of variation fields of parameters, calculated on extreme deviations of input data, given on the same figure. One can see that for 100 and more trials the deviation fields on both methods are slightly differ. So approximate estimation of variation parameters, according to the extreme deviation method, may be use for preliminary analysis of the opportunities of ballistic systems with sufficient accuracy for practice.

For replying to question about statistical significance of got results and the choice function, adequately describing Monte-Carlo method results, it is necessary to make estimation of coefficients in the law describing probability distribution of random values output parameters on limited sample from general population $P(\alpha < X < \beta) = \sum_{x>\alpha}^{x<\beta} P_x$. For χ^2- distribution, for level of confidence probability α=0.05, the average significance $\overline{p_д} = 56.3$ MPa with value of confidence dispersion Sx =0.09746 MPa (for n=300) was gotten. That

for the execution of condition $P\left\{t_{\alpha/2} < \frac{\bar{x} - \mu_x}{S_{\bar{x}}} < t_{1-\alpha/2}\right\} = 1-\alpha$ gives for probability P=0, 975 crictical significance $t_{0,975}$ =2, 26. Then confidence interval for muzzle pressure will compose 56.05 $\leq \overline{p_д} \leq$ 56.50. Analogically for muzzle projectile velocity it will have gotten: 680.3$\leq \overline{V_д} \leq$682.3 m/s.

Practical application of got distributions may be use for solution of whole row tasks: the calculation of dispersion or hit probability in a target, serviceability estimation of recoil mechanisms and other aggregates of guns, bore stress and the dynamics of it vibrations and so on. As example of using got results on Fig.4 are given epures of tangential stresses in 4 cross-sections of bore wall, calculated according to formula $E_{et} = \frac{2}{3}P_1\frac{r_1^2}{r^2}\frac{2r_2^2+r^2}{r_2^2-r_1^2} + \frac{2}{3}P_2\frac{r_2^2}{r^2}\frac{2r_1^2+r^2}{r_2^2-r_1^2} + \frac{1}{3}\sigma_z$ at P_2=0, σ_z= 0 and the random assignment of gas pressure on walls inside a bore.

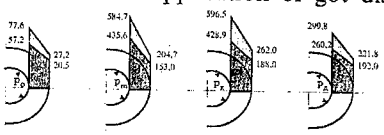

Fig. 4. The distribution of tangential stresses in different bore cross-sections

NOMENCLATURE

1. Орлов Б.В. "Внутренняя баллистика артиллерийских систем", М., 1978.
2. Серебряков М.Е. "Внутренняя баллистика" , II изд., М., 1949.
3. Чуев Ю.В. "Проектирование ствольных комплексов", М., 1976.
4. Чурбанов Е.В. "Внутренняя баллистика", Л., 1975.
5. Белов А.В. "Основы проектной оценки надежности артиллерийских орудий" БГТУ, С.-Пб., 1986.
6. Dr. Zakharenkov V.F., Dr. Belov A.V. " The Estimation of Work Capacity of Electrothermal Chemical Launcher by Reliability Method", Proceedings of Fifth European symposium on electromagnetic launch technology, France, Toulouse, 9-14 April,1995, paper N 48.

BURNING OF 7 AND 19-HALLS POWDER GRAINS WITH TAKING INTO ACCOUNT REAL GEOMETRY OF SMALL PRIZMS AFTER COLLAPSE

V. F.ZAKHARENKOV, Baltic State Technical University, 198005, Russia, Saint-Petersburg

The calculation of burning parameters and the geometry of powder grain with n halls until a moment of collapse does not present difficulties and may be carried out according to M.E. Serebriakov or J. Corner methods [1], [2]. Geometrical characteristics of powder grain before the start of burning and at the moment of collapse (when halls meet each other) are shown on Fig.1.

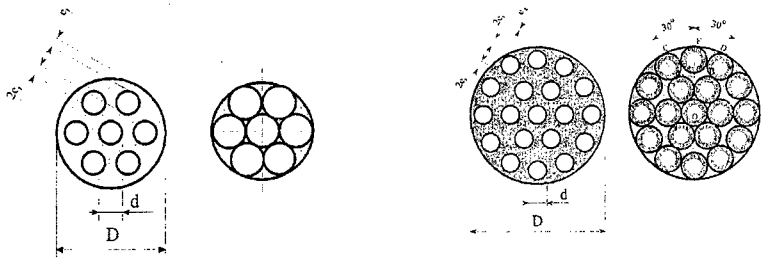

Fig.1 Geometry of 7-and 19-halls powder grain

The calculation of post-collapse parameters requires the accounting of real geometrical shape of collapse elements - curvilinear small prizms. The complex form of such prizms demands, for calculation of their burning surface, application of mathematical apparatus of analytical geometry and computer technique for providing of necessary calculations. The existing methods [1], [2] were created during a time when there were no computer technique and demanded the elaborating of simple calculation methods. As a result, two schemes of such calculations have been developed. In accordance with the first scheme the relative thickness of powder grain at the moment of collapse z_s was accepted equal to unit as to the second one - less then a unit. In the practice of powder grain parameters calculation in Russia the first scheme (method prof. M.E.Serebriakov [1]) found it's application. The second scheme is widly used in the countries of West Europe, USA, China and some other countries. In Russia the second scheme was developed by professor prof.V.E.Slukhotsky [1].

In accordance with the first scheme under $z_s = 1$ the burnning outside and inside surfaces are connected and collapse of grains on several groups of curvelinear prizms takes place: for 7-hall grains - 2 groups; for 19-hall grain -3 groups (Fig.2). After collapse of grain a local groups of prizms burn indepedently.

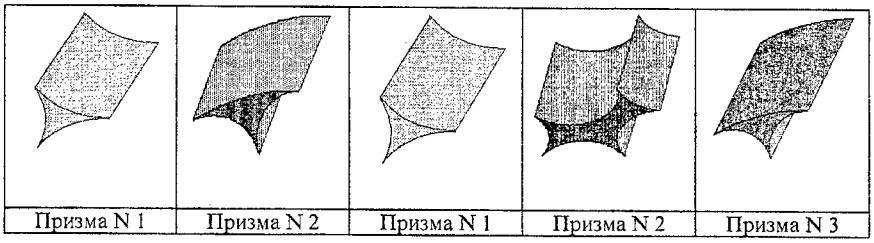

Fig.2 Shape of prizms of 7 and 19-halls powder grains at the collapse moment

The calculation of surface burning grain during this period may be given on relative burning thickness for whole groups of prizms or as to real geometry. Classical ballistics is based on the first approach, theoretical bases of which in Russia have been developed by professors G. V. Oppokov, M.E. Serebriakov, K. K. Greten and I.P. Grave [1]. The essence of the given approach consists in the calculation of relative burning thickness z_l which change in a range from 1 to z_k at alteration ψ from ψ_s to 1. By this the value $z_k = \frac{e_1 + \rho_1}{e_1}$, where ρ_1 - the radius of circle inscribing into outside prizm of 7-hall powder grain and calculated as to formula I.P. Grave $\rho_1 = 0{,}1772(d+2e_1)$. On the basis of geometrical approach (Fig.3) the following formulas for calculation of radiuses of prizms inscribing circles were got by us

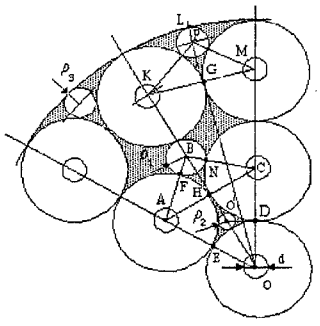

Fig.3 The calculation scheme of the grain geometry

$$\rho_1 = \left(\frac{3-\sqrt{3}}{4-\sqrt{3}}\right)(d+2e_1);$$

$\rho_2 = \left(\frac{2\sqrt{3}-3}{6}\right)(d+2e_1)$. In 19-hall grain the third group of prizms appears at the moment of collapse. The radius of circle ρ_3, inscribing into the section of these prizms is equal to

$$\rho_3 = \frac{25 - 40\cos 15^\circ + 16\cos^2 15^\circ}{12 - 8\cos 15^\circ}(d+2e_1).$$

The calculation results of geometrical characteristics of standard $(d = e_1)$, $(2\ell = 2{,}5D)$ 7 and 19-halls powder grain and burning's parameters before and after collapse for both approaches are given in Table 1.

Таблица 1

Параметр	Модель 1		Модель 2	
	4/7	11/19	4/7	11/19
l_1, мм	0,4	1.16	0,4	1.16
d_3, мм	0,2	5,8	0,2	5,8
D, мм	2,2	9,86	2,2	9,86
l	5,5	24.65	5,5	24.65
$ж_1$	0,7343	0,5804	0,7343	0,5804
λ_1	0,2337	0,4162	0,2337	0,4162
μ_1	-0,02174	-0,02162	-0,02174	-0,02162
ψ_s	0,8536	0,8094	0,8536	0,8094
z_k	1,5316	1,5316	0,6529	0,6529
$ж_2$	0,5508	0,7170	-0,8436	-1,0982
λ_2	-0,9406	-0,9406	1,4406	1,4406
σ_s	1,4022	1,7676	1,4022	1,7676

For calculation of current burning surface of prizms under the assumption of layers parallel burning, i.e. as to geometrical law, it is necessary to know the thickness of burned layer e_2^i in every moment of time. This thickness may be computated on the basis of power law of burning $U = U_1 p^{\nu}$. As $U_i = \frac{de_2^i}{dt} = \frac{dz_i}{dt} e_o^i$, then $e_2^i = \int_t U_1 p^{\nu} dt$. From this follows that, by grains burning at the same pressure and physical-chemical and kinetical characteristics of powder material, the value e_2^i for all prizms will be alike and it may be put $e_2^i = e_2$. Under such conditions prizm with radius ρ_2 will over burn the first, then - with radius ρ_3 and the last - with radius ρ_1. Thus, during the calculation of burning parameters of all prizms the identical thickness step value $d\rho = \rho_2 / N$ may be set. The last one is determined as to smallest radius ρ_2, where N - the number of radius divisions on elementary thicknesses. Then current thickness is $e = id\rho$, where $i = 1,2,...,N_1$ and $N_1 = \rho_1 / d\rho$. At such conditions full burning of prizms will be determined by following constraints: for prizms with radius ρ_2 : $e \geq \rho_2$; for prizms with radius ρ_3: $e \geq \rho_3$; for prizms with radius ρ_1 : $e \geq \rho_1$.

The calculation of current prizm's surfaces is held as to following generalized formulas , describing coordinates of point C ($y_c = 2R_o Cos30^\circ; x_c = 2R_o Sin30^\circ$) and radius $(x - X_c)^2 + (y - Y_c)^2 = R^2$, and areas of prizm's faces also $S = \int_0^{x_1} y_1 dx - \int_0^{x_1} y_2 dx$, the lengths of arcs prizm's surface $\ell_s = \int_{x_1}^{x_2} \sqrt{1 + (y')^2} dx$, lengths of stright-line segments $\frac{x - x_1}{x_2 - x_1} = \frac{y - y_1}{y_2 - y_1}$ and angle of crossing between them $tg\alpha = \frac{a_2 - a_1}{1 + a_1 a_2}$, where a_1 and a_2 - angular coefficients of every straight. The calculation of point G coordinates (Fig.3) shows that circles with centers in points K and M are not touch in this point as it takes place in 7-hall grain.

Subcontractory points have coordinates $G(1{,}0782R_0;3{,}85196R_0)$, $G'(0{,}99216R_0;3{,}875R_0)$, that speaks about presence of narrow bridge between outside and middle prizms. Difference in coordinates is $\Delta x_G = 0{,}08604R_0; \Delta y_G = 0{,}02304R_0$. On the base of expounded above it may be drawen the conclusion: **19-halls powder grain at the collapse moment of inner prizms does not provide simultaneously collapse of 12 outside prizms**. The presence of web with thickness $\Delta=\sqrt{\Delta x_G^2+\Delta y_G^2}=0{,}0891R_0$, that constitute about 9% from initial radius up to join's point of 7-hall powder grain leads to form of prizms 19-halls grain shown on Fig.4-a. The view of the same prizm at the moment of it secondary collapse (after that web was burned) is shown on Fig.4-b. Full collapse of complex prizm occurs at the moment when thickness equal to $\Delta/2$, i.e. $0{,}04555R_0$ will burn over. At $R_2 \geq 1{,}04455R_0$ the powder grain breaks up and points G and G' merge into one overall point G with coordinates $x_G = 1{,}0356R_0$, $y_G = 3{,}8636R_0$. Mentioned peculiarity of collapse were considerated at the development of the calculation program for ECM. Below are presented the results of computer calculations of current burning surface and relative mass of gases for 7 and 19-hall grains versus parameter z.

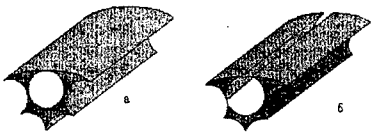

Fig.4 View an element of 19-halls powder grain at the moment of premier collapse prizms (a) and at the moment of secondary collapse prizms (b)

The 7-hall grain. The calculations of perforated tube carried out as M.E. Serebriakov and suggested methods for powder grain with burning web thickness $2e_1 = 1{,}2$ mm and type sizes of hall diameters $d=e_1$, outside diameter of rosette $D=4e_1+3d=6{,}6$ mm and length of tube $2c = 2{,}5D = 16{,}5$ mm. The calculation results of grain geometric form function coefficients before and after the halls will meet each other and parameters of progressivity and end of burning, computated as to method prof. M.E. Serebriakov are given in tabl.1. The character ψ and σ changing versus z during the post-collapse period collapse, i.e from value z=1 to z_k, is shown on Fig.5.

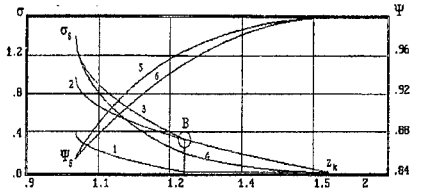

Fig.5 Dependence of σ and ψ for 7-halls powder grain versus thickness z

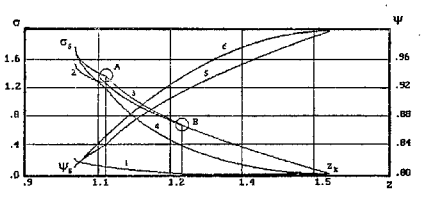

Fig.6 Dependence of σ and ψ of 19-halls powder grain versus thickness z

1-σ small prizm; 2-σ big prizm; 3-summary change of burning surface; 4-σ on M.E.Serebriakov's method; 5- ψ on offered method; 6- ψ on M.E.Serebriakov's method; B-the burning end of small prizm; A- point of secondary grain collapse

19-hall grain. The calculations were held as to method M.E. Serebriakov and the supposed method for powder grain with thickness of burning web 1,2 мм too.The calculation results of geometrical form function coefficients before and after collapse and also parameters of progressivity of burning computated as to M.E.Serebriakov method are given in Table 1 and on Fig.6.

From pictures anyone can see that 19-hall grain has more sugnificant burning progressivity in comparison with 7-hall grain and hence the less value of maximal pressure in comparison with the last. For comparison of powders of progressive and degressive burning ballistic calculations of 152 mm caliber cannon on both methods were carried out by means of KOBRA special program package. The qualitative results of influence of 1, 7 and 19-halls powder grain on pressure and projectile velocity are shown on Fig. 7 and 8.

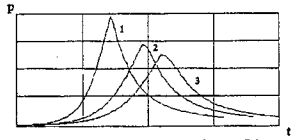

Fig.7 Influence of progressivity of burning on pressure

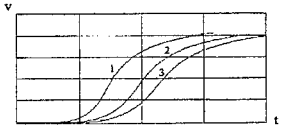

Fig.8 Influence of progressivity of burning the projectile velocity

1- degressive burning; 2- progressive burning of 7-hall grain; 3- progressive burning of 19-halls grain

The analysis of calculation results shows that more degressive powder (one-hall) gives more gases and the higher level of maximal pressure.The application of progressive gun powder decreases maximal pressure and increase the muzzle pressure. This is accordingly leads to the decreasing of muzzle velocity (Fig.8). Such character of alteration of ballistic parameters permits to provide the desired muzzle velocity at given level of maximal pressure on account of selection of combined (composed) charge characteristics. For example, the division of charge mass between degressive and progressive burning components in ratio 0,4:0,6 allows to decrease maximal pressure on 14% while the muzzle velocity decrease on 2,3% only.

REFERENSES

1. М.Е.Серебряков, К.К.Гретен, Г.В.Оппоков Внутренняя баллистика, Оборонгиз, 1939, 592 с.

2. J.Corner Theory of the interior Ballistics of Guns, John Willey & Sons, Inc., London, Chapman & hall, 1950, 443 p.

THE TRANSVERSAL FLUCTUATION OF PRESSURE IN TRANS-PISTON VOLUME OF BALLISTIC LAUNCHER

V. A. GOLUBEV, V. F. ZAKHARENKOV, Baltic State Technical University, 198005, Russia, Saint-Petersburg

Knowledge of pressure fluctuations in trans-piston volume and parameters, defining their appearance in the series of applied tasks is more essential, as the lasts can accord noticeable influence on the character of piston motion in the bore.

In check cross-section experimentally recorded (Fig.1) the presence of sudden change local transversal pressure gradients. The last ones as to absolute value account for 10-15% from maximal value of average ballistic pressure. The explanation of appearance this phenomena may be given on the basis of fluctuations modeling.

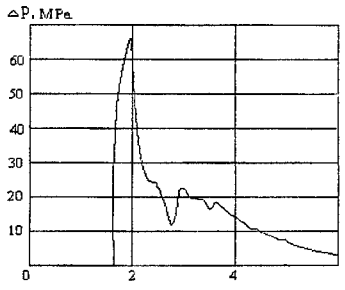

Fig.1 Pressure drop

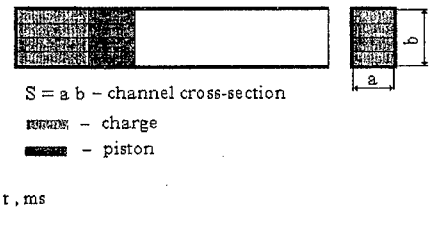

Fig.2 Structural model

Physical-mathematical model is built on the representation of trans-piston volume of the ballistic set-up as a set of longitudinal layers with sub-volumes W_i (Fig.2). Correspondingly the piston is represented as a set of local sub-pistons too. Mass of each sub-piston is q_i and there number is equal to the number of selected layers. Mass and energy transfer through this contact planes takes place due to pressure, temperature or density gradients. Gas parameters inside each layer is taken as average on sub-volume. Division of powder volume on a number of rectangular sub-volumes demands to take account of disturbance wave propagation rates from one layer to another [1]. This circumstance leads to the necessity of time step choice $\Delta\tau$, for integration of ballistic equations, satisfying to condition $\Delta\tau = I_{ki}\frac{\Delta z_i}{p_i} \langle\langle \tau_i = \frac{b}{Nc_i}$. Velocities and travels of sub-pistons on each integration time step is calculated from ballistic parameters in every i-layer. However stiff connection between local pistons make to tie on temporary time-layer values of velocity and paths of

local pistons on considered transversal distance to the average velocity and path of pistons on the whole by means of equations:

$$\frac{dV_i}{dt} = \frac{s_i p_i}{\varphi_i q_i} \; ; \; \frac{d\ell_i}{dt} = V_i \; ; \; V = \frac{1}{N}\sum_{i=1}^{N} V_i \; ; \; \ell = \frac{1}{N}\sum_{i=1}^{N} \ell_i \; ; \; V_i^{\tau-1} = V \; ; \; \ell_i^{\tau-1} = \ell \; ;$$

$$P_i = (f_i \omega_i \psi_i - 0{,}5\theta_i \varphi_i q_i V_i^2) / W_i ; \Delta p_i = P_i - P_{i-1} \; ; \; \Delta\rho_i = \rho_i - \rho_{i-1} \; ; \; \Delta\omega_i = \mu \frac{\Delta p_i F_i \Delta\tau}{c_i} \cdot \frac{\Delta\rho}{\rho}.$$

In given equations are admitted following signs: ψ - the relative weight of burned part of powder charge; z - the relative thickness of burned part of powder charge; J_k - the burning impulse of gunpowder ; p- pressure ; $\Delta\omega$ - mass of gas, removing from layer to layer; s - transversal cross-section area of layer; ℓ - transient way of piston(s); V- piston(s) velocity; φ - coefficient of the accounting of secondary works; t - time; $\Delta\tau$ -integration time step; f- powder energy ("force" of gunpowder); $\theta = k - 1$- adiabatic coefficient ; q- mass of piston(s); - gas density; c - speed of sound in the layer(s); F- contact surface of layers; N- total number of layers; i-number of layer.

Worked out mathematical model was realized as computer program for ECM IBM PC. Below are presented the results of numerical examinations for the case of two-layer transversal division of trans-piston volume for set-up with rectangle channel with the following data:

$s_1 = s_2 = 61\ sm^2$, $\omega_1 = \omega_2 = 5$ kg, $q_1 = q_2 = 3$ kg and time step less then 10^{-5} s.

The initial stage of examinations was devoted to determination of ballistic parameters in trans-piston volume under the same constructive and technological features and loading conditions in sub-volumes. As a result the reference variant of solution without the accounting of transversal pressure fluctuations and identical burning of powder charge in layers was found. Later on it was used for the examinations of one-percent deviations mass of charges, burning impulses, force and density of powder influence on values of maximal and finite pressure drops.

Fig. 3 shows the curves p=f(t) and Δp=f(t) for the case of one-percent deviation of "force" of powder only. Anyone can see that the duration of pressure fluctuations is comparable with the time of piston moving along the bore.

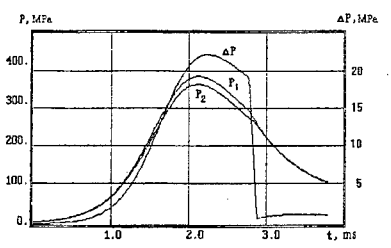

Fig.3 Gas pressure change inside sub-volumes

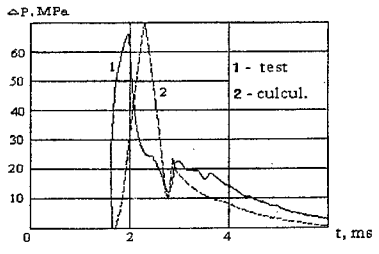

Fig.4 Comparison of pressure calculation with experimental data

The particular interest presents the examination of transversal pressure fluctuations at the same parameters of loading in sub-volumes for modeling of charge's destruction in layers. Such investigation allows to wide representation about real processes , taking place in trans-piston volume of ballistic sets. So, for instance, at the destruction of charge in layer 1 at ψ_1=0,45 and in layer 2 - at ψ_2=0,55 with coefficients of crushing charges as 2 and 3 accordingly, calculation curve $\Delta P = f(t)$ satisfactorily consists with experimental curve on Fig.1 not only in qualitative but and quantitative relation (Fig.4). At t=1,8 ms, as like how calculations, experimentally detected the beginning of pressure fluctuations.

Thus worked out model allowed:

- to bring out the conditions of transversal pressure fluctuations appearance within the trans-piston volume of ballistic launchers;
- to give quantitative estimation of various factors influence on the value of transversal pressure gradients in the trans-piston volume, which, depending on constructive-technological parameters and of charge loading conditions, can achieve 10÷15 % from P_m value and ought to be taken into account during the designing and experimental testing of ballistic sets-up;
- to bring out the sensitivity of transversal pressure fluctuations to deviations of charge parameters and to conditions of charge loading, nomenclature and value of which can be specified during further researches of specific ballistic sets.

REFERENCE

1. Повх И. Л. Техническая гидромеханика.Машиностроение, Л.,1976

18

BRAKE DEVICES OF BALLISTIC SET-UP WITH A RING GAS WITHDRAW

V.A. GOLUBEV, V.M. ALEKSEEV, V.A. VASIN
Baltic State Technical University, 198005, Russia, Saint-Petersburg

There are many types of brake devices of ballistic sets-up utilizing the residual energy of gases with the purpose of the recoil pulse reduction. Such brake devices begin to work after the piston pass through the muzzle. The variety of such brake devices can be explained by aspiration to find the optimal design, which would provide the least load on the ballistic set-up, the least perturbation on the piston inside the brake device chamber and the least mass of device.

The questions connected with asymmetrical action of gases on the piston inside the device chamber become more urgent as power of both set-up and brake devices increasing. Widely used in practice earlier created perfect brake devices, have the constructive characteristic $\alpha \geq -0.26$.

In the present paper some results of research of brake devices with the ring gas supply from the trans-piston volume are submitted. Using such devices one can gain effective reduction of the recoil pulse and minimize the piston perturbation. The fragment of set-up with the brake device of such type is shown at the below drawing.

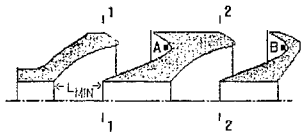

Contouring of the muzzle brake is aimed at obtaining of the directed change of the gas flow. In the brake device the gas flow is divided on central and peripheral flows proportionally to the areas of central window and ring entrance in the peripheral channel. Thus, up to the entrance in the peripheral channel, the gas flow is not exposed to asymmetrical transformations and, accordingly, is not a source of asymmetrical perturbation on the piston inside such chamber.

The distance L_{min} (from the beginning of peripheral expansion of gases up to forward edge of central hole) is rather important for determination of the rational size and mass characteristics of the brake device.

For the two-chamber brake device, with a ratio of the areas of central and peripheral channels in cross-sections 1-1 and 2-2 equal to 1:4, size L_{min} should be not less then the diameter of the central channel. The efficiency of such scheme of brake devices is checked up experimentally for $\alpha = -0.7$ as applied to two-chamber design of the brake device. The calculated pressure distribution on chambers surface, in accordance with channels geometry, is proved to be true by measurements of gas pressure in points A and B, which make 10,5 MPa and 2,5 MPa accordingly, i.e. are in the ratio 1:4,2.

19

MATHEMATICAL MODELING OF A SHOT WITH DISPERSIVE MONOBLOCK CHARGES

A.N. ISCHENKO, J.P. KHOMENKO

Institute of Applied Mathematics and Mechanics at Tomsk State University

One of the ways to increase the efficiency of an artillery shot consists in use monoblock powder charges, which in comparison with usual granulated and tubular have some doubtless advantages: more higher density and additional concentration of energy, opportunity of gradually ignition and controlled progressive combustion during a shot, redistribution of energy in burning space and other. It is probably to use monoblocks in various circuits of a shot. The most known and distributed is the circuit with the monoblock in the chamber of a trunk (MK). Alongside with this monoblock can be used as travelling charge (PZ), and also in the various combined circuits of a shot together with granulated or tubular charges.

It is necessary to mean, that if for monoblocks manufacturing to use usual ballistit gunpowder, with burning speed about centimeters in a second, than necessary gasflow is possible to create by an only advanced surface of burning. It means, that the charges will be porous and the porosity can be as gastransfer and to be present at the monoblock in an initial condition, and opened, i.e. appearing during burning fuel. In any case the burning of such charge will be accompanied by dispersion of a porous matrix on separate particles. In a common case the received mix will include a few factions, each of which is moving and burning on its own laws.

The similar picture is observed and in the usual classical circuit of a shot. By virtue of the technological and statistical reasons powder elements always differ from each other and will form a polydispersive mix. Moreover in regular shots are as often used the charges, consisting from different grades of gunpowder, and also there are other charges elements: ignitor, burning down cartridge and etc.. Thus, practically always at account of a artillery shot it is necessary to collide with a problem of polydispersive gas-powder mix. In known models of internal ballistics it while is not completely solved. Is as a rule used biphase, two-high-speed (gas - gunpowder) approximation. The line of the authors allocates as the third phase the ignitor, but it is considered to move with the gas speed. In the given work new mathematical model of a shot, taking into account the polydispersive mix and opportunity to disperse of the monoblocks is offered.

The model is based on the following assumptions. The powder mix includes N factions, each of which moves with the own speed and burns under the own laws. The products of combustion of all factions are identical on thermodynamic properties and will form uniform carrying environment. The gas is considered unviscous and unheat-transfered, and the influence of viscosity is taken into account only in interaction of phases. Particles are not compressable, and are burning under the geometrical law /1/ with stationary speed. The transition of particles from one faction in other is away. The initial period of a shot is not taken into account, heat-transfer to the walls of the channel we neglect.

The basic system of the equations includes the laws of preservation of weight, pulse and energy for a gas phase, laws of preservation of weight and pulse for each faction of particles, equation of burning and change of number of particles. At the description of transformation of monoblocks it was supposed, that the porous fuel (as MK, and PZ) partially burns down in a plane mode, and partially disperses on particles, burning down in depth of the volume. Dispersive products of PZ will form only one, for example, m-th_ a faction, and at MK — l-th faction of a general mix of n-factions. The front of burning is replaced by a surface of gasdynamics break, through which with identical speed flow gas products and dispersive particles.

At realization of accounts a grid was used mobile similar differencive net, one end of which fastened at the front of PZ burning, and second — at the front of MK burning. At absence of monoblocks borders of settlement area served bottom of the chamber of a trunk and mobile shell. The two-step-by-step obvious circuit was applied. At a first stage the Lax-circuit with a step on the top temporary layer, and at second stage — the integrated laws of preservation was used. Peculiarity of numerical algorithm was occurrence of an additional condition of stability by the right part, connected with presence of interphases force resistance.

For testing offered model of a shot and developed numerical technique two series of experiments on a model ballistic installation were spent. In first was used combined granulated charge, consisting from fine single-channel and large seven-channel gunpowder, and in second — plane and single-channel gunpowder. Comparison of settlement and experimental results has shown, that a divergence on the maximum pressure of a shot does not surpass 2 %, and on initial speed of a shell - 1.2 %. The gasdynamics analysis of a picture flow in the burning space has shown, that the larger faction of seven-channel gunpowder is burning longer single-channel and takes a great interest less for a shell.

On the basis of the advanced approach are investigated gasdynamics peculiarity of the combined shot circuit with use of dispersive PZ. With this purpose a series of experiments is carried out and comparison settlement and

experimental dates is spent. The parameters of the coordination were served by dispersive speed and characteristic of dispersive phase. Dynamics of dispersive products area is investigated and is shown, that the flow of powder gases from PZ carries dispersive faction to the middle of volume, where it mixs up with particles of granulated gunpowder. The zone of mixture does not reach bottom of the chamber as fast dispersal PZ and shell, connected with increase of pressure and reduction of PZ weight begins. The back front of particles takes a great interest for the PZ and up to a moment of complete dispersion PZ "is accompanied" by a dispersive zone in width 0.2-0.25m. After PZ complete dispersion between bottom of a shell and the dispersive zone will form area of pure gas, which in due course extends. Thus forward front of m-th faction particles is designated. To a moment of an exit of a shell from a trunk it practically completely burns down.

Parametrical researches on the basis of offered model have allowed to establish, that the circuit of a shot with MK use can be applied to modernization hunting and sporting shot /2/. Thus is shown, that at presence at MK fuel of necessary delay of ignition, it is possible not only in common to use with granulated gunpowder, but also to keep thus weight regular charge. The given effect has completely proved to be true at realization of experimental tests, during which the speed of fraction is increased up to 20 % without increase of the maximum pressure of a shot.

1. Серебряков М.Е. Внутренняя баллистика ствольных систем и пороховых ракет. М.: Оборонгиз, 1962, 703с.

2. Ischenko A.N., Starchenko A.V., Khomenko J.P. The peculiarities of combustion of granulated and combined powder charges in a sporting gun. Abst. Int. Worksh. On Chem. Gasdyn. And Comb. Energ. Mater. Tomsk, 1995, p.85-86.

22

METHOD and RESULTS of the DECISION of a RETURN PROBLEM of INTERNAL BALLISTICS

EROFEEV V.K., GRIGORIEV V.V.
BSTU, St.-Petersburg

Non-stationary problem on definition of the necessary laws of change gas-and thermodynamic parameters in combustion chamber of in volume of any structures. The problem discusses with the account of physics and chemical conversions, burning surface of a solid fuel, assuring given laws of changes of parameters in volume, kinematics and dynamic laws of movement of the object.

There are known the decisions of a number of return problems of internal ballistics. As a rule, there are the problems of PAD designing, which have to guarantee the necessary ejection. As the other turn there are the problems of volumes desiging in structures for creation of the required laws of parameters changing. The works devoted of deciding the complex return problem and for the volume, where combustion products from the PAD are flow in are not known by the authors. The same words one can say about the PAD's combustion chamber in view of the possibility to account the physics and chemical reactions of gas mix for the different object's assignment laws.

The mathematical model of such complex return problem consists of two equation systems, describing processes, occurring in given volume (1-9) and in a combustion chamber (10-14).

$$G_k = \frac{P_c\left[G_c + \frac{P_c}{R_cT_c}\frac{dV_c}{dt} + \frac{V_c}{R_cT_c}\left(\frac{dP_c}{dt} - \frac{P_c}{T_c}\frac{dT_c}{dt}\right)\right]}{P_c + \frac{P_c}{R_c}\sum_{\gamma} R_{\gamma c}\left(\xi_{\gamma *} - \xi_{\gamma c}\right)}; \tag{1}$$

$$\frac{dT_c}{dt} = \frac{1}{\frac{\rho_c C_{v_c} V_c}{\mu_c} + \frac{A}{B}\frac{P_c^2 V_c}{R_c T_c^2}}\left[G_0\left(\frac{A}{B}P_c - R_cT_c\right) + P_c\frac{dV_c}{dt}\left(\frac{A}{B}\frac{P_c}{R_cT_c} - 1\right) + \right.$$

$$\left. + \frac{dP_c}{dt}\frac{A}{B}\frac{P_c}{R_cT_c}V_c - V_c\sum_{\gamma} H_{\gamma c}W_{\gamma c} - V_cT_c\sum_{\gamma} R_{\gamma c}W_{\gamma c} - \frac{dQ_c}{dt}\right]; \tag{2}$$

$$\frac{d\xi_{\gamma}}{dt} = G_k\frac{R_cT_c}{P_cV_c}\left(\xi_{\gamma *} - \xi_{\gamma c}\right); \tag{3}$$

$$W_{\gamma} = \frac{P_c}{R_cT_c}\frac{\xi_{\gamma}^1 - \xi_{\gamma}^0}{\nabla t} - \frac{\xi_{\gamma *} - \xi_{\gamma}^1}{V_c}G_k; \tag{4}$$

$$G_c = \frac{\varphi q F_{c*} P_c}{\sqrt{R_cT_c}}; \tag{5}$$

$$\frac{dQ_c}{dt}=\alpha_{эф}\left(T_c-T_{ст1}\right)S_c=\frac{dQ_{ст1}}{dt};\qquad(6)$$

$$\frac{dQ_{ст2}}{dt}=\frac{\lambda_{ст}}{h_2}\left(T_{ст1}-T_{ст2}\right);\qquad(7)$$

$$\frac{dQ_{ст3}}{dt}=\frac{\lambda_{ст}}{h_3}\left(T_{ст2}-T_{ст3}\right);\qquad(8)$$

$$G_{k\,ср}=\frac{G_{k\,нас}G_{k\,кон}}{G_{k\,нас}-G_{k\,кон}}\frac{G_{k\,нас}}{G_{k\,кон}}\Big/S_k;\qquad(9)$$

where $A=\dfrac{H_k}{\mu_k}-\sum_{\gamma}\dfrac{H_{\gamma c}Z_{\gamma}}{\mu_k}+T_cR_k$; $B=P_c+\rho_cT_c\sum_{\gamma}R_{\gamma c}\left(\xi_{\gamma *}-\xi_{\gamma c}\right)$;

$$\frac{dP_k}{dt}=\frac{1}{V_k}\left(\rho_{т}S_{т}u_{т}\chi\gamma_kR_kT_{\nu}-G_k\gamma_kR_kT_k\right);\qquad(10)$$

$$\frac{dV_k}{dt}=S_{т}u_{т};\qquad(11)$$

$$P_k=\rho_kR_kT_k;\qquad(12)$$

$$\frac{dT_k}{dt}=\begin{cases}\left(\dfrac{2T_k}{P_k}-\dfrac{T_kC}{D}\right)\dfrac{dP_k}{dt}-\dfrac{T_k}{R_k}\dfrac{dR_k}{dt}+\dfrac{T_k}{D^2}\left(A\dfrac{d\gamma_k}{dt}+B\dfrac{dP_k}{dt}\right)-2\dfrac{\sqrt{R_kT_k^3}}{F_{*k}P_kD}\dfrac{dG_k}{dt}- \\ \qquad\qquad\text{when } \left(\dfrac{2}{\gamma_k+1}\right)^{\frac{\gamma_k}{\gamma_k-1}}\pi\dfrac{P_c}{P_k}\le 1; \\ \dfrac{2T_k}{P_k}\dfrac{dP_k}{dt}-\dfrac{T_k}{P_k}\dfrac{dR_k}{dt}-T_k\dfrac{d\gamma_k}{dt}\left(\dfrac{1}{\gamma_k}-\dfrac{2\sqrt{\gamma_k}}{\Gamma}L\right)-\dfrac{2\sqrt{R_kT_k^3}}{P_kF_{*k}\Gamma}\dfrac{dG_k}{dt}-\text{when } 0\le\dfrac{P_c}{P_k}\le\left(\dfrac{2}{\gamma_k+1}\right)^{\frac{\gamma_k}{\gamma_k-1}};\end{cases}\qquad(13)$$

$$S_{т}=\begin{cases}\left[\dfrac{V_kP_k}{R_kT_kD^3}\left(A\dfrac{d\gamma_k}{dt}+B\dfrac{dP_c}{dt}\right)-G_k\left(\gamma_k+1+\dfrac{CP_k}{D^2}\gamma_k\right)-\dfrac{2V_k}{\sqrt{R_kT_k}F_{*k}D}\dfrac{dG_k}{dt}\right]/ZN- \\ \qquad\qquad-\text{when } \left(\dfrac{2}{\gamma_k+1}\right)^{\frac{\gamma_k}{\gamma_k-1}}\pi\dfrac{P_c}{P_k}\le 1; \\ \dfrac{\dfrac{V_kP_k}{R_kT_k}\dfrac{d\gamma_k}{dt}\left(\dfrac{1}{\gamma_k}+\dfrac{2\sqrt{\gamma_k}}{\Gamma}L\right)-G_k\left(1+\gamma_k\right)-\dfrac{2V_k}{\sqrt{R_kT_k}F_{*k}\Gamma}\dfrac{dG_k}{dt}}{\left[\dfrac{P_k}{R_kT_k}-\rho_{т}\left(1+\chi\gamma_k\dfrac{T_{\nu}}{T_c}\right)\right]u_{т}}\text{ - when } 0\le\dfrac{P_c}{P_k}\le\left(\dfrac{2}{\gamma_k+1}\right)^{\frac{\gamma_k}{\gamma_k-1}};\end{cases}\qquad(14)$$

where $ZN=\frac{P_k}{R_k T_k}-\rho_t\left(\chi\gamma_k\frac{T_v}{T_c}+1+\frac{CP_k}{D^2}\chi\gamma_k\frac{T_v}{T_c}\right)u_t$; $A,B,C,D-f\left(\frac{P_c}{P_k},\gamma_c\right)$; $\Gamma,L-f(\gamma_c)$.

At development of mathematical models the following assumptions were accepted:

- the products of combustion represent an ideal gas;
- the concentration changing of gas's mix substances, occurs at the expense of a solid fuel burning and at the physics and chemical reactions;
- gas- and thermodynamic parameters in a PAD's combustion chamber are rounded.

The equation system is realized as a calculation program for IBM computers. The (1-9) equation system is decided by Runge-Kutt method. The (10-14) system is rigid and for its decision the Girs method, enabling for easy integrating such systems is used.

The (10-14) system for approximate valuation of burning surface can be lead to the next algebraic equation:

$$S_\tau=\frac{\bar{G}_k-\bar{G}_{k0}}{u_\tau}\left(1-\frac{\gamma_k}{\gamma_k-1}\frac{\bar{P}_k}{1+\bar{P}_k}\right)^{-2}+\frac{\bar{u}_{\tau 0}}{\bar{u}_\tau}\left(\frac{1-\frac{\gamma_k}{\gamma_k-1}\frac{\bar{P}_{k0}}{1+\bar{P}_{k0}}}{1-\frac{\gamma_k}{\gamma_k-1}\frac{\bar{P}_k}{1+\bar{P}_k}}\right)^2-$$

$$-\frac{\frac{\gamma_k}{\gamma_k-1}\sqrt{\gamma_k}\bar{F}_{k*}}{\left(1-\frac{\gamma_k}{\gamma_k-1}\frac{\bar{P}_k}{1+\bar{P}_k}\right)^2}\left[\frac{1}{2}\left(\frac{\bar{P}_k}{1+\bar{P}_k}-\frac{\bar{P}_{k0}}{1+\bar{P}_{k0}}\right)+\right.$$

$$\left.+2\left(\sqrt{1-\frac{\bar{P}_k}{1+\bar{P}_k}}-\sqrt{1-\frac{\bar{P}_{k0}}{1+\bar{P}_{k0}}}\right)-\frac{2}{3}\left(\sqrt{\left(1-\frac{\bar{P}_k}{1+\bar{P}_k}\right)^3}-\sqrt{\left(1-\frac{\bar{P}_{k0}}{1+\bar{P}_{k0}}\right)^3}\right)+\frac{1}{2}\frac{1+\bar{P}_{k0}}{1+\bar{P}_k}\right]; \quad (15)$$

where $\bar{G}_k=\frac{G_k}{\omega_\tau}$; $\bar{F}_{k*}=\frac{F_{k*}\sqrt{R_k T_v q}}{V_\tau(\gamma_k-1)}$; $\bar{u}_\tau=\frac{u_t S_{\tau 0}}{V_\tau}$; $\bar{P}_k=\frac{P_k(\gamma_k-1)}{\rho_\tau R_k T_v}$; $\bar{S}_\tau=\frac{S_\tau}{S_{\tau 0}}$.

The numerical researches results permit to generalize about serviceability of an offered technique and opportunity of using with considerably smaller costs, than at the decision of a direct problem, in design work.

THE ACCOUNT OF PERCUSSION CAP PRESSURE WITH BALLISTIC CALCULATIONS OF THE SMALL ARMS AMMUNITIONS WITH LOW BALLISTICS

MAKAVEYEV A. T., BALTIC STATE TECHNICAL UNIVERSITY, 198005, S.- PETERSBURG, RUSSIA

The initial pressure in chamber renders big influence on a course of ballistic process in the channel of a barrel. Particulary, the quantity of the powder which has burned during a shot depends from one for the weapon with low density of loading. With realization of ballistic calculations of artillery systems the prime device p_v is accepted as initial pressure which will be formed as a result of smoky gunpowder combustion of the prime cartridge but the pressure of shock structure of percussion cap is not taken into calculations as it is a very small in comparison with pressure from smoky gunpowder of prime device and main charge of smokeless powder. However there is a necessity of the account of percussion cap pressure with ballistic's calculations of stopping action ammunitions and hunting ammunitions. It is caused by the several reasons: throwing bodies of this ammunitions have the small meaning of parameter C_q, but starting pressure p_o and shock structure of percussion cap pressure p_{vk} are comparable to pressure from burning of powder p. Today two kinds percussion caps applies for ignition of powder charge in hunting ammunition- opened and closed. Cap of " Tsentroboy" type concerns to first, and second type is "Zhevelo". Cap "Tsentroboy" is less powerful on own action and is usually used with equipment of smoky gunpowder ammunition as this powder is easily ignited. It is more preferable to use cap "Zhevelo" with equipment ammunition by smokeless powder. Cap "Zhevelo" is applied also in ammunition of stopping action of 23-mm rifle shot gun KS-23, which was accepted on arms of interior security troops in 1991.

Percussion cap "Tsentroboy" (State Standard N 7574 - 71) exists two versions: TsBO - with shock structure on a basis of $Hg(ONC)_2$ and TsBO-N - with anticorrosive structure on a basis of $C_6H(NO_2)_3OPb{\cdot}H_2O$. Prescriptions of shock structures of these caps are following (in % on weight):

TsBO	%	**TsBO-N**	%
$Hg(ONC)_2$	16,5 ± 1,5	$C_6H(NO_2)_3OPb{\cdot}H_2O$	35 ± 3
$KClO_3$	55,0 ± 3,0	$C_6H_8ON_{10}$	3 ± 1
Sb_2O_3	28,5 ± 1,5	$Ba(NO_3)_2$	42 ± 3
		PbO_2	5 ± 2
		Granule mix of Sb_2O_3 and Al	15 ± 2

Weight of shock structure in "Tsentroboy" type percussion caps is 0,03 ± 0,002 g. Percussion cap "Zhevelo" (State Standard N 24579 - 80) also exists two versions: "Zhevelo-N" (anticorrosive) - with structure on a basis $C_6H_8(NO_2)_3OPb{\cdot}H_2O$ and "Zhevelo-M" (powerful) - with structure on a basis $Hg(ONC)_2$. Prescription of shock structure of cap "Zhevelo-N" is the same as at cap TsBO-N, and prescription of structure of "Zhevelo-M" is following:

$Hg(ONC)_2$ - 50 %;

$KClO_3$ - 33 %;

Sb_2O_3 - 17 %.

Weight of shock structure in percussion caps of this type is 0,05 ± 0,003 g. Percussion caps with shock structure on a basis $Hg(ONC)_2$ have got the greater practise than anticorrosive structures because of their high energy, in particular for ammunition of pomp gun KS-23 where " Zhevelo-M" cap is only applied. Prescription of shock structure renders big influence on the physical characteristics of products of combustion. The physical data for two shock structures on a $Hg(ONC)_2$ are resulted below.

Cap	**TsBO**	**Zhevelo - M**
Specific volume of gases with normal conditions, 10^{-3} m^3 / kg	107,2	210
Flame temperature of gases, ° C	4600	4500
Adiabatic coefficient	1,11	1,27
Quantity of gases in products of combustion, %	34,3	68,62
Quantity of the solid rest, %	65,7	32,28

Calculation of pressure, created percussion cap, is possible to make under the formulas of classical internal ballistics. The pressure, which is created by products of combustion of shock structure in volume of cap, is determined on the formula:

$$p_k = f_k w_k y_g / (W_k - w_k y_t / d_t) , \qquad (1)$$

where w_k - weight of shock structure; f_k - force of shock structure; W_k - internal volume of cap; d_t - density of the solid rests of products of combustion shock structure; y_g - relative quantity gas products of shock structure combustion; y_t - relative quantity of the solid rests of shock structure combustion.

The force of shock structure of percussion cap can be calculated as :

$$f_k = R_k T_{1k} , \qquad (2)$$

where R_k- specific gas constant for a mix of gas products; T_{1k} - explosive temperature of shock structure.

Gas constant for a mix of combustion gas products is defined from the energy equation of Clapeyron-Mendeleev:

$$R_k = p_a W_{1k} / T_o , \qquad (3)$$

where p_a = 0,1013 MPa - normal atmospheric pressure; T_o = 273 K; W_{1k} - specific volume of gases with normal pressure and temperature T_o = 273 K.

Pressure, which is produced by products of combustion of shock structure in free volume of a chamber, is possible to define from the equation of adiabatic process:

$$p_{vk} = p_k \left(\left(W_k - w_k y_t / d_t \right) / \left(W_o - w / d + W_k - w_k y_t / d_t \right) \right)^k , \qquad (4)$$

where W_o - initial volume of chamber; w - weight of powder; d - density of a grain powder , k - adiabatic coefficient.

The calculations under the formulas (1), (2), (3) and (4) for two caps have given the following results:

Cap	**TsBO**	**Zhevelo-M**
Gas constant, R_k, J/(kg K)	39,8	77,9
Force of shock structure, f_k, MJ/kg	0,194	0,372
Pressure of explosion products in cap volume, p_k, MPa	30,7	170,2
Pressure of explosion products in free volume of a chamber, p_{vk}, MPa	1,5	6,3

The ballistic calculations of 23-mm standard ammunition of shot gun KS-23 have shown that if not to take into calculation pressure from gases of shock structure of percussion cap then the mistake with calculation of muzzle velosity makes from 15 up to 30 percents depending on density of loading.

REFERENSES

1. ГОСТ 24579-81. Капсюли-воспламенители "Жевело". - М.,1981.
2. ГОСТ 7574-71. Капсюли-воспламенители центрального боя для патронов охотничьих ружей. - М., 1993.
3. Карпов П. П. Капсюли-воспламенители и капсюли-детонаторы. - Л., 1935.

This Page Intentionally
Left Blank

Section 2
INTRA-CHAMBER PROCESSES

MATHEMATICAL MODELING OF THE IGNITION ABNORMAL MODE DEVELOPMENT IN THE SOLID PROPELLANT ROCKET MOTOR, CAUSED BY THE NONESTIMATED ACTIONS

Alexey M. LIPANOV, Alexander N. LUKIN and Ali V. ALIYEV

Institute of Applied Mechanics, Ural Branch of the Russian Academy of Sciences
222, Gorky Str., Izhevsk, Udmurt Republic, 426001, Russia
Tele.: int. +7-(3412)-752731; Fax: int. +7-(3412)-231713
E-Mail: lam@lam.ipm.udm.ru

The tendency of development of the modern large-sized solid propellant rocket motors (SPRM) is characterized by increase of the combustion chamber filling degree by propellant and operation loads level. Improvement of the modern large-sized SPRM characteristics, reduction of terms and material expenses on their improvement and manufacturing depends largely on reached results in understanding the regularities of a course and possible accuracy of the anomalous physico-chemical processes prediction, which arise during the operational period. There are a class of the large-sized SPRM with a high intrachamber loading coefficient ($\geq$ 0,95). The main peculiarity of the structural diagrams of such propulsion systems is that the firmly fastened internal channel charge has a partially non-fastening and unarmoured end face surfaces in the vicinity of the front bottom. In these conditions the end face combustion surface can make up to 50 % and more from the whole total combustion surface. The charge end face is usually fastened with the engine front bottom with using of the boot (the sealing ring). On the fig. 1 the typical structural diagram of such SPRM is shown (1 - is the fiber glass case; 2 - is the

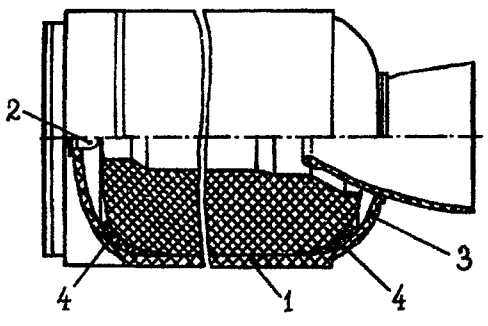

Figure 1.

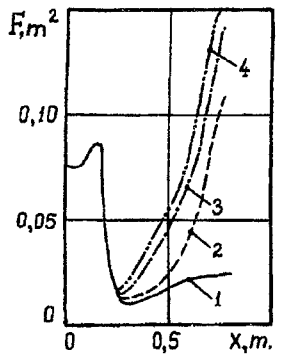

Figure 2.

pyrotechnic ignition system; 3 - is the nozzle bottom; 4 - is the boot (the sealing ring)). The other peculiarity of this class of SPRM is that, in normal conditions, at which the propulsion systems storage is provided, the clearances width between the engine case front bottom internal surface and the charge end face surface $\Delta \leq 0.001$ m. In the process of the intrachamber volume filling by the high-temperature combustion products (CP), coming from the ignition system (IS) and from the propellant already ignited part, there are joint elastic deformations of the propellant charge and engine case. The engine case has a "cocoon" type design and is executed from the organic plastic materials. In these conditions, the thickness of the not-flowing clearance between the SPRM case front bottom internal surface and the charge end face surface can increase in 20 - 100 times at the operating pressures in the combustion chamber 5 - 10 MPa. On fig. 2 is submitted the dependence of the front face clearance cross section area in a vicinity of the engine front bottom from the longitudinal coordinate in various time moments: 1 - $t = 0$ sec., 2 - 0.036 sec., 3 - 0.048 sec., 4 - 0.060 sec. Here the significance of coordinate $x = 0$ corresponds to the boundary between the end face cavity and the engine front volume. In a number of cases, listed peculiarity of the considered SPRM can cause the increased sensitivity of the SPRM operation initial stage to a various kinds of the nonestimated actions. In general case, under the "nonestimated actions" are implied not only deviations of working parameters of the separate units and elements of the SPRM, but also supposed design errors, violations of technological process modes and aging of the materials of the elements, both of the design of SPRM, and the charge.

In a considered situation, the reason of an anomalous mode of ignition and combustion in the SPRM combustion chamber beginning can serve the nonestimated action from the pyrotechnic IS. Such noncalculated effect result in nonmonotonicity of the working processes course during the propellant charge ignition.

In a number of cases, realization of the situation is possible, when from the moment of beginning of the high-temperature CP outflow from the IS and up to the moment of the flame occurrence on the propellant charge surface, mentioned nonflowing end face clearance, having significant elongation, has no time to expand up to the necessary sizes. Beginning of a similar situation, in the most responsible period of activity of this class of the SPRM, can initiate a number of anomalous physico-chemical processes, which capable to affect essentially on the engine further operation. The most probable sequence of the ignition anomalous mode development can look like as follows. The clearance, representing a poorly warmed up stagnant zone, will hinder to supply of enough heat quantity, necessary for the charge front end face ignition. And in case of absence of beforehand organized distribution of the CP flows from the IS on directions can result in much greater irregularity of the heat supply to the charge various surfaces. It will lead to increase of the front end face

ignition time delay and to the nonmonotonicity of all process of the charge ignition. Besides, in the beginning of IS functioning, the CP flowing into as from the IS, and from charge sections already joined to combustion, will affect on the initial gas, placed in the end face clearance, as a piston. Thus, into the depths of the end face clearance will begin propagate the compression waves, which, as a rule, are transformed into an intensive shock wave. The last, when reaches the area of interface of the engine bottom with the boot and the charge end face, is reflected at simultaneous build up pressure in this place. Then, propagation of a reflected shock wave begins, and the initial gas, which contiguous to the area of interface of the engine bottom with the boot and the charge end face, will contract up to the high pressure. The considered phenomenon of gradually strengthening compression waves propagation was for the first time investigated in the ordnance science, in 1876 - 1878 by Major-General of the Russian Army Nickolay V. Kalakoutsky, the outstanding Russian scientist in the fields of metallurgy, physical metallurgy and ordnance. As a result of sequential development of an indicated phenomenon, in the area of interface of the end face clearance cavity with the boot, which fastening the charge end face with the engine bottom, can arise a strong local dynamic loads, causing either to the boot breaking-off, or to the boot breaking-off from the engine case and from the charge. The numerical analysis shows [1], that at the clearance value equal to Δ = 0.001 m. the pressure maximum level in the end face clearance cavity is surpasses more than in 13 times the pressure level, corresponding to the clearance value equal to Δ = 0.1 m.

The boot breaking-off (or rupture) from the engine case is accompanied by opening of a new cavity, in which the incandescent CP begins inflow. The last circumstance change over the anomalous process development on a new qualitative level, which characterized already more large scale action on the intrachamber processes in the SPRM. The further development of the non-stationary physico-chemical processes can represent hazard for the normal functioning of the SPRM in all. In case, if the surface on which there is the boot breaking-off is great, the intraballistics processes development in the engine chamber can happen on a following way. The CP pressure in the vicinity of the boot breaking-off place on a some time interval can decrease, and on the SPRM chamber, as the corollary, will be propagated the rarefaction wave. In case of the strong rarefaction wave appearance, can take place either extinction of the propellant charge (complete or temporary) or transition to the propellant charge unsteady burning mode (the SPRM "chuffing") [2]. Propagation of the compression wave along the cavity, formed at the boot breaking-off, can result in ignition of the propellant opened surface and to create dangerously large pressures in the vicinity of the upper boundary of an indicated cavity. And it, in turn, can result in the propellant charge destruction. The investigations of the flame propagation processes along the propellant surface, which placed in the narrow deaf and deformable channel, through the opened boundary of which, from the IS the CP flow into inwards, were conducted in the papers [1], [3]. The difference of the

present research from indicated papers is, that here is considered the situation, when on the boundary between the narrow deaf end face clearance with boot, during boot breaking-off a new cavity is opened. This cavity also representing a deaf channel.

The numerical modelling of anomalous physico-chemical processes development in the SPRM chamber after the boot breaking-off is carried out in the following statement. The CP flow in the propellant charge central channel and in the end face clearances is considered in one-dimentional gasdynamics statement. Thus it is supposed, that the CP are the chemical nonreacting mixture of several components. The heat flows from CP in the propellant charge and the SPRM case are determined with use of criteria relationship [1]. Warm-up of the propellant surface and its ignition is determined on the models of Professor R. Ye. Sorkin of Russia. It is supposed, that the boot breaking-off happens instantly, and the parameters in the vicinity of breaking-off are described in the one-dimentional statement. The gasdynamics equations are solved numerically by the "large particles" method [4], which developed by academician Yu.M. Davydov of Russia, with utilization of a number of modifications [1].

For the complex check-up of the developed mathematical model of the physico-chemical processes, the numerical calculations results have been compared with the fire stand tests results. The pressure gauge was installed in the engine front bottom area, namely in the IS flange plug (fig. 1, (2)).

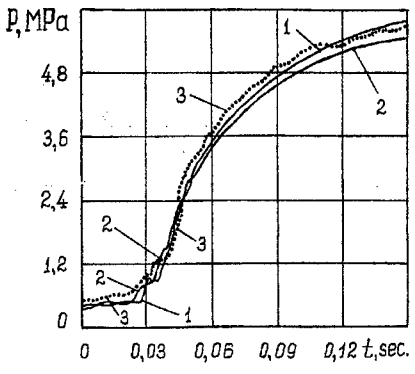

Figure 3.

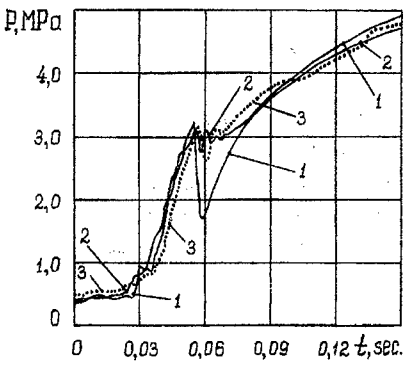

Figure 4.

On the fig. 3 presented the results, which corresponds to the processes development without boot breaking-off: 1 - is the calculated CP pressure on the boundary between the front end face clearance and the boot; 2, 3 - are the computational and experimental CP pressure in the SPRM front volume. On the fig. 4 presented the results, which corresponds to the processes development at boot breaking-off: 1 - is the calculated CP pressure on the boundary between the front end face clearance and again opened cavity; 2, 3 - are the computational and experimental CP pressure in the

SPRM front volume. During the calculations, the volume of the opened cavitny relied equal to $W_0^{calc} \approx 0.13 m^3$. Thus, the boot breaking-off calculated pressure has appeared equal to the value $P_*^{calc} \approx 3.225$ MPa, and the breaking-off pressure value, obtained by an experimental way has made $P_*^{exp} \approx 3.153$ MPa.

The numerical investigation of the non-stationary physico-chemical processes development regularities after the boot breaking-off, was executed taking into account the influence of a number of the factors: the boot breaking-off pressure value, the cavity volume which opened after breaking-off, the length on which there is the boot breaking-off and the duration in time the boot breaking-off period. Established, that the non-stationary processes, caused by the boot breaking-off, are the most dangerous to the SPRM functioning at instant breaking-off. Conducted numerical investigations permit to make a conclusion that the velocity of the flame propagation along the propellant surface, which opened after the boot has breaking-off, weakly depends on the boot breaking-off pressure and on the length, on which the breaking-off occurs. However, the increase of the above mentioned pressure and the length results to increase of the propellant ignition time delay in the opened cavity.

Realization of the described above, or similar, ignition anomalous mode in the large-sized solid-propellant boosters of the Reusable Transport Space System (RTSS) (fig. 5) is extremely undesirable. The asymmetry of two solid-propellant boosters distribution in the lay-out diagram put in the essential limitation on instability level of the ignition processes and subsequent combustion in the boosters combustion chambers. Realization of the described above an ignition anomalous mode in one of the boosters can lead to infringement of the symmetry of the RTSS total thrust distribution and appearance of the destabilizing moment. And it, depending on the boosters thrusts misalignment level, can provide essential influence on the RTSS motion stability on a planned trajectory, to create nonexpected actions on the payload and even lead to loss of the RTSS controllability.

Executed calculations demonstrate, that the described above ignition

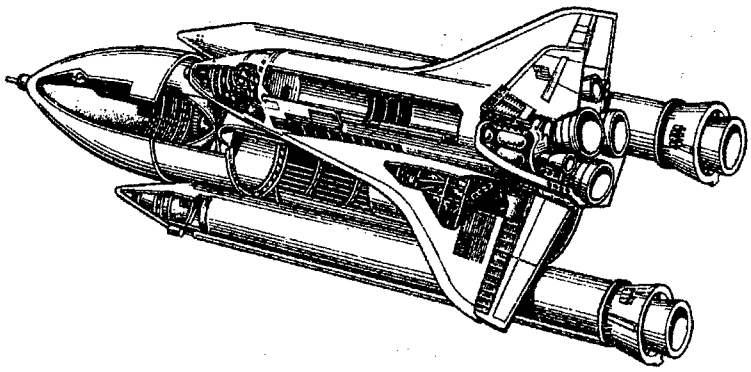

Figure 5. The RTSS lay-out diagram.

abnormal mode appearance in the SPRM it is possible to prevent through the monotony of the engine operation during the start period providing, by means of the IS CP flows selection both on the direction, and on the time. It can be realized by means of using of the IS special design scheme, which can provides at first the CP supply only in the SPRM charge channel. In this case, joint elastic deformation both the propellant charge and the SPRM case will be proceed. And it lead to the face clearances volumes increase still up to the moment of the flame appearance on the propellant charge surface. Then, the CP supply in the deformed face cavity begins, that will be the favorable factor for the initial stage of the SPRM operation. For example, in this conditions the $\partial P/\partial t$ maximum values are reduced, the flame propagation velocity along the face clearance increase in some times, the time straggling of the propellant surface, located in the face cavity connecting to combustion have decreased, and the boot breaking-off probability is essentially reduced.

REFERENCES

1. *Lipanov, A.M., et al.,* Numerical experiment in the theory of the SPRM / *Lipanov, A.M., Bobryshev, V.P., Aliyev, A.V., Spiridonov F.F., Lisitsa, V.D.*, Ural publishing firm "Nauka", Ekatherinburg, 1994, 303 p., (in Russian).

2. *Price E.W. L* - Instability / Nonsteady Burning and Combustion Stability of Solid Propellants. Chapter 9 // Progress in Astronautics and Aeronautics, AIAA Volume 143, 1992, pp. 325 - 359.

3. *Lipanov, A.M., et al.,* The Flame Propagation in the narrow deaf deformable channel / *Lipanov, A.M., Aliyev, A.V., Bodnar T.A., Druzhbin-Chodos V.M., Litvinov L.A.* // J. Physics of Combustion and Explosion, 1990, Vol. 26, N 3, pp. 27 - 33, (in Russian).

4. *Davydov Yu.M.* Large particles method / On: Encyclopaedia of Mathematics, Vol. 5. - Kluwer Academic Publishers: Dordrecht / Boston / London, 1990, pp. 358 - 360.

THE NUMERICAL STUDY OF THE POROUS COOLING EFFECT ON THE CALCULATION EXAMPLE OF HEAT TRANSFER IN ZONE OF THE SHOCK-WALL INTERACTIONS

ISAEV S.A., SADOVNIKOV G.S. (CIVIL AVIATION ACADEMY)
LEONTIEV A.I., NOSATOV V.V. (MSTU by him N.E.Baumann)

The numerical study of injection effect on thermal output at the hypersonic flow of viscous gas at the presence of heat transfer district in the place of the shock drop has target the substantiation of the concept of porous cooling in the heat protection systems for power plants of modern aircraft. Elaborated on of the solution by the determining method of discretizied by means of explicit-implicit MacCormack scheme Navier-Stokes equations for the laminar regime of flow and Reynolds equations, closed by means of two-parameter dissipative model of turbulence, program package [1 - 3] is applied for the task solution about laminar hypersonic prewall flow of viscous gas with a drop shock. Whereat for the constriction of the calculating region sizes it's accommodated symmetry of flow concerning top controlling plane, parallelled low wall and coming out from sharp of the shock generator. Thus, it's considerred the development of the hypersonic flow of viscous gas in the channel of variable transversal section with convergent middle partly. At the task solution it's neglected possible at such velocities of flow by physics and chemical conversions. At the assignment of initial conditions the parameters of gas into all calculated grid points are admitted to the equal parameters of gas in nondisturbed flow. On entrance the parameters of flow are supported continual constant. On exit ones are set of soft boundary condition or the conditions of the solution continuation. On lower стенке in the calculation process traditional slip conditions are fulfilled, while the wall temperature is supported constant. On the overhead surface of the shock generator conditions corresponding to thermally insulated wall are admitted.

In carried out analyses calculated region broke by grid with the bodying of points at the walls, especially at lower wall and in the field of shock drop, where recircuting zone is formed. Grid contained 81x61 calculated points. Minimal step at lower wall was chosen approximately 10^{-4}. It's necessery to notice , that the height of channel section on region exit was considered as an characteristic linear size, and velocity and the density of gas stream are chosen as an scales variable. Comparative analysis of the calculated results for hypersonic viscous flow near impenetrable wall and wall with the district of porous cooling at the presence of falling the shock is carried out in the approach of the laminar regime of flow (Reynolds number is chosen equal to 5000). Mach number was assigned 8.2, and the value of wall temperature and input through the porous

insertion of gas was admitted equal to 0.27. The district of porous cooling was situated in the most heat transfer place (with x=14 till x=16) corresponding to place of the shock dropping on the wall. The impulse of gas injection was fixed and was chosen equal to 5%.

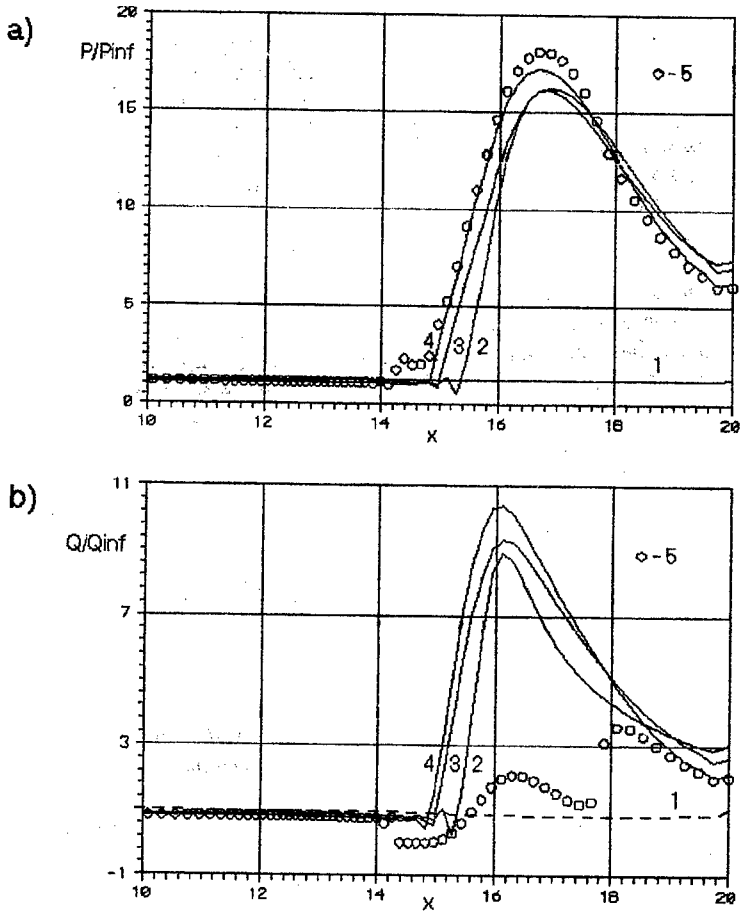

On the picture are presented the results of the comparative analysis of distributions along the wall relative pressure P/Pinf (a) and relative heat current Q/Qinf (b) in the various moments of time (1 - T=3; 2 - 10; 3 - 15; 4 - 20; 5 - 20) without injection (1-4) and with (5). Here index «inf» characterizes the gas parameter for hypersonic flow along flat wall. The analysis of the characteristics field is carried out at the achievement of the solution determining, i.e. at the

achievement of the steady regime of the gas flow. This state is achived at times over 15. The pattern of the stationary viscous prewall flow discovers the decelerating zone in the most heating place - the place of the shock dropping. The recirculating zone is created in pointed place, although in the case without injection it's expressed rather weakly. The presence of cooled insertion does not accord, just like followed to expect, of essential influence on the flow field. This is acknowledges comparative analysis of the graphic distributions of pressure and temperatures in the prewall fields at presence and absence injection.

Transformation with the time of the superficial distributions of the relative values of static pressure and heat current demonstrates the process determining at prewall flow without injection with formation of thermal stress zones corresponding to place the shock-boundary layer interactions. In this case interestingly to mark|, that flow pattern and distributions of local force and heat load generally are formed to the moment of time T=10. Injection does practically not accord sizeable influence upon the profile of relative pressure on the wall. There is noticeably only some increasing of pressure in the place of the beginning of gas injection. The analysis of calculated heat current on the wall displays that realization of injection through porous insertion lets essentially to take off heat loading on the wall, what stimulates the effectiveness of this type of cooling. This conclusion is confirmed in physical experiments [4]. Thus, in carried out numerical analyses is substantiated the concept of the porous cooling of thermal stress places of the flow around elements of the objects of various destination. Whereat is marked local character of the actions of this type of cooling, not bringing to essential influence on the pattern of flow around the object.

This work is carried at financial support of RFFI under the project N96-01-00298.

REFERENCES

1. Epifanov V.M., Isaev S.A., Nosatov V.V.//Abstract of papers of Int.Symp.Heat Transfer Enhancement in Power Machinery (HTEPM' 95). M.: MSTU, 1995. V.2. P.151-152.

2. Isaev S.A., Nosatov V.V.,Sadovnikov G.S., et al. // The proceedings of III Minsk Inter. Forum "Heat and mass transfer-MIF-96": V.1, Convective heat and mass transfer, pt.1. Minsk: IHMT, 1996. P.105-108.

3. MacCormak R.V. // Airspace technics. 1983. V.1. N 4. P.114-123.

4. Holden M., Sweet S.// AIAA Paper. 1994. N2475. P. 1-24.

MAGNETIC FIELD EFFECT ON HEAT EXCHANGE AT THE BURNING SURFACE

I. G. BOROVSKOY, A.B. VOROZHTSOV

RESEARCH INSTITUTE OF APPLIED MATHEMATICS AND MECHANICS, TOMSK, RUSSIA

A laminar flow of a noncompressible conducting medium in a plane channel of height $2b$ exposed to a transverse uniform magnetic field is considered. The bottom and top walls of the channel are the burning surfaces of a solid propellant, the conducting lateral walls being shorted. The variation of channel height due to propellant consumption is ignored. The magnetic flux density vector in the Cartesian coordinates is $\mathbf{B} = (0, B_y, 0)$ and has one component in the flow zone, $B_y = const$. The value of electric current density $\mathbf{j}$, according to generalized Ohm's law, also has one component $j_z = \sigma u_x B_y$, with electric currents shorting to the lateral walls of the channel and the ponderomotive force vector opposing the flow $\mathbf{f} = (f_x, 0, 0)$, $f_x = -j_z B_y$.

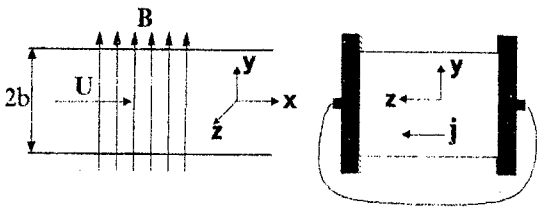

It follows from the solution of Hartman's problem for the considered flow in the absence of heat and mass exchange with the channel walls [1] that with other conditions being equal the increased magnetic induction of the external field leads to increased friction stress near the wall. Accepting the Reynolds assumption that the dynamic and thermal fields are similar for the given problem [2], one should expect certain intensification of the heat transfer to the channel walls. This in turn can increase the surface temperature and burning rate since usually for solid propellants valid is the exponential dependence of the mass burning rate m on the surface temperature θ_s at a constant pressure [3]

$$m(\theta_s) = m_k \exp(-e_k/\theta_s), \qquad (1)$$

where $\theta_s = T_s/T_g$ is the ratio of the propellant surface temperature T_s to the gas temperature T_g in the flow core, m_k and e_k are constants.

The approximate value of magnetogasodynamic effect on burning surface temperature is estimated from the heat balance

$$\alpha (T_g - T_s) = c_k m(\theta_s) (T_s - T_\infty), \qquad (2)$$

Dividing both sides of Eq. (2) by T_g and taking into account the Stanton number definition

$$St = \frac{\alpha}{c_p m_g},$$

where m_g is the mass gas velocity in the flow core, after transformations we have

$$St \frac{c_p m_g}{c_k m_k} \frac{1-\theta_s}{\theta_s - \theta_\infty} = exp(-e_k / \theta_s). \quad (3)$$

Equation (3) applies both to the case with applied magnetic field (in this case the parameters are marked with the index H) and to the case with the magnetic field absent (index o). To estimate the Stanton number in the presence of magnetic field we make use of the solution of Hartman's problem

$$w(Ha) = \frac{Ha^2}{3} \frac{th(Ha)}{Ha - th(Ha)}, \quad (4)$$

where $th(Ha)$ is the hyperbolic tangent of the Hartman number Ha.

Then, substituting the Reynolds analogy, which in terms of Eq. (4) has the form $St_H/St_o = w(Ha)$, into Eq. (3) we have the final equation

$$St_o' \; w(Ha) \frac{1-\theta_s}{\theta_s - \theta_\infty} = exp(-e_k/\theta_s), \quad (5)$$

where the Stanton number St_o' constitutes the heat exchange coefficient α_o in the absence of magnetic field, the constant m_k, and the specific heat coefficient of solid propellant c_k. This substitution is possible if the magnetic-field-induced changes in the mass velocity of combustion products in the flow core (unlike the mass burning rate) are neglected.

Figures 1 show the numerical solution of nonlinear equation (5) at the dimensionless parameter ranging within $e_k \in [0, 2]$. The ratios θ_s^H / θ_s^o and m_H/m_o are independent of the Stanton number St_o' and weakly depend on the temperature θ_∞. The results obtained suggest that with increasing Hartman's number the propellant surface temperature increment is 15 % (at $Ha < 20$), while the burning rate shows more than two-fold increase, which is accounted for by the exponential dependence (1).

The results presented are qualitative and are indicative of possible essential influence of external magnetic field on the combustion of solid propellants. The authors did not extend the range of Ha variation at $m_H/m_o >> 1$ since the intense efflux from channel walls would violate the assumptions accepted in the approximation of both laminar and turbulent boundary layers [2]. Hence, Eq. (4) used as the basis for the present analysis, could also be violated. Thus, a detailed investigation of the problem can be performed and quantitative results can be obtained only by the solution of the complete Navier-Stokes equations for a compressible gas, supplemented by equations for diffusion and magnetic induction as well as by the right sides responsible for the chemical reactions proceeding in the gas flow and at the burning surface.

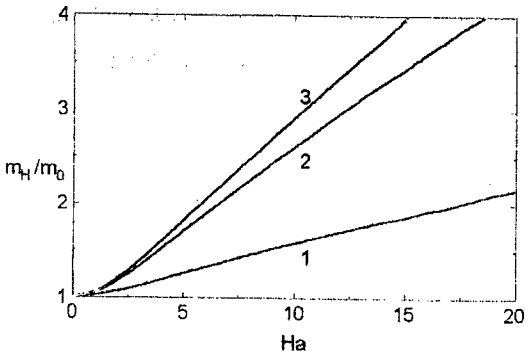

Fig. 1. Plots for dimensionless mass burning rate versus Ha and e_k. 1- e_k =0; 3-1.0; 5-2.0.

References

1. Loitsanskii, L. G., *Fluid and Gas Mechanics*, Nauka, Moscow, 1987.
2. Kutateladze, S. S., Leont'ev, A. I., *Heat and Mass Transfer and Friction in Turbulent Boundary Layer*, Energoatomizdat, Moscow, 1985.
3. Novozhilov, B. V., *Transient Combustion of Solid Propellants,* Nauka, Moscow, 1973.
4. Borovskoy I.G., Vorozhtsov A.B. *Magnetic Field Control of Burning Rate and Thrust in Solid Rocket Motors* // Jour.Prop.and Power, 1995, V.11, N.4, P.824-829.

42

THE EFFECT OF EXTERNAL ELECTRIC FIELD ON HEAT AND MASS TRANSFER CHARACTERISTICS IN THE POWER FACILITY COMBUSTION CHAMBER

YAGODNIKOV D.A., VORONETSKII A.V., PELEVIN F.V.

Bauman Moscow State Technical University

Experimental study results of the external electrical field (EEF) effect on operating process characteristics and heat and mass transfer peculiarities in a model porous-wall combustion chamber (CC) are given. It is found, that when a 900 V constant negative potential is applied to the CC the combustion products heat flow to CC wall is increased, and in case of a positive potential the heat flow is decreased. In both case, it was been established that ignition and combustion processes is intensified and blow-off velocity grows. The data obtained is explained by means of ionic wind coinciding in direction with positive ions movement. With negative voltage CC the ionic wind directed toward to chamber wall interacts with the wall boundary layer and determines a modification of its geometrical and thermophysical parameters.

MATHEMATICAL MODELLING OF TRANSITIONAL REGIMES FOR CONVERSION OF HIGH ASH BITUMINOUS COAL IN THE PRESSURISED CIRCULATING FLUIDIZED BED FACILITY

MAYSTRENKO A. Yu., PATSKOV V.P., TOPAL A.I.
Coal Energy Technology Center (CETC)
National Academy of Sciences of Ukraine
MINENERGO of Ukraine

The conversion (pyrolysis, combustion and gasification) of low grade high ash coals in the combined cycle units using pressurised circulating fluidized bed combustion (PCFBC) is one of the promising ways to increase the efficiency of combustion while decreasing NO_x and SO_x emissions [1].

As a part of activity aimed at implementation of new clean coal technologies, the Coal Energy Technology Center (CETC) is developing pilot-scale facility with coal consumption of 1 ton/hr to carry out investigation on conversion of bituminous coals at the PCFBC under pressure of up to 2.5 MPa and with high number of recirculation (more than 100) [1]. The main components of the facility being developed are: 1) pyrolyser with slowly movable bed of fuel at the return circuit of coke residue, 2) reactor, hydrodynamically separated at fluidized bed zone and freeboard space, to produce syn-gas, 3) cyclone-separator.

The mathematical models, algorithms and program for numerical analysis of transitional regimes of conversion process for polyfractional high ash coal in the above PCFBC facility are considered.

The mathematical model of pyrolyser is made using the fixed bed assumption. The interaction of two phases are considered, namely: solid phase, including porous coal particles, coke residue and ash, which are entered from above and gas phase, containing components of fuel pyrolysis, which are passed through bed from below. The fuel pyrolysis components consist of light gaseous products (CO_2, CO, H_2O, H_2, N_2, CH_4, C_2H_4, C_2H_6) and tar vapour as well as hydrocarbons of phase (evaporation-condensation) and chemical reactions inside the porous structure of coal particles [2]. The tar composition is modelled by seven key components: benzol, toluol, phenol, phenatren, undekan, dimetilnaphthaline and metiltetralin [3]. The mass and energy transfer over the bed is due to effective diffusion and heat conductivity, filtration and convective heat/mass transfer between fuel particles and ash inside

the free space of the bed. The effective diffusion and heat conductivity, convective and filtration transfer, primary extraction of vapour and volatile, tar and hydrocarbons phase transition (evaporation-condensation), secondary heterogeneous gasification reactions for coke residue with pyrolysis components are considered for porous coal particles. It is also taken into account the heating up of inert ash particles of bed.

The main assumptions made for the fluidized bed zone of the reactor producing syn-gas are as follows: non-stationary diffusive model that accounts for longitudinal effective diffusion and heat conductivity for solid phase transfer, gas component filtration, phase-to-phase heat/mass transfer, convective and radiative heat/mass transfer between fuel and inert ash particles and gas flow, near wall heat transfer, surface heterogeneous reactions of combustion/gasification of coke residue, homogeneous reaction for CO oxidation.

The transfer processes for bubble phase are described using non-stationary model of ideal forcing out that takes into account phase-to-phase heat/mass transfer and homogeneous reaction of CO oxidation.

The surface concentrations of gas components, temperature of coke and inert ash particles are calculated taking non-stationary model of ideal mixing that takes into account convective heat/mass transfer between particles and flow in gas phase, radiative heat transfer between particles and gas, surface reactions of fuel combustion/gasification.

The size distribution functions for solid particles are determined basing on non-stationary diffusive model that accounts for effective longitudinal diffusive and circulation of particles as well their change due to surface chemical conversion and carry over [4].

In the freeboard space of the reactor producing syn-gas, the upstream movement of polyfractional fuel coke surrounded by high temperature gas flow in the entrained flow regime is considered. The process models are based on theory of multi-rate penetrating phases and turbulent heterogeneous streams [5] in one and two dimension non-stationary statements. The surface heterogeneous reactions of combustion and gasification of coke residue, homogeneous reaction of CO oxidation, convective heat/mass transfer between phases, convective and radiative heat transfer between particles, flow and facility walls, turbulent transfer, gravitation forces, pressure drop, phase-to-phase friction, heating up of reactor walls are taken into account.

The models of transfer processes in the cyclone are based on Lagrange trajectory theory of particle movement inside the twisted gas flow and Eiler assumption on gas.

The balance boundary conditions which bind proposed assumptions into the whole mathematical description of the process in the facility are formulated.

The iterative algorithms of process calculation (like Zeidel method) for each components of the facility are developed.

The solution of the equations describing the pyrolyser process is provided by double-sweep method. An special feature of the algorithm is an additional assumption for the system about thermodynamic balance between gas and condensed phase inside the pores of coal particles, that is necessary for iterative estimation of phase transition rates of liquid tars and hydrocarbons [2].

The systems of equations for solid phase of fluidized bed and for size distribution functions are solved by double-sweep methods, as to bubble phase and single particles - like relaxation method for solving of systems of hyperbolic differential equations.

The systems of equations for the freeboard space and the cyclone, when one dimension statement is used, are solved the same manner. To solve two dimension tasks, the longitudinal-cross double-sweep method is used [5].

The method of automatic choice of time step provided by Richardson extrapolation is used for each algorithms.

The program to calculate process parameters for the facility is made using Fortran-77 (v.1.0 for Wiindows)

References

1. Maystrenko A.Yu., Dudnik A.N., Yatskevich S.V. Coal gasification technologies for combined cycle power plants. Kyiv: Znanie, p.68
2. Patskov V.P., // XIII Int.Conf.on Chem.React. Novosibirsk: IK SO RAN,1996 pp.251-257
3. Khalinenko R.A., Levicky A.A., Pollak L.S. et al // Kinetic and catalysis. 1985 v. XXV. issue 6. pp. 1336-1343
4. Patskov V.P., Korchevoy Yu.P., Maystrenko A.Yu. // Chem.phys. proc.for comb.and expl. Chernogolovka: IHF RAN, 1996.- v.1, ch.1, pp.138-140
5. Patskov V.P., Kulchicky I.V. // Test method math.model.in boiler tech.: abstract. conf: Krasnoyarsk: SIBVTI, 1996. pp. 50-52

GAS DYNAMIC EXPERIMENTAL DATA BASE OF SURFACE GROUND STRENGTHS

Vasin V.A., Sannikov K.A.
198005, Russia, St.-Petersburg, Baltic State Technical University,

The data accrued in data base (DB) are used as training and examining sampling at execution prognosticate of accounts on erosion of surface ground strengths.The necessary volumes of experimental data are accumulated by statement of special laboratory experiments on physical models.The unique data on erosion of surface ground strengths in conditions are used as the basic points for checks of accuracy of statistical models, constructed on results laboratory model of tests. The opportunity of direct valuation of parameters crater by direct carry given model of experiment on nature the object is provided.

The gas dynamic experimental data base of surface ground strengths represents the managing programme and information environment, ensuring in regime of interactive dialogue with personal computer (PC):

- management and accumulation of base of experimental data;
- fast search of necessary information;
- updating of structure DB;
- initial formation for correlation, regression and variance of analysis;
- prognosis the accounts of sizes crater;
- documenting of results.

The data composition.

Accrued in supervision bank for erosion by processes in surface ground strengths the information is directed on use of her in quality of training sample of statistical models given at set-up for forecasting of sizes forming in ground crater. The statistical uniformity is reached criterion by form of representation of data. Quality of determining criteria of similarity, forming structure of data, nominates the criteria, pursuant to which the gears of formation crater act. The most representative by criteria of similarity for processes considered here the numbers Maha and Fruda are considered. Because of inconsistency of requirements to structures size invariant of similarity, propound by these criteria, kind of data, accommodate in bank, is defined alternatively on some of one of mentioned criteria.

At use in quality of determining criterion of similarity of number Maha, table of supervision is made following unsizing parameters and sizing invariant of similarity:

Characteristic gas dynamic level of load:

- impulse, on unit of working volume nozzle $J' = J / d^3$, $H\ s/m^3$; - average traction, on unit of working area of target section traction $P'=P/d^2, N/m^2$; - traction armament of product $T=gm/p$; - the relative distance from null level traction to ground $y'=y/d$; - unsizing the time of effect of jet on ground (number Struhal) $t' = t \cdot v / y$;

The physical-mechanical properties of ground:

- indication dynamic densitometer $C_{уд}$, quantity of impacts / the depth of immersing; - humidity w, %; - pore e; - density ρ; - pressure σ, N/m^2; - module E, N/m^2;

The sizes crater:

- relative diameter D / d; - relative depth H / d.

At use in quality of determining criterion of similarity of number Fruda in table of supervision unsizing the parameters remain the same, that and in previous item. Sizing invariant of similarity present to base object on formulas:

$$J' = J \cdot \frac{K_L}{d^3}; \quad P' = P \cdot \frac{K_L}{d^2}; \quad \sigma' = \sigma \cdot K_L; \quad E' = E \cdot K_L,$$

Where $K_L = d_H / d_M$- the scale factor (factor of reduction); d_H, d_M - diameters of target section of nozzle of base and observable objects; J', P', σ', E' - adduced pecific pulse, specific traction, pressure of ground and its module.

The base object nominates the most the characteristic object from considered class. At placing in bank the data informations, received by laboratory tests of physical models, as such object is used prototype of model.

The data are adduced in natural kind. Transformed to mentioned above by way in criterion form, these data are united with other data, received in other operational conditions. Thus the statistical uniformity of incorporated data is preserved, and training sample becomes more representative one.

The increase of reliability prognosis valuations of sizes crater at simultaneous decrease of operational restrictions on possible area their distributions can be achieved by updating DB by new data, received on ground platforms with other properties, at other constructive - composite and traction characteristics booster.

The structure of DB.

DB is executed in kind of user interface, is constructed on system of multilevel menu. DB is written on language Clipper5.1. The data are placed on groups:

– supervision for model by start-up, classified on types of ground, criteria, scales of simulation and prototypein natural measurement of parameters;

– supervision for natural by start-up, classified on objects in natural measurement of parameters;

– supervision for start-up in criterion kind.

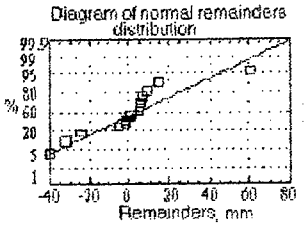

Fig.1

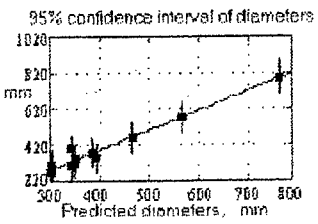

Fig.2

On fig. 1 and 2 the results of statistical processing of tests on gas dynamic base of surface gritty strengths are submitted. The volume of tests has made about 40 experience. The analysis of accuracy and adequacy of model is conducted. The schedule on fig. 1 is constructed on "paper probability value", ropriate to normal law of distribution. The remainders arrange on direct line, that peaks about weak interrelation between remainders, i.e. about their casual character. Fig. 2 illustrates the examples of arrangement settlement craters on attitude to nature to objects for gritty ground of various humidity, pore and density. The analysis of accuracy and adequacy of statistical model is conducted. On fig. 2 by vertical strokes the 95 % the confidence intervals for settlement significances of diameters craters are shown.

Section 3
TWO-PHASE FLOWS

50

NUMERICAL INVESTIGATION OF TURBULENT TWO-PHASE FLOW IN THE CHANNEL WITH POROUS WALLS

EMELYANOV V.N., VOLKOV K.N.

Baltic State Technical University

The sections of gaseous highways with penetrable walls are one of most encountered hydrodynamic compound units of thermal and power devices. The flow in the channel with distributed gas blowing is a model of flow solid propellant combustion products in the gap maked up wall of combustion chamber and burning surface cartridge.

Turbulent flow with the suspended particles has been simulated on the basis of averaged equation systems of interpenetrating continuum mechanics, turbulent viscosity conception and equations of two-parameter dissipative turbulence model. Correlative moments and additional source terms ε_p and Φ_p associated with dispersed phase have been calculated out of spatial and temporal averaging method [1] in local and uniform approximation. Iterphase iteraction have been defined with the drag force according to Stokes formula. Admixture particles are rigid undeformed spheres of equal diameters. Thermal and physical properties of phases have been assumed permanent values. The frame of reference has selected so that axis x coinsides with the channel centerline and axis y has directed perpendicularly it. Positive reference of lateral component has been conducted to the side contrary of blowing direction.

The simulation of two-phase turbulent flow in the channel with porous walls has been developed in the framework of calculation general conception of accelerating gas-particle flows proposed by the authors [1, 2]. Let us introduce dimensionless coordinates $\xi = x / r_w$, $\eta = y / r_w$ and shall seek the solution in the form

$$\rho_g u_g y^\chi = \rho_w v_w \xi U_g(\eta) r_w^\chi, \quad \rho_g v_g y^\chi = -\rho_w v_w V_g(\eta) r_w^\chi, \quad \vartheta_g = \vartheta_w T_g(\eta),$$

$$\rho_p u_p y^\chi = \rho_w v_w \xi U_p(\eta) r_w^\chi, \quad \rho_p v_p y^\chi = -\rho_w v_w V_p(\eta) r_w^\chi, \quad \vartheta_p = \vartheta_w T_p(\eta),$$

$$k = v_w^2 K(\eta), \quad \varepsilon = v_w^3 E(\eta) / r_w,$$

where r_w — half width of channel, v_w — blowing rate, $\chi = 0$ for planar flow and $\chi = 1$ for axially symmetric flow.

Then, neglecting with the terms of multiplicity of a ξ^2, the turbulent two-phase flow calculation in the duct with distributed gas blowing has been reduced to the solution of boundary problem for nonlinear ordinary differential equations

$$U_g - V_g' = 0;$$

$$(U_g U_g)' - (V_g U_g')' = \left[\left(\frac{1}{\mathrm{Re}} + c_\mu \frac{K^2}{E}\right) U_g'\right]'' - f_1 \varkappa_p \left(U_g' - U_p'\right);$$

$$(U_g T_g) - (V_g T_g)' = \left[\left(\frac{1}{\mathrm{Pr}} + \frac{c_\mu}{\mathrm{Pr}_t} \frac{K^2}{E}\right) T_g'\right]' + f_2 \varkappa_p \vartheta \left(T_g - T_p\right);$$

$$U_p - V_p' = 0;$$

$$(U_p U_p) - (V_p U_p)' = f_1 \left(U_g - U_p\right) + \left(\mathcal{F}_{12}^2 c_\mu \frac{K^2}{E} U_g'\right)';$$

$$(U_p T_p) - (V_p T_p)' = f_2 \left(T_g - T_p\right) + \left(\mathcal{F}_{22}^3 \frac{c_\mu}{\mathrm{Pr}_t} \frac{K^2}{E} T_g'\right)'.$$

$$(U_g K_g) - (V_g K)' = \left[\left(\frac{1}{\mathrm{Re}} + \frac{c_\mu}{\sigma_k} \frac{K^2}{E}\right) K'\right]' + P - E - E_p;$$

$$(U_g E) - (V_g E)' = \left[\left(\frac{1}{\mathrm{Re}} + \frac{c_\mu}{\sigma_\varepsilon} \frac{K^2}{E}\right) E'\right]' + \frac{E}{K} \left(c_{\varepsilon 1} P - c_{\varepsilon 2} E\right) - \Psi_p;$$

where

$$f_1 = 1/\mathrm{Sk}_D, \quad f_2 = 1/\mathrm{Sk}_T, \quad E_p = r\varepsilon_p / v_w^3, \quad \Psi_p = r^2 \Phi_p / v_w^4.$$

Mathematical formulation of the problem has been completed with the representation of boundary conditions at the centerline and channel walls. The boundary conditions for averaged flow properties under the $\eta = 1$ have been determined by means of assignment of wall's temperature, no-slip condition for longitudinal component velosity and normal blowing predicate

to the channel walls for lateral velosity component of the carry phase. The symmetry flow conditions have been supposed under the $\eta = 0$.

The obtained distributions of turbulence kinetic energy and energy dissipation rate have been used for statistical simulation of particles motion trajectories in the stochastic and inhomogeneous medium.

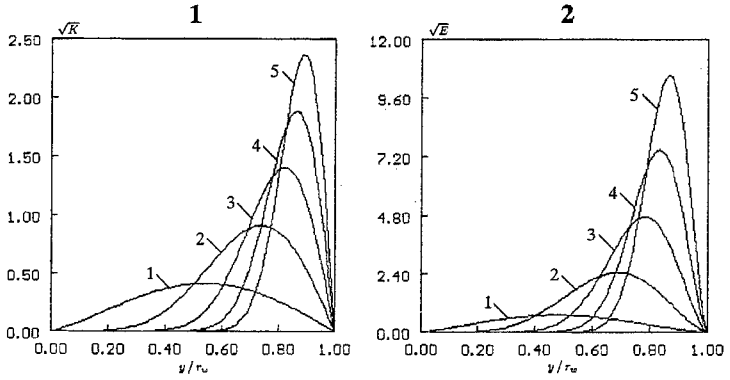

Distributions of turbulence kinetic energy (**1**) and energy dissipation rate (**2**) at the various cross-section of the channel with porous walls. The lines correspond to the following values $\xi =$ 5 (1); 10 (2); 15 (3); 20 (4); 25 (5).

Turbulent structure formation and particle-phase flow patterns in channels are studied depending on size and volume fraction of particles. The obtained results are most efficiently can be used for solution of applied problems and for recommendation establishment according to practical implementation of optimal operating conditions of intra-chamber processes in the rocket solid propellant motors and power devices. Developed models are the base for investigations of turbulent transfer processes in the domains with more complicated geometry.

References

1. Shraiber A.A., Yatsenko V.P., Gavin L.B., Naumov V.A. Turbulent flows in gas suspensions. — New York: Hemisphere publishing corporation, 1990. — 248 p.

2. Volkov K.N., Emelyanov V.N. Numerical investigation of turbulent two-phase flow near the stagnation point. // Intra-chamber processes, combustion and gas dynamics of dispersed systems. — S.-Petersburg: BSTU, 1995. — pp. 87–89.

3. Emelyanov V.N., Volkov K.N. Effects of turbulence and heterogeneity on heat transfer in accelerating flows. // III Minsk International Heat and Mass Transfer Forum. — Minsk: HMTI, 1996. — pp. 103–104.

TWO–PHASE GAS–SOLID FLOW AROUND A CYLINDER: EFFECTS OF PARTICLE SIZE DISTRIBUTION AND PARTICLE–PARTICLE COLLISIONS

A.N. VOLKOV, YU.M. TSIRKUNOV
Baltic State Technical University, 198005 St. Petersburg, Russia

In computational models of gas–solid particle flows particles are usually assumed to have an equal size. At the same time there is always a particle size distribution, and a particle radius can vary in a rather wide range.

The kinetic model and the DSMC method were proposed in papers [1,2] for the simulation of mono–sized particle phase motion in transient flow regime on the Knudsen number in the pseudogas of particles. The DSMC method is similar to the one in rarefied gas dynamics. It can be extended rather simply to the case of different particle sizes in the dispersed medium. The aim of the present work is to study how the particle size distribution influence the dispersed phase flow field and the action of particles on the streamlined surface. The cross–flow of a dilute gas–particle mixture around a circular cylinder is considered as an example.

The particle size distribution can be described by the particle concentration distribution function in a particle radius r_p. It is often convenient to deal with the particle volume concentration α_p ($\alpha_\mathrm{p} g^\circ(r_\mathrm{p})\mathrm{d}r_\mathrm{p}$ is the volume concentration of particles with a radius from r_p to $r_\mathrm{p}+\mathrm{d}r_\mathrm{p}$) [3]. For the DSMC simulation the distribution function $g^\circ_\infty(r_\mathrm{p})$ at the entrance boundary of the calculational domain must be given (the entrance boundary is located in an undisturbed flow). A random radius r_p of each new particle flying into the calculational domain is sampled from the distribution function $f^\circ_\infty(r_\mathrm{p})$ of the number particle density $n_{\mathrm{p}\infty}$ ($f^\circ_\infty(r_\mathrm{p}) = r_\mathrm{p}^{-3} g^\circ_\infty(r_\mathrm{p}) / \int r_\mathrm{p}^{-3} g^\circ_\infty(r_\mathrm{p})\mathrm{d}r_\mathrm{p}$). The particle phase macroparameters, such as the volume concentration α_p in an arbitrary point in the flow and the energy flux E_w from particle phase to a body surface are determined from the integrals taken over translational and rotational velocities and over radiuses r_p of particles

$$\alpha_\mathrm{p}(\boldsymbol{r}) = \frac{1}{\rho^\circ_\mathrm{p}} \int m_\mathrm{p} f(\boldsymbol{r}, \boldsymbol{z}_\mathrm{p}) \mathrm{d}\boldsymbol{z}_\mathrm{p}, \quad E_\mathrm{w}(\boldsymbol{r}_\mathrm{w}) = \int\limits_{\boldsymbol{v}^-_\mathrm{p}\cdot\boldsymbol{n}_\mathrm{w}<0} \Delta E_\mathrm{p} |\boldsymbol{v}^-_\mathrm{p} \cdot \boldsymbol{n}_\mathrm{w}| f(\boldsymbol{r}_\mathrm{w}, \boldsymbol{z}^-_\mathrm{p}) \mathrm{d}\boldsymbol{z}^-_\mathrm{p}. \quad (1)$$

Here $\boldsymbol{r}$ is a radius–vector of a point in the physical space, $\boldsymbol{r}_\mathrm{w}$ a radius–vector of a point on the body surface, ρ°_p and m_p the material density and the mass of a particle; $\boldsymbol{z}_\mathrm{p} = (\boldsymbol{y}_\mathrm{p}, r_\mathrm{p})$, $\boldsymbol{y}_\mathrm{p} = (\boldsymbol{v}_\mathrm{p}, \boldsymbol{\omega}_\mathrm{p})$; $f(\boldsymbol{r}, \boldsymbol{z}_\mathrm{p})$ is the distribution of particles in velocities, radiuses and locations in the physical space ($\int f(\boldsymbol{r}, \boldsymbol{z}_\mathrm{p})\mathrm{d}\boldsymbol{z}_\mathrm{p} = n_\mathrm{p}(\boldsymbol{r})$ is the number particle density at the point with the radius–vector $\boldsymbol{r}$,

$\int f(\boldsymbol{r}, \boldsymbol{z}_\mathrm{p})\mathrm{d}\boldsymbol{y}_\mathrm{p} = n_\mathrm{p}(\boldsymbol{r})f^\circ(\boldsymbol{r}, r_\mathrm{p}))$, $\boldsymbol{n}_\mathrm{w}$ is the outer surface unit normal at the point with the radius–vector $\boldsymbol{r}_\mathrm{w}$; $\Delta E_\mathrm{p} = E_\mathrm{p}(\boldsymbol{z}_\mathrm{p}^-) - E_\mathrm{p}(\boldsymbol{z}_\mathrm{p}^+)$, E_p is the kinetic energy of a particle, $\boldsymbol{z}_\mathrm{p}^-$ и $\boldsymbol{z}_\mathrm{p}^+ = \boldsymbol{z}_\mathrm{p}^+(\boldsymbol{z}_\mathrm{p}^-, \boldsymbol{n}_\mathrm{w})$ are parameters of a particle before and after its rebound from a surface at the point with the radius–vector $\boldsymbol{r}_\mathrm{w}$. E_w in (1) is one of the key parameters in the process of abrasive erosion of a body in the gas–particle flow.

In the present study the log-normal law is accepted for the particle distribution in an undisturbed flow [3]

$$g_\infty^\circ(r_\mathrm{p}) = \frac{1}{\sqrt{2\pi} r_\mathrm{p} \ln\sigma} \exp\left[-\left(\frac{\ln r_\mathrm{p} - \ln r_m}{\sqrt{2}\ln\sigma}\right)^2\right]. \qquad (2)$$

When calculating the motion of particles, the aerodynamic force, the Magnus force and the damping torque are taken into account as it was done in [1, 2]. The influence of the particle phase on the carrier gas flow is assumed to be negligible. The semiempirical impact model proposed in [4] is used to determine parameters of a particle just after its rebound from a body surface. Hydrodynamic interaction between particles are not taken into account. Velocities of two particles after their binary collision are calculated from the classical impact theory for undeformable rotating spheres with the use of two restitution ratios a_{rn} and a_{rt} for the normal and tangential components of the contact point velocity [5]. Kinetic energy losses of colliding particles depend on the values of a_{rn} and a_{rt}.

Motion of particles of synthetic corundum in the potential incompressible flow of the carrier gas (air) around a cylinder of mild steel is studied numerically. The governing parameters have the following values: $a_{rn} = 0.5$, $a_{rt} = 0.9$, $\rho_\mathrm{p}^\circ = 3950$ kg/m^3, $v_\infty = 100$ m/s, $\rho_\infty^\circ = 1.197$ kg/m^3, $\mu_\infty = 1.71 \cdot 10^{-5}$ kg/(m·s), radius of a cylinder has been taken equal to 1 m. The particle volume concentration $\alpha_{\mathrm{p}\infty}$, the most probable particle radius in an undisturbed flow $\bar{r}_\mathrm{p} = r_m \exp\left[-\ln^2\sigma\right]$ and the parameter σ in the formula (2) are varied. The last parameter describes the particle size dispersion in an undisturbed flow $\mathbf{D}r_\mathrm{p} = \bar{r}_\mathrm{p}^2 \exp[3\ln^2\sigma]\left(\exp[\ln^2\sigma] - 1\right)$.

In the numerical simulations the truncated distribution function $\hat{g}_\infty^\circ(r_\mathrm{p})$ approximating $g_\infty^\circ(r_\mathrm{p})$ with high accuracy is used ($\hat{g}_\infty^\circ(r_\mathrm{p}) = g_\infty^\circ(r_\mathrm{p})/C$, where $C = \int_{r_{\min}}^{r_{\max}} g_\infty^\circ(r_\mathrm{p})\mathrm{d}r_\mathrm{p}$, $r_\mathrm{p} \in [r_{\min}, r_{\max}]$). Boundary values $r_{\max}$ and $r_{\min}$ have been determined from the conditions: $g_\infty^\circ(r_{\max})$ and $g_\infty^\circ(r_{\min}) \le 0.01 g_\infty^\circ(\bar{r}_\mathrm{p}), C \ge 0.99$. In all calculations $r_{\max}$ and $r_{\min}$ satisfy the following inequalities: $r_{\min} \ge 1$ μm и $r_{\max} \le 250$ μm.

The scheme of the algorithm and the parameters of the numerical method (size of a mesh cell, a number of modelling particles, *etc.*) are given in [2].

The particle volume concentration distribution along the axis of symmetry depending on σ is shown in figure 1,*a*. These results refer to the case of

infinitely small particle concentration in the undisturbed flow when particle–particle collisions are negligible. One can see that the distribution changes strongly when particle size dispersion increases (σ changes from 1 to 1.2^3). Peaks usually observed in the case of mono–sized particles, first become smooth and then disappear at all. Conversly, the particle size dispersion plays no role in distribution of macroparameters (1) along the body shape (curves 1–3 in the figure 2 practically coincide).

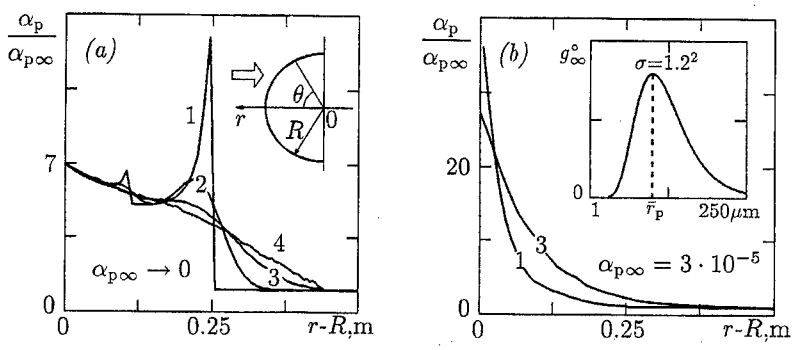

Figure 1. Distribution of the relative particle concentration $\alpha_p/\alpha_{p\infty}$ along stagnation streamline $\theta = 0$ in the flow around a cylinder. $\bar{r}_p = 100$ μm; (*a*) collisionless particle phase motion, (*b*) particle phase motion with particle-particle collisions. Curve 1, $\sigma = 1$ (monodisperse particles); 2, $\sigma = 1.2$; 3, $\sigma = 1.2^2$; 4, $\sigma = 1.2^3$.

Opposite situation takes place when particle–particle collisions are essential. In this case the particle flow field structure does not change qualitatively when the particle size dispersion is varied in the wide range (see fig. 1,*b*). But the particle concentration distribution along the body shape and the distribution of the dispersed phase energy flux to the surface change noticeably (see curves 4–6 in the figure 2). It should be noted that the role of particle–particle collisions in forming of particle–phase flow structure decreases with increasing of σ. In particular, the distributions of both, the particle concentration and the particle energy flux to the surface along the cylinder contour, calculated at $\sigma = 1.2^2$ are closer than at $\sigma = 1.2$ to those obtained for the collisionless particle phase model.

The same results are obtained for the other values of $\bar{r}_p$ (for $\bar{r}_p = 25\mu$m and 50μm).

Thus, even rather large dispersion of a particle size $\hat{\mathbf{D}}r_p$ calculated for the truncated distribution $\hat{g}^\circ_\infty(r_p)$, results in the change of macroparameters (1) at the front surface of a cylinder only in $10 \div 20\%$ compared with those in the flow of mono–sized particles of radius $\bar{r}_p$. Therefore, force and erosive

effects of the particle phase on a blunt body are expected to depend on $\hat{\mathbf{D}}r_\mathrm{p}$ slightly enough.

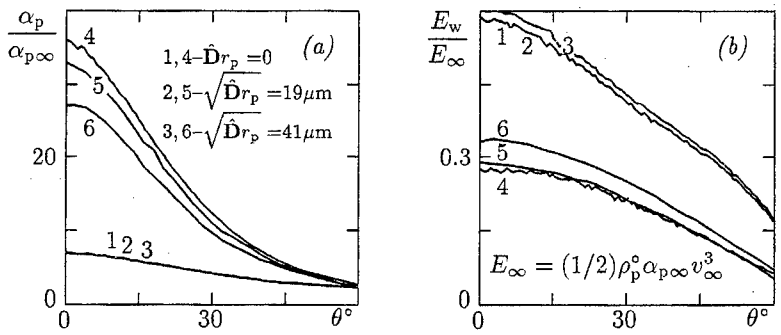

Figure 2. Distribution of the relative particle concentration $\alpha_\mathrm{p}/\alpha_{\mathrm{p}\infty}$ and the relative particle energy flux to the surface E_w/E_∞ along the cylinder contour. $\bar{r}_\mathrm{p} = 100$ μm; curves 1–3, $\alpha_{\mathrm{p}\infty} \to 0$ (collisionless particle phase motion); 4–6, $\alpha_{\mathrm{p}\infty} = 3 \cdot 10^{-5}$ (particle phase motion with particle-particle collisions); 1, 4, $\sigma = 1$ (monodisperse particles); 2, 5, $\sigma = 1.2$; 3, 6, $\sigma = 1.2^2$. $\hat{\mathbf{D}}r_\mathrm{p}$ is the dispersion of the truncated distribution function $\hat{g}^\circ_\infty(r_\mathrm{p})$.

This study was supported financially partly by the Russian Foundation for Basic Research (grant No. 96-01-01467) and partly by the St. Petersburg University Competitive Centre of Basic Natural Sciences (grant No. 95-0-4.2-5).

REFERENCES

1. Volkov, A.N. and Tsirkunov, Yu.M. *Proc. Int. School on Models in Continuum Mechanics, St. Petersburg, June 27 – July 3, 1995.* St. Petersburg University Press, pp. 133–140, (1996) (in Russian).

2. Volkov, A. and Tsirkunov, Yu. *Proc. Third ECCOMAS Computational Fluid Dynamics Conf., 9-13 September 1996, Paris, France.* Wiley, pp. 662-668, (1996).

3. Kouzov, P.A. Fundamentals of Disperse Analysis of Industry Dusts and Granular Materials. Khimiya Press, Moscow, 1987 (in Russian).

4. Tsirkunov, Yu.M., Panfilov, S.V. and Klychnikov, M.B. *Journal of Engineering Physics and Thermophysics*, Vol. 67, Nos. 5–6, pp. 1018–1025, (1994) (English translation).

5. Babukha, L.G. and Shraiber, A.A. Particle–particle interaction in two–phase flows with a particle size distribution. Naukova Dumka Press, Kiev, 1972 (in Russian).

NUMERICAL SIMULATION OF REFLECTION OF SOLID PARTICLES FROM THE ROUGH SURFACE IN TWO-PHASE FLOW

S.V. PANFILOV, YU.M. TSIRKUNOV
Baltic State Technical University, 198005 St. Petersburg, Russia

In two-phase gas–solid flow around the bounding rigid surface coarse-grained particles collide with the surface and rebound from it. Reflected particles can essentially influence the two-phase flow structure near the surface. The motion of reflected individual particles is largely determined by their rebound parameters which depend, first of all, on the particle collision velocity and the particle collision angle given by particle trajectory inclination, as well as on the physical and mechanical properties of the particle and surface materials [1,2]. At the same time the appreciable dispersion of parameters of reflected particles is always observed in experimental studies [1]. The reasons of this phenomenon are random in nature. Among them are particle size distribution in real gas–particle mixtures, possible rotation of particles, deviation of a particle shape from a sphere, as well as surface roughness.

Up to now there are no sufficient detailed experimental data to develop mathematical models of particle–wall collisions taking account of all factors named above. In this connection the analysis of every separate factor is of significant interest, because it allows to formulate and investigate assumptions which then can be used in more complete physical and numerical models, taking into account all important features of the collision process.

At present the two sufficiently developed semiempirical models of a spherical particle collision with the smooth wall are known [3,4]. They are based on the momentum and the angular momentum equations for a particle and contain two experimental coefficients.

In the paper [3] the model of irregular particle reflection from the surface with stochastic roughness profile was also proposed. A local collision angle was represented as a sum of the regular collision angle α_1 between the particle collision velocity vector and the smooth surface, and the inclination γ arising due to surface roughness. The roughness profile was not considered by itself and γ was assumed to be a random value with a Gaussian distribution with a mean value of 0° and a given standard deviation of $\Delta\gamma$. Under a suitable value of $\Delta\gamma$ this model gave very good agreement between numerical simulations and experiments in two examples, namely on distributions of the normal velocity restitution ratio for particle reflection from a target, and on profiles of particles' velocity fluctuations along the flow direction in the plane channel two–phase turbulent flow.

Nevertheless the model of irregular reflection [3] calls for further analysis and justification. First, the point is that the distribution function of random angle γ depends in fact on α_1 for the given roughness profile, and therefore it must be related with both the roughness profile and the regular collision angle α_1. However, the question of how to determine this relation has been only touched on in [3] and remains open. Besides, the particle rebound angle distribution depends not only on the distribution of local collision angles $\alpha_1 + \gamma$, but also on the kinematics of the reflection process (for example, on the possibility of multiple collisions within one hollow) that can not be taken into account in the model [3].

The purpose of the present work is the numerical simulation of the particle reflection angle distribution functions for two types of the roughness profile, periodic (sine–shaped) and stochastic, and for different values of the regular collision angle α_1.

The roughness profile and the particle motion were supposed to be two–dimensional and the particle shape to be spherical. The characteristic scales of roughness profiles (the amplitude and the period of sinusoid or the roughness depth and the mean cycle of roughness) were given from the ranges mentioned in [3]. The stochastic roughness profile $y(x)$ was simulated as a cubic spline drawn through N points with coordinates (x_i, y_i), that were determined as follows: $x_1 = 0$, $x_i = x_{i-1} + h/2 + \xi$, $(i = 2, 3, \ldots, N)$; $y_i = \eta$, $(i = 1, 2, \ldots, N)$, where the step h was equal to the mean cycle of roughness, and random values ξ and η were sampled from the Gaussian distribution with a mean value of zero. Standard deviations $\Delta\xi$ and $\Delta\eta$ can be determined from measurements of real roughness profiles. Typical values of the governing parameters were taken as follows: $N = 50$, $h = 100\mu$m, $\Delta\xi = 5\mu$m and $\Delta\eta = 3\mu$m. In the computational simulation of the distribution of particle reflection angles α_2 for each considered value of α_1 a number of particle–wall collisions was taken equal to 7500 for the sinusoidal roughness and about 10000 for the stochastic one. In calculations the presence of "shady" zones on the profile which particles can not fall into at the sufficiently small value of α_1 and the possibility of multiple particle–surface collisions within a roughness hollow were taken into account. The semiempirical particle–wall collision model [4] was used to determine the particle parameters after every single rebound. The particle radius was varied within the range $r_p = 5 \div 50\mu$m and the particle collision velocity was taken equal to 100m/s.

Typical patterns of the considered roughness profiles and the corresponding particle scattering indicatrixes, i.e. the reflection angle distributions in polar coordinates, are shown (for $r_p = 5\mu$m) in the figure.

For the sinusoidal profile there are two dominant directions of particle reflection. The similar profile was considered earlier in [5]. It should be noted, however, that the model [5] for particle reflections from a sine–shaped surface in the case of sufficiently small α_1 is invalid because the local surface inclination angle was determined in [5] from the profile equation

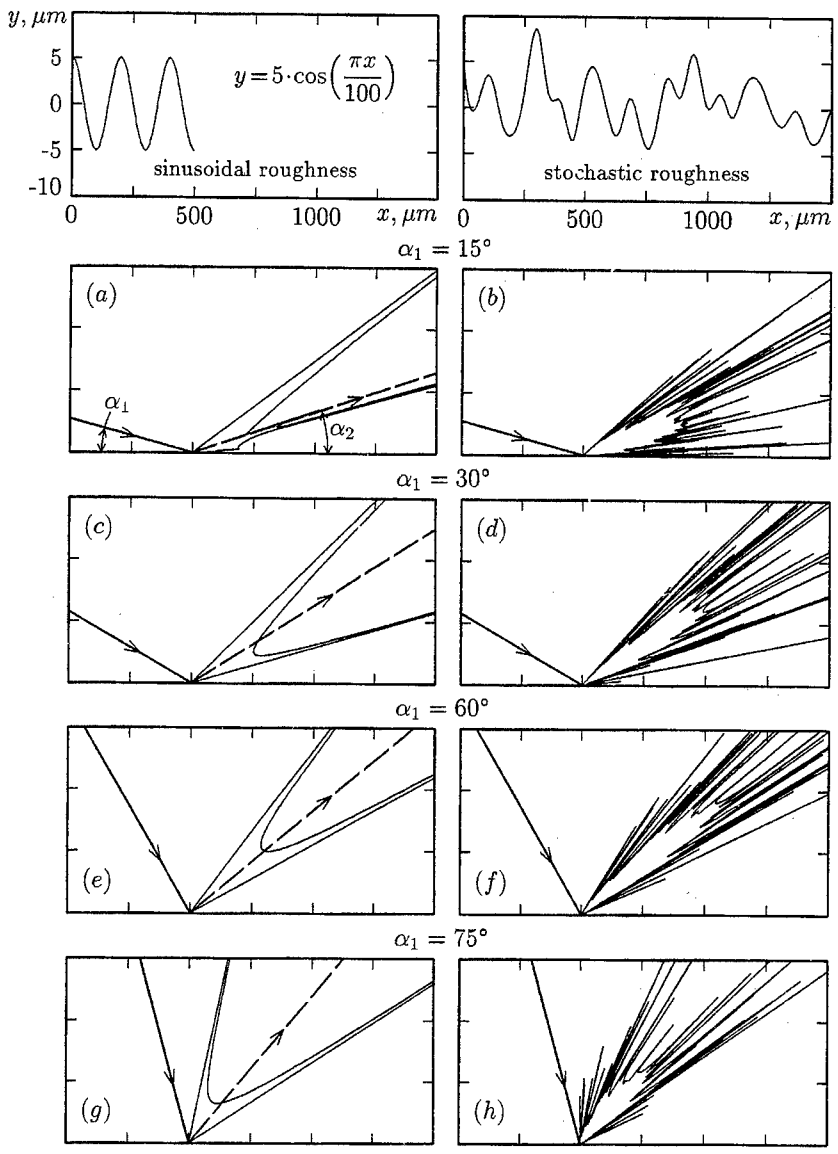

Scattering indicatrixes of particles reflected from the surface with sinusoidal (a, c, e, g) and stochastic (b, d, f, h) roughness; — — —, regular reflection of particles from the smooth surface.

$y = a\sin(2\pi x/L+\varphi)$, where the random phase φ was considered as distributed uniformly in the range $[0, 2\pi]$. Such distribution of φ is accurate only at $\alpha_1 = 90°$ but the distribution of φ differs significantly from the uniform one when α_1 is small.

It is seen from the figure that the configuration of particle scattering indicatrixes for the stochastic roughness differs qualitatively from the case of the periodic one. In spite of multiple outliers, the distribution tends to become monomodal which, possibly, can be obtained with significant increasing of the surface length (with increasing of N). But a mean value of the particle reflection angle distribution will differ from the regular angle α_2, at least for small α_1 (see the figure).

This study was carried out due to the financial support of the Russian Foundation for Basic Research (grant № 96-01-01467) and the St. Petersburg University Competitive Centre on Basic Natural Sciences (grant № 95-0-4.2-5).

REFERENCES

1. Tabakoff, W., Malak, M.F. and Hamed, A. Laser measurements of solid–particle rebound parameters impacting on 2024 Aluminium and 6A1–4V Titanium alloys. *AIAA Journal*, Vol. 25, № 5, pp. 721–726, (1987).

2. Lashkov, V.A. On experimental determination of the velocity restitution ratios of particles reflected from a surface in gas-particle flows. *Inzhenerno–Fizicheskii Zhurnal*, Vol. 60, № 2, pp. 197–203, (1991). (in Russian).

3. Sommerfeld, M. Modelling of particle–wall collisions in confined gas–particle flows. *Int. J. Multiphase Flow*, Vol. 18, № 6, pp. 905–926, (1992).

4. Tsirkunov, Yu.M., Panfilov, S.V. and Klychnikov, M.B. Semiempirical model of impact interaction of a disperse impurity particle with a surface in a gas suspension flow. *Journal of Engineering Physics and Thermophysics*, Vol. 67, Nos 5-6, pp. 1018–1025, (1994). (English translation).

5. Matsumoto, S. and Saito, S. Monte Carlo simulation of horizontal pneumatic conveying based on the rough wall model. *J. Chem. Engng. Japan*, Vol. 3, pp. 223–230, (1970).

MODEL OF PROBE PARTICLES IN APPLYING TO GAS-PARTICLE FLOW COMPUTATIONS.

D. K. ZAITSEV
St.Petersburg State Technical University

Gas-particle flows are found in many industrial applications such as cyclone separators and classifiers, pneumatic transport of powder, droplet and coal combustion systems, spray drying and cooling, sandblasting and so on. Such flows are usually characterised by considerable coupling between phases. For instance, when a spray is injected into a hot gas stream, one observes thermal coupling through heat transfer to the droplets, momentum coupling through aerodynamic drag responsible for droplet motion, and mass coupling through evaporation.

Two basic approaches are successfully used to model behaviour of discreet phase in such flows: Lagrangian and Eulerian. In the Eulerian approach, a "gas" of particles is introduced and both phases are treated as separate interpenetrating continua, each one with its specific density, velocity, temperature, etc. The governing equations with phase coupling terms are solved mutually for all phases (components). Probably the weakest point of this approach is the necessity of specifying effective transport coefficients for the "gas" of particles in turbulent carrier flow; all the developed closure models need some experimental fitting for the particular flow type considered. Many artificial assumptions have to be introduced in respect of the effect of particles on the carrier flow turbulence. One more disadvantage of the Eulerian treatment of dispersed phase concerns modelling the particles-boundary interaction; in fact, the boundary conditions required by the governing equations do not correspond to the physics of the phenomenon.

The Lagrangian approach is known to be less efficient while computations but more physically correct and simple in implementation than the Eulerian one. In this approach, a lot of probe particles are tracked using a previously computed carrier flow field, and an averaging procedure is employed to obtain local parameters of the particle cloud and generate phase coupling terms needed for the carrier flow governing equations. Two-way coupling between the phases can be achieved through global iterations. Effect of the carrier flow turbulence is typically modelled by introducing random fluctuations of the flow field while tracking the particles. Since all the probe particles are tracked independently of each other, the Lagrangian approach is only applicable to dilute mixtures with no or negligible particle collisions. The conventional upper limit of the volume fraction of particles in gas-particle flows is 0,001 that corresponds to the mass loading of order unity. Below this limit the model of probe particles yields well predictions of turbulent gas-particle flows while introducing relatively simple and physically clear closure assumptions.

Several modifications of the model of probe particles are reported in the literature; the formulations differ from each other by some details of generating random quasi-turbulent flow field as well as by the physical effects taken into account while particle tracking. A simple model presented below is aimed at simulation of a steady-

state dilute gas-particle flow with solid spherical particles; heat and mass transfer between the phases are not considered.

Motion of a probe particle is governed by the equation (1). The aerodynamic force on the particle is represented by the drag one (2); other forces are negligible because of high particle-to-gas density ratio.

$$m\frac{d\vec{v}}{dt} = m\vec{g} + \vec{F}\ ; \quad \frac{d\vec{r}}{dt} = \vec{v} \tag{1}$$

$$\vec{F} = 3\pi\mu\delta(\vec{u} - \vec{v})\left(1 + 0.179\sqrt{Re_p} + 0.013\,Re_p\right),\ Re_p < 6\cdot 10^3 \tag{2}$$

To simulate particle dispersion due to turbulence, the actual velocity $\vec{u}$ of the carrier gas along the particle trajectory is represented as the sum of the local mean velocity (available from the computed flow field) and some fluctuation (3). The fluctuation is randomly sampled from the normal (Gaussian) distribution with mean zero and standard deviation according to the turbulent energy k; the turbulence is assumed isotropic. The sampled fluctuation is associated with an eddy whose size l_e and life-time t_e are evaluated through the turbulent energy k and the rate of its dissipation ε; the constant C_T=0.28 was chosen by comparing numerical results with fundamental derivation by Hinze (1975) for turbulent dispersion of light particles.

$$\vec{u} = \bar{\vec{u}} + \vec{u}'\ ; \quad \overline{u_i'^2} = \frac{2}{3}k\ ; \quad t_e = C_T\frac{k}{\varepsilon}\ ; \quad l_e = t_e\sqrt{\overline{u_i'^2}} \tag{3}$$

It is accepted that, the generated fluctuation remains unchangeable within the eddy during its life-time. As soon as the life-time has expired or the particle has left the eddy, a new fluctuation is chosen assuming no correlation with the previous sample.

Neglecting fluctuations of gas density and the volume fraction of particles in the mixture, the carrier flow field is governed by the equations (4). They differ from corresponding single-phase equations by particle-induced source terms (5); the corner brackets denote time averaging along a particle trajectory and summation over all the probe particles within a control volume. Except the last one, the source terms are available from particle tracking and do not need artificial modelling.

$$\nabla\cdot\left(\rho\bar{\vec{u}}\right) = 0\ ; \quad \nabla\cdot\left(\rho\bar{\vec{u}}\otimes\bar{\vec{u}} + p\vec{I} - \bar{\vec{\tau}}_t\right) = \vec{F}_p$$

$$\nabla\cdot\left(\rho\bar{\vec{u}}k - \frac{\mu_t}{\sigma_k}\nabla k\right) = P - \rho\varepsilon + P_p \tag{4}$$

$$\nabla\cdot\left(\rho\bar{\vec{u}}\varepsilon - \frac{\mu_t}{\sigma_\varepsilon}\nabla\varepsilon\right) = \frac{\varepsilon}{k}\left(C_{\varepsilon 1}P - C_{\varepsilon 2}\rho\varepsilon + C_{\varepsilon 3}P_p\right)$$

$$\vec{F}_p = -\left\langle\vec{F}\right\rangle\ ; \quad P_p = -\left\langle\vec{u}'\cdot\vec{F}\right\rangle\ ; \quad C_{\varepsilon 3} \approx 1.0 \tag{5}$$

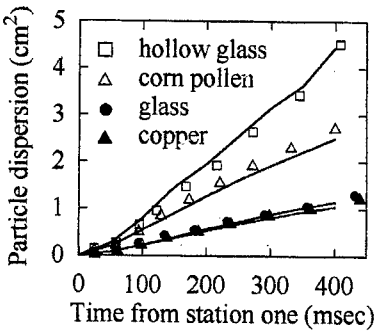

The model has been implemented using arbitrary structured multiblock 3D grids. Several tests were made to validate the developed code. Particularly in the diagram to the left, numerical results on dispersion of separate particles in a grid-generated turbulence are compared with measurements by Snyder & Lumley (1971). The carrier flow field was specified according to the experimental data. Injection of 10000 probe particles provided statistically stationary solution with the true Gaussian distribution of particle deflection from the flow axis.

As another test, computations were made for a planar mixing layer with polydispersed (3-100mkm) water drops according to flow conditions reported by Chang *et al.* (1993). Unlike the former test, both the carrier flow and particle trajectories were simulated; measured flow parameters were used as inlet boundary conditions while at computations. Following the reported data, 8 fractions of probe particles were introduced. To obtain a statistically stationary solution, 19200 trajectories were computed (2400 particles in each of the eight fractions; 800 particles per cell at the inlet). The prediction was encouragingly accurate except the lateral component of the carrier gas velocity; as a result the lateral velocity of particles was slightly underestimated too.

The developing region ($x/D<12$) of a particle laden round jet was investigated by Mostafa *et al.* (1989); the measurements provided a basis for testing the model at relatively high mass loading of the flow (up to unity). 13200 probe particles were used in computations. A satisfactory agreement between measured and computed flow fields was obtained despite rather unreliable data on the inlet conditions.

The work has been carried out under support of "Research in Brussels 95" grant.

REFERENCES

Chang K. C., Wang M. R., Wu W. J., Liu Y. C., 1993, "Theoretical and Experimental Study on Two-Phase Structure of Planar Mixing Layer", *AIAA Journal*, Vol.31, No.1, pp.68-74.

Mostafa A. A., Mongia H. C., McDonell V. G., Samuelsen G. S., 1989, "Evolution of Particle-Laden Jet Flows: A Theoretical and Experimental Study", *AIAA Journal*, Vol. 27, No. 2, pp. 167-183.

Snyder W. H., Lumley J. L., 1971, "Some Measurements of Particle Velocity Auto-correlation Functions in a Turbulent Flow", *Journal of Fluid Mechanics*, Vol. 48, pt. 1, pp. 41-71

Hinze J.O., 1975, *Turbulence*, McGraw-Hill, New York, 790 p.

64

LASER DOPPLER SYSTEM FOR DIAGNOSTICS OF HIGH-SPEED KINETIC FLOWS

ANISIMOV YU.I., AGAPOV A.S., LASHKOV V.A., MASHEK I.CH., MASHEK A.CH.

St.-Petersburg State university

High-speed kinetic flows of dispersed particles (flows of particles by the sizes 5-300 microns with speeds 2-15 Km/s without gas), are investigated now rather heavily.

Such flows, created in laboratory conditions, can simulate micrometeoric influence on elements of space vehicles, to serve for researches in the field of high-speed impact, to be used in technological purposes. Diagnostics of particle parameters over body, reflected and scattering flows of matter at surface of target is the special interest at research of processes interaction of such kinetic flows with target.

The laser system, serving for diagnostics of the specified flows, consists of the single frequency tuning and stabilized Argon-ion CW laser with output power up to 100 mW, the system of illumination of researched area of a flow, the gathering system of scattering radiation, the absorptive frequent detector on vapor molecular iodine-127, two channels of measurement of scattering light: measuring (past through frequent detector) and basic (falling on detector), two-channel fast ADC and the computer. The main principles of operation of Doppler systems with the frequent molecular detector and their application to diagnostics of stationary flows are described in the papers /1, 2/. Peculiarity of the system described in the present work is its high temporary and space resolution, received at the expense of application of fast light detectors with threshold frequency more than 100 MHz, and fast ADC with operation time 25 ns. The specified parameters of channels of measurement of scattering light have allowed to receive measuring volume with characteristic sizes 0,5x0,5x1,0 mm at diagnostics of flows with speeds up to 15 Km/s. A particle, passing through area of measurement scatters laser light, forming pulse of radiation by duration 10^{-7} - 10^{-5} s. The system measures scattered light in two channels simultaneously - basic and measuring. Their attitude does not depend on amplitude of light pulse and is determined by Doppler shift frequency of scattering radiation and kind of the gear characteristic of the absorption frequency detector. The subsequent numerical processing of signals, made in view of temporary width of each pulse spectrum, permits to receive distribution of particle speeds. The quantity of registered particles for one cycle of measurement is determined by volume of internal memory used ADC (four F4226 in standard CAMAC, two ADC on channel, started synchronously, with shift 25 ns). Maximum time of measuring process for one cycle is 50 - 100 mks. The described system at first stage permits to measure only one projection of speed of researched flows,

however potential opportunities of a described method permit to create the similar analyzer as for two, and for three components of a vector of speed.

References

1. Anisimov Ju.I., Mashek I.Ch., Chaika M.P. Molecula iodine vapor as a linearly absorbing medium for frequency- sensitive detectors in Doppler velocimetry. Opt. Spectrosc., 1992. -.72. -. 1083-1985.

2. Anisimov Yu.I., Lashkov V.A., Mashek I.Ch. Two dimesional laser Doppler analyser of velocity and concentration in two- phase flows. Proceedings of international seminar "Intra- chamber processes, combustion and gas dynamics of dispersed system". S.-Peterburg, 1995. P.71-72.

66

COMPARATIVE NUMERICAL ANALYSIS OF VISCOUS AND INVISCID FLOWS IN A SQUARE CAVITY

Lobov S.L., Romanov O. Y.
The Baltic State Technical University

The main features of the inner flows in SRM chamber are the recirculation zones. These zones arise due to main body of the gas flow separating from a rigid wall, which caused by joint action of positive pressure gradient and viscosity.

Since the gaseous products of solid propellant burning have a very small viscosity (large Re), the numerical computation of the Navier-Stokes equations present great difficultes. The first is that the conventional schemes with small numerical visconsity have very strong stability limitation on the grid size and time step [1].The second, in each gridpoint finite-difference solution is qualitatively viscous only when local grid Reynolds number not more than 2 and, consequently, the local grid size is comparatable with kinematic viscosity coefficient [2]. That why, a method that enables to obtain a stable and accurate solution is limited by the computing time and storage available.

One of the possible ways to solve this problem is to use an inviscid vortical flow model. The above assumption is undoubtedly true in cases where the streamlines are open-ended. There are some cases, in which the main body separating from the ridig wall is determinated by boundary conditions without apparent viscosity influence. For instance, this takes place in a case of flow in a region bounded extermaly by ridig wall with rectangular elementes, or in a point of joint of mass injection part of boundary and solid wall. Batchelor G. K. has theoretically proved that for small but non-zero values of kinematic viscosity in two-dimensional closed flow the central part asymptotically approached to 'inviscid core' with uniform vorticity. However, the rålation between value of vorticity inside the recirculation zone (W0) and the same on boundary line of main stream body (W1) remains to be determinated by the conditions that the viscous boundary layer surrouding this region must also be in steady motion [3].

The parametric numerical investigations based on viscous and on inviscid models have been fulfiled to definite above mentioned relation and to find a lowest Reynolds value, since which the vorticity in the centre of cavity became quasi uniform. The classical cavity flow problem has been modified by the entering of boundary part of main flow body to the computational domain. The scale size equal to the hight of cavity (H) . The computional grid is rectangular and uniform. The equation system is written in term of a vorticy-stream function. The task is resolved in axisimmetric variant but at large values of radial coordinates (R>8H). The govering equations are used here in implicit finite-

difference formulation. All metric derivatives are evaluated by central difference formulas.

The calculations demonstrated, that at the Re=800 in vorticity distribution in central part of cavity the plate appeared. When the Reynolds number further grows, this plate increases and occupies the most of the cavity space. In the main flow zone vorticity distribution apparently trends to consideration of vorticy along streamlines since Re>200. The relation (W0/W1) is near 5-6.

The accurate viscous flow solutions obtained for the peculiar geometric elements then applied to solve the global flow problem in whole domain of SRM inner volume using approximate inviscid model. Thus, the presented technique ensures the required accuracy at resonable computing time and storage requirements.

REFERENCES

1. Белов И.А., Исаев С.А., Коробков В.А. Tasks and methods of account отрывных of currents несжимаемой жидкости.-ice.: Су- достроение, 1989 г, 270 with.

2. Андерсен, Дж. Танненхилл, Р.Плетчер. Computing гидромеха- ника and теплообмен. - М.: World, т.2,1990 г, 726 with.

3. Batchelor G.K. On steady laminar flow with closed streamlines at large Reynolds number. Journal of Fluid Mechanics, 1956, vol.1, pt.2, p177.

COMPUTATION OF TWO-PHASE FLOW AND SLAG MOTION IN SOLID ROCKET MOTOR

Lobov S.L., Romanov O.Y.
The Baltic State Technical University

The combustion of an alumized solid propellant produces not only gases but also liquid particles. These particles are the source of slag material that may remain in the motor during firing and thereby cause excessive heating and subsequent insulation erosion where they collect.

A time-dependent, axisymmetric numerical solution technique has been developed to analyse the coupled gas-particle flow and the motion liquid slag in a solid rocket motor.

In this work for description of two-phase flow numerical model based on a combined Eulerian-Lagrangian analysis was used [1]. The time-dependent flow description was ensures by simulating the quasi steady-state flowfield at sequence of burn times.

The previously-computed single-phase flow results are taken as the initial quess for the two-phase flow. This quasi gas phase solution is solved in Eulerian mesh. Initialy the gas is inviscid, vortical and incompressible, without chemical reactions. The mathematical formulation for gas is used here in term of vorticity-stream function.

This model treats the particles as a discrete phase. The discrete particle phase solution is obtained by integrating their dynamical equation of motion along their trajectories. The combustion of an aluminized solid propellant produces AL/AL_2O_3 agglomerates and small particles on the propellant burning surface, which are ejected into the gaseous surrouding. Along agglomerate trajectory remained in agglomerate metal is oxidized. Some of the new AL_2O_3 is shed as small particles, while the rest remains attached to the AL/AL_2O_3 agglomerate. This events lead to bimodal size distribution of k-phase, consisting of large AL/AL_2O_3 composite particles and small 'smoke' particles [2]. The 'smoke' particles have neglectible values of velocity lag from gas, that why the particle phase analysis is only by agglomerate solution restricted. In this study agglomerate burning and breacup are accounted for. In a SRM, the particle-to-gas density ratio is usually lage, therefore, the only important forces on a particle are the inertia, drag and external acceleration.

In model the relationship between the metal burning rate and spread gaseous oxidizer density distribution in inner volume of SRM is also account for.

The time-dependent slag motion solution is solved in a Eulerian mesh. The slag material is considered as chemically inertial film flow along axisimmetric surface. The important forces on a film are the gas pressure gradientes, the viscous friction between gas and film and external acceleration. The local momentum and mass flux density also influences on a slag motion.

The particle flow and slag motion information has been used to estimate the amount of slag in a apogee SRM, which agrees favourably with availible test data. The results of numerical investigation were:

1)the distribution of mass flux density for oxide and nonburned metal along the countour of aft chamber bottom and submerged nozzle;

2) space distribution of combustion effeciency for solid propellant charge body;

3) the time-dependent slag form, determinated by slag material motion.

The prezented numerical solution technique gives the possibility to determinate the behavior of the particle laden gas as it moves in the motor, and the slag, which remains in the chamber. This knowledge is neccesary for optimum design of SRM.

REFERENCES

1. Golafshani M.,Hai-Tien Loh. Computation of Two-Phase Viscous Flow in Solid Rocket Motors Using a Flux-Split Eulerian-Lagrangian Technique//AIAA Paper.-89-2785.-1989.-P1-14.

2.Babuk V.A.,Vasiliev V.A., Lobov S.L., Romanov O.Y.,Hodosov V.V. Evolution of metal fuel in rocket engine chamber. International Conference on Combustion, Moscow, St.-Petersburg, 1993, p.34-35.

70

COMPUTATION OF CHARACTERISTICS OF LARGE-SIZE OXIDE PARTICLES IN CHAMBER OF ALUMINIZED SOLID PROPELLANT MOTOR

V.A.BABUK, V.A.VASILYEV, O.V.VODOVOZOV, O.YA.ROMANOV
Baltic State Technical University, Saint Petersburg, RUSSIA

Abstract

Combustion of aluminized solid propellants (ASP) is characterized by formation of particles of two different sizes. Large size particles may reach up to hundreds and thousands micrometers. It is these particles that cause slag deposition in rocket chambers and some accompanying phenomena. Large-size oxide particles are formed as the result of evolution of agglomerates in the combustion product flow after they leave the burning propellant surface. A model for large-size particle formation is developed as a result of experimental and theoretical investigation. Parametric analysis of the model as applied to a large dimension rocket engine had revealed that characteristics of large-size oxide particles depend on propellant properties, engine geometry, time of their presence in a combustion chamber. The model allows to predict large-size particles properties, to improve the technique for calculation of two phase flows in the chamber and, in turn, to obtain more precise characteristics of a "propellant-engine" system.

Introduction

Burning of aliminized solid propellant (ASP) produces condensed phase combustion products (CPCP) which consist of two types of particles: large-size and small-size. The former may reach hundreds and even thousands micrometers, the latter is about 1 micrometer in size. In the rocket chamber the small-size particles are in equilibrium with gas phase. The large-size particles are characterized by their velocity lag as compared with gas. It is precisely these particles that cause slag deposition on the inner surfaces of the chamber and accompanying phenomena connected with additional transfer of substance and energy, i.e., more intensive destruction of heat isolation and slag deposition.

The CPCP are formed in the course of two processes: metal agglomeration on the burning propellant surface and CPCP evolution in the combustion product flow. Agglomeration leads to the fact that the CPCP leaving the burning propellant surface consist of agglomerates and highly dispersed oxide particles (HDOP) of about 1 micrometer in size. Quantitative proportion of agglomerates and HDOP and their dispersity are determined by peculiarities of the agglomeration process. The evolution of CPCP includes a number of physical and chemical transformations of the particles in combustion product flow. This paper is devoted to modeling of large size particle formation in combustion chamber with agglomeration characteristics assigned. To solve this problem it is necessary to model the evolution of a single agglomerate and the evolution of two phase flow.

Modeling of a Single Agglomerate Evolution

The model was developed on the base of various experimental data on agglomerate characteristics at different stages of evolution [1]. The model takes into account the following phenomena:

- burning of agglomerate metal in gaseous phase mode,
- chemical interaction of metal and oxide in agglomerate with formation of gaseous products;
- structure of agglomerate composed of metal, oxide, and gaseous products in different proportion;
- deposition on agglomerates of HDOP from the flow.

The developed model combines a number of individual models for specific phenomena occurring in the evolution [1,2]. As these models are rather complex and require much computer time when used then fast-operating formal models were developed for some specific phenomena. Reliability of single agglomerate evolution model was confirmed by comparison of the model and experimental data on evolution of agglomerates in linear flow.

Modeling of Two Phase Flow Evolution

Two phase flow consists of two interacting objects: 1. gas phase with HDOP and 2. large-size particles of CPCP. Chemical, termal, and dynamic interactions between this objects take place in the flow that causes changes in velocity, chemical contents, and temperatures

of the objects. In the particle burning zone HDOP are formed and then transported to gas phase. In turn, HDOP of the gas phase may deposit on the large- size particles.

Modeling of the flow evolution in rocket chamber is based on the following approach. Velocity field of the gas phase is calculated on the base of a model for vortex motion of non viscous and incompressible gas developed by V.N.Emelyanov at Baltic State Technical University (Saint Petersburg, Russia). Then on the base of the gas velocity field, motion of large-size particles is calculated. In this procedure the model of single agglomerate evolution is used that allows to take into account all the phenomena occurring in the evolution. Calculations are made for different fractions of the particles and for different places on propellant burning surface which produce the particles.

Chamber cavity is divided into sells. Dimensions of a sell depend on precision of calculations. Temperature, oxidizer and HDOP concentrations in each sell are calculated as a result of evolution of agglomerates crossing a gas stream which passes through the sell. This parameters are determined with the help of equilibrium thermodynamic approach.

A problem of modeling HDOP formation in solid propellant combustion has not been solved completely yet. However, an experimental data are obtained which allow to think that HDOP dispersity depends on sizes of the agglomerates. At the burning propellant surface, mass-medium diameter δ_{43} of HDOP is about 0.8 - 0.9 μm. These HDOP are formed as a result of burning process of metal particles which do not take part in the agglomeration [3]. Agglomerate combustion may change this value up to 4 - 5 μm [4,5]. It may be assumed also that agglomerate lag influences dispersity of HDOP formed in agglomerate burning process. These facts allow to believe that HDOP dispersity may change significantly during two phase flow evolution in rocket chamber. In this paper, HDOP dispersity was accepted to be constant during evolution but dependent on the portion of metal involved in agglomeration (Z_m^a): HDOP diameters increase if parameter Z_m^a increases.

In computer modeling it was accepted that agglomerate deposition takes place if agglomerate trajectory crosses inner surface of combustion chamber. However, behavior of deposited

agglomerates is not examined. The model allows to calculate parameters of large- size fraction of CPCP in any section of the chamber. Input information for the calculation is the following:

- geometry of propellant charge and combustion chamber;
- propellant burning rate and chamber pressure;
- parameters of CPCP at propellant burning surface (proportion of agglomerates and HDOP, agglomerate size distribution);
- HDOP size;
- thermodynamic characteristics of the propellant.

Computer Modeling

Computer program was developed for above model. The program was used for calculating behavior of large - size CPCP particles in the last stage of their evolution in rocket chamber. CPCP evolution in combustion chamber is considered to end with either agglomerate deposition on chamber inner surface or agglomerate entry into motor nozzle where their evolution continues in supersonic two- phase flow.

Results of the agglomerate deposition are represented in Fig.1 and 2. Fig. 1 shows section of rocket chamber and propellant burning surface. Computations were made for the following conditions: pressure P = 6MPa, acceleration 1.5g, oxide part in agglomerate by mass η=0.35, parameter Z_m^a =0.72, HDOP diameter δ=2μm, agglomerate mass-medium diameter D_{43} =327μm. Fig. 2 shows distribution of CPCP deposition along the inner surface ABCDEFGH of the chamber. The deposited CPCP consist of 80% oxide by mass.

The study allows to find out characteristics of propellant and combustion chamber which strongly influence deposition intensity. Obvious ways to deposition reduction are decrease of gas velocity, curvature of flow lines, agglomerate size and their quantity. The same task may be solved with unusual approaches: by temperature increase and/or organization of local zones with oxidizing potential increased in gas phase. These factors may cause intensification of reaction between aluminum and alumina in the agglomerate, and, in a limiting case, fragmentation of agglomerates.

Propellant features influence parameters of large- size CPCP changing characteristics of agglomeration process. In turn, parameters of two- phase flow at propellant burning surface have

strong influence on the flow evolution process. Decrease in size of agglomerates and oxide content in them leads to intensification of reaction between aluminum and oxide in agglomerates. Reductions in Z_m^a parameter, HDOP size, and agglomerate velocity lags cause decrease of HDOP deposition on the agglomerates.

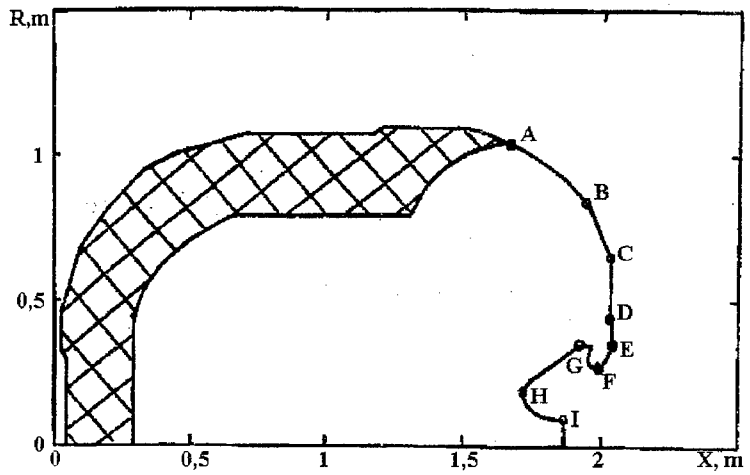

Figure 1. Section of solid propellant motor chamber.

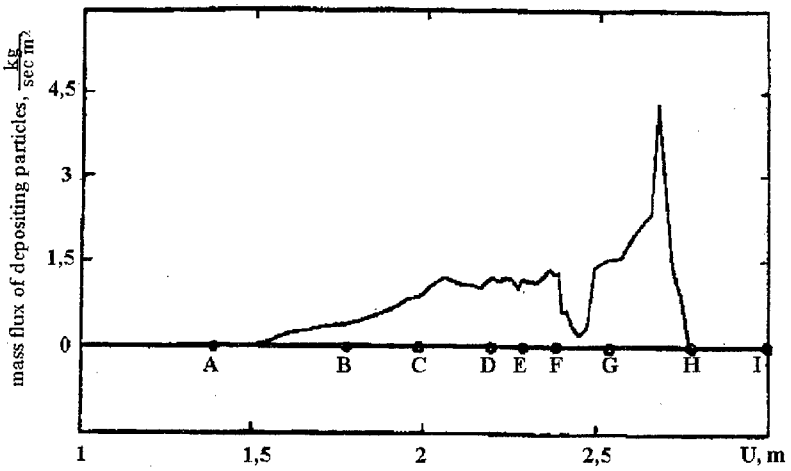

Figure 2. Distribution of particle deposition.

CPCP evolution in one-dimensional flow was calculated for different two phase flow conditions provided by using two different propellants: Prop.N1 and Prop.N2. Figures 3 and 4 show results of the calculation: agglomerate size distribution at propellant burning surface and in the last stage of the evolution process when combustion efficiency reaches up to 95%

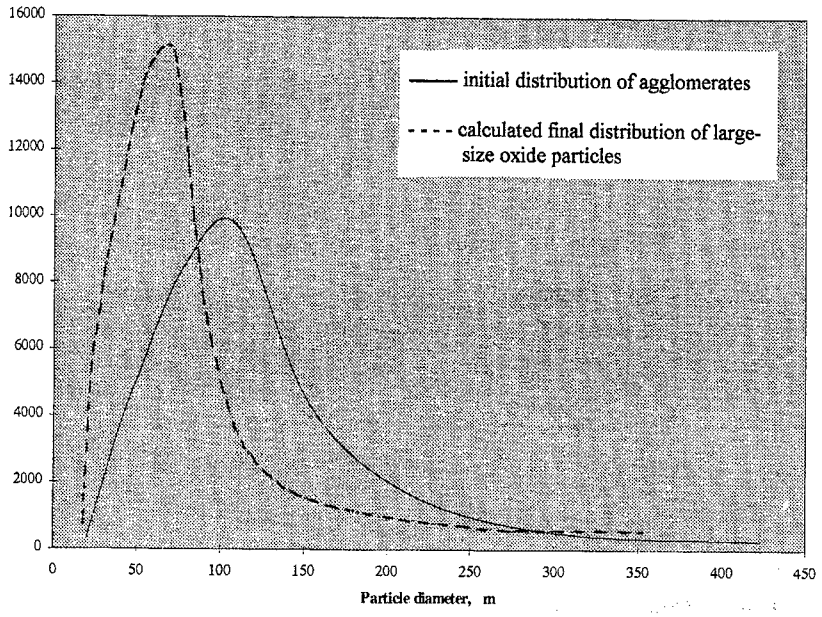

Figure 3. Comparison of particle size distribution for Prop.N1.

Prop.N1 is characterized by the following initial parameters of CPCP (near propellant surface): D_{43}=130μm, Z_m^a=0.26, η=0.34. These values provide predominance of oxide removal from agglomerates in comparison with HDOP deposition. Therefore in the case of Prop.N1, CPCP evolution is accompanied by decreasing agglomerate sizes in consequence of metal burning and oxide removal. As a result, dispersity of large- size particles increased and the distribution function changed as it is shown in Fig.3. Initial

parameters of CPCP for Prop.N2: D_{43}=327μm, Z_m^a=0.72, η=0.35 provide much lower rate of oxide removal and more intensive deposition of HDOP on agglomerates. These facts reduce dispersity of large- size particles (Fig. 4).

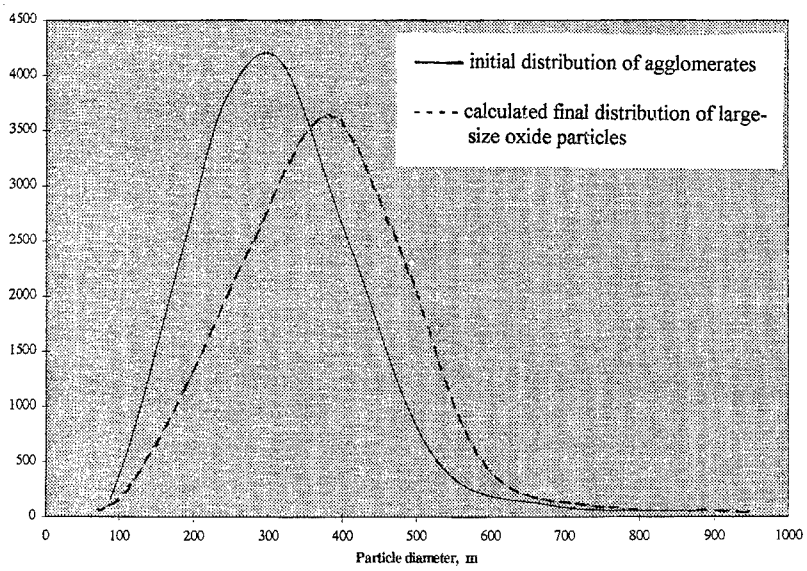

Figure 4. Comparison of particle size distribution for Prop.N2.

Structure of large- size CPCP particles is changing during evolution (Fig.5). When leaving the burning propellant surface, agglomerates are aluminum drops with oxide "caps" [6]. Agglomerate may contain gas cavities (bubbles) which are results of gaseous products formation in the chemical reaction between metal and oxide of agglomerates. The agglomerate structure is near to equilibrium and it is determined by surface properties and amounts of the substances in the agglomerate. Intensification of the reaction and decrease in "cap" thickness may lead to out-break of bubbles through the "cap" and, consequently, to oxide removal from the agglomerate. At the last stage of the evolution, the above reaction may continue but oxide removal stops in consequence of agglomerate structure transformation (oxide "cap" thickness increasing) because of metal

burning out. Thus, conditions for bubble existence in agglomerates remain in final stage of the evolution. The bubbles merge and after metal burned out, agglomerates turn into oxide drop with one bubble, as a rule. Size of the final bubble depends on pressure, particle size and temperature. The bubble may amount to 25 - 40 % of the oxide drop volume and be not located symmetrically in the drop.

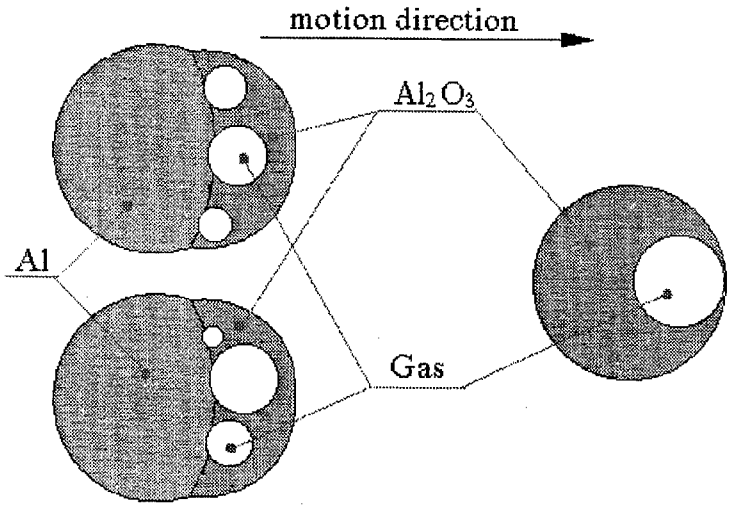

Figure 5. Scheme of agglomerate transformation to final oxide particles.

Thus, at the last stage of the evolution, large-size particles of CPCP are oxide drops containing bubbles displaced from the drop center in direction of the drop motion. This drop structure is rather steady for a wide range of conditions of two phase flow of combustion products in rocket chamber.

Conclusion

The work is based on contemporary knowledge about large- size particle formation in rocket solid propellant combustion. The work resulted in developing methods for prediction of large- size particles

characteristics in rocket chamber. The result of the work would be useful for optimization of the "propellant - motor" system.

References

1. Бабук, В.А., Васильев, В.А., Романов, О.Я. и др., 1993. "Физико- химические превращения капель Al - Al2O3 в активном газовом потоке," *Физика горения и взрыва*, N3, с.129-135.

2. Babuk, V.A., Vasilyev, V.A., Romanov O.Ya., 1994. "Combustion of Aluminum Particles in a Flow of Solid Propellant Combustion Products," *Proceedings of the Zel'dovich Memorial,* Vol.2, pp.152-155.

3. Babuk V.A., Malahov M.S., 1995. "The Method of Experimental Research of Formation Highly Dispersed Oxide Particles Process in Burning Solid Propellant," *Proceedings of the International Seminar on Intra-Chamber Processes, Combustion and Gas Dynamics of Dispersed Systems*, pp.140-143.

4. Бахир, Л.П., Левашенко, Г.И., Таманович, В.В., 1973. "Исследование размера капель Al2O3 вблизи горящей поверхности топлива," *Физика горения и взрыва*, N6, с.842-849.

5. Федоров, Б.Н., Плечов, Ю.Л., Тимохин, Э.М., 1982. "Исследование дисперсности частиц Al2O3 в продуктах сгорания конденсированных систем," *Физика горения и взрыва*, N1, с.22-27.

6. Бабук, В.А., Белов, В.П., Ходосов, В.В. и др., 1988. "Исследование структуры агломератов при горении алюминизированных смесевых конденсированных систем," *Физика горения и взрыва*, N5, с.52-57.

Section 4
COMBUSTION OF DISPERSED SYSTEMS

80

ON REASONS FOR STABILITY LOSS OF MAGNESIUM VAPOR-PHASE COMBUSTION

U.I. GOLDSHLEGER, E.Ya. SHAFIROVICH
Institute of Structural Macrokinetics, Russian Academy of Sciences
Chernogolovka, Moscow 142432, Russia

Combustion of metals, in spite of the often observed unsteady phenomena (a decrease in light emission intensity, jets, explosions, fragmentation), is usually considered a quasi-steady vapor-phase or heterogeneous process. It is generally agreed that for volatile metals ignition always leads to stable vapor-phase burning. However, in experimental investigation of magnesium interaction with CO, a pulsating combustion mode has been unexpectedly found [1]. Later, in thermogravimetric studies of Mg oxidation in carbon oxides, a "slow heterogeneous combustion" mode has been found, with kinetic self-acceleration of heterogeneous reaction being inherent [2, 3]. In CO_2 atmosphere the temperature existence region of such a mode separates slow oxidation and fast vapor-phase burning, the low boundary of this region coinciding with the melting point of Mg. In CO atmosphere a high-temperature mode of "slow heterogeneous combustion", apart from the low-temperature one, is observed that separates regions of pulsating and vapor-phase combustion.

In the present paper a possible mechanism of interaction between macro-kinetically characteristics and physical/chemical processes in a surface film and gas phase is discussed that makes it possible to explain, in the framework of a unified concept, the existence of the unusual combustion modes of Mg mentioned above.

Analysis of experimental results has shown that the slow heterogeneous combustion process is mainly determined by heat and mass transfer of liquid magnesium through a growing porous oxide film and by its evaporation from surface of menisci in pores. Good wetting by liquid Mg of its own oxide results in continuous pulling of metal into the porous film. The pressure difference needed for the liquid movement is caused by capillary forces on the liquid/gas interface in the pores and on surface of a bubble that forms inside the metal drop and grows during the process. Due to high velocities of capillary flow, the vapor-gas reaction occurs close to the film/oxidizer interface. The growth of the film leads to increasing the effective surface of evaporation and, therefore, to macro-kinetic acceleration of chemical reaction. Moreover, with increasing the bubble the curvature of concave liquid menisci in the pores decreases. Pressure of vapor above the metal surface increases (Thomson effect). This is an additional reason for the kinetic self-acceleration of reaction during slow heterogeneous combustion.

Let us consider features of metal vapor-phase combustion in strong (CO_2) and weak (CO) oxidizers.

During combustion of Mg in CO_2 the gas-phase reaction occurs in a thin zone detached from the particle surface. The great heat flux from high-temperature flame

results in the high rate of metal vaporization. The vaporization occurs in Stefan mode with noticeable gas velocities in space between the particle surface and the flame zone. For this reason, the oxidizer concentration close to the particle surface is low and the oxide film structure, formed at initial phases of the process, does not change during vapor-phase combustion. The burning phase, in spite of possible formation of an "outer" oxide shell in the flame, may be considered a stable quasi-steady process.

During combustion of Mg in CO, when the adiabatic flame temperature is low, the gas-phase reaction occurs, on the contrary, occurs in an extended zone adjusting the particle surface. In this case the temperature difference between the flame zone and the particle surface is noticeably less. Since the heat flux from the flame is small, the evaporation mode is close to the diffusion-controlled one. Therefore, the counter-flow of Mg vapor (that prevents ingress of CO to the particle surface) is significantly weaker than in the combustion in CO_2. For this reason, in the mode of Mg vapor-phase combustion in CO, together with the gas-phase reaction in volume, the heterogeneous reaction may always occur on the particle surface at the temperature close to the boiling point of Mg. The increase in the particle surface during vapor-phase inflammation promotes great thermal acceleration of the heterogeneous reaction. On the other hand, the characteristic grain size of the surface film falls exponentially with increasing the temperature, resulting in drastic changes in the film properties. This may entail the great kinetic inhibition of the heterogeneous reaction that is not compensated by the higher rate of heat release.

The changes in the film properties are an inhibiting cause with respect to both heterogeneous and gas-phase reactions. With the capillary mechanism of metal transport to the outer boundary of the film, the decrease in the characteristic size of pores results also in the decrease in the effective surface of evaporation. Simultaneously the saturated vapor pressure of Mg decreases due to the increase in the meniscus curvature in the pores. Both these causes decrease flow of Mg vapor to the flame zone, resulting in the decrease in the gas-phase reaction intensity, and therefore, to stability loss of vapor-phase burning.

Therefore, existence of feedback between the rate of heat release and the changes in structure and properties of the film at the vapor-phase burning phase may lead to instability, particularly to the pulsating mode observed experimentally. The feasibility for realization of this mode depends on the state and properties of the film formed at the pre-ignition phase. If the oxide film formed at the initial phases of the process is loose, only partial healing of the pores may take place, insufficient for cessation of vapor-phase burning. With increasing the ambient temperature the density of the original film increases. For the reasonably dense film fast healing of the pores and extinction of the flame may occur after vapor-phase ignition. The particle returns to the slow heterogeneous combustion mode when the characteristic size of the film pores is sufficiently great and, therefore, the growth of the film does not prevent from thermal self-acceleration of reaction, resulting in a repeat flash. As this take place, the higher the particle temperature at the phase of slow heterogeneous combustion, the shorter the time before the repeat flash.

To realize the pulsating combustion mode, it is necessary that the activation energy of the healing process is higher than that of chemical reaction. In this case, the value of temperature always exists theoretically when the characteristic size of pores at the phase of slow heterogeneous combustion is small to an extent that thermal self-acceleration of reaction is not sufficient for equilibrium breakdown in the system. As a result, at high ambient temperatures the combustion mode may become heterogeneous again, as we observed in the experiments.

This work was supported by the Russian Foundation for Basic Research (Grant 95-03-09829).

References

1. Shafirovich, E.Ya., and Goldshleger, U.I., "Combustion of Magnesium Particles in CO_2/CO Mixtures," *Combustion Science and Technology*, Vol. 84, 1992, pp. 33-43.

2. Shafirovich, E.Ya., and Goldshleger, U.I., "On the Role of Surface Films in the Ignition and Combustion of Metal Particles," *Combustion, Detonation, Shock Waves: Proceedings of the Zel'dovich Memorial, Vol. 2*, Moscow, 1994, pp. 208-211.

3. Shafirovich, E.Ya., and Goldshleger, U.I., "Combustion of Magnesium Particles in Carbon Dioxide and Monoxide," AIAA Paper 95-2992, 1995.

STUDY OF DISPERSE PHASE OF HMX-BASED ALUMINIZED PROPELLANTS. 1. STEADY-STATE COMBUSTION CHARACTERISTICS

O. G. GLOTOV, V. E. ZARKO, V. V. KARASEV

Institute of Chemical Kinetics and Combustion
Russian Academy of Sciences, Novosibirsk 630090, Russia

The efficiency of use of aluminized propellants in solid rocket motors is determined not only by conversion of chemical energy in the heat of combustion but also by formation of condensed combustion products that causes two-phase loss of specific impulse, slagging in the combustion chamber and erosion of the nozzles.

The objective of this study was to get experimental information about generation of condensed combustion products by HMX-based model metalized propellants with inert and energetic binder both in steady-state and nonsteady regimes of combustion (the last one is the topic of companion paper). The data obtained by sampling technique [1-2] on size distribution in the range from 0.5 μm to D_{max} and on content of non-consumed *Al* in condensed combustion products (CCP) formed in course of stationary combustion are reported in present paper.

Two metalized propellants were designated as I and E in accordance with the nature of binder. The propellants characteristics are presented in Table 1. The inert binder consists of butadiene rubber 20%, transformer oil 76%, and additives 4% while the energetic binder consists of nitryl rubber plasticized with DEGDN 98% and additives 2%. Propellant E contained numerous macro pores and thus had relatively low density.

Table 1. Propellant formulations (% mass.) and characteristics

Propellant	Energetic binder	Inert binder	Al D_{30}=14 μm	AP 200-315 μm	AP S=6000 cm^2/g	HMX >315 μm	Density, g/cm^3	$r = B \cdot P^{\nu}$, r in mm/s, $6<P<64$ atm
I	-	15	16.8	13.1	31.8	23.3	1.7	$r = 1.13 \cdot P^{0.65}$
E	20	-	20	18	7	35	1.6	$r = 1.88 \cdot P^{0.52}$

Coarse size CCP particles, propellant I

The combustion behavior of propellant I is characterized with a weak agglomeration of *Al* particles. At all pressures under study (6, 22, 64 atm) no more than 10% of mass of sampled CCP belong to particles with size exceeding 100 μm. In fact, the coarse particles give negligibly small contribution into total mass of unburnt *Al*. The mass size distribution data are presented in Table 2 in a form of mean sizes D_{mn} calculated in the size range 120-1000 μm. The mean sizes decrease with pressure. A similar trend (Table 2, 2nd column) is revealed for incompleteness of *Al* combustion which is determined in present work as the ratio of mass of unburnt *Al* in CCP particles m_c^{Al} and mass of original metal in the propellant sample m_p^{Al}: $\eta = m_c^{Al} / m_p^{Al}$. Such

observations are typical for aluminized propellants combustion [3]. A trivial explanation of this trend is in the fact that the smaller time is available for *Al* particles to melt and agglomerate on the burning surface with enhanced burning rate under elevated pressure. A possible cause of relatively weak agglomeration of *Al* in combustion of propellant I could specific properties of binder which prevents adhesion between metal particles in preheat layer. According to the observations made with high speed movie and morphological analysis the aggregates of *Al* particles leaving the surface are only partially sintered clusters which ignite mostly at a finite distance above the surface. It should be underlined, however, that total completeness of *Al* combustion for propellant I is rather high due to relatively small particle sizes and their fast burn out in flame.

Coarse size CCP particles, propellant E

An agglomeration of *Al* particles in combustion of propellant with energetic binder is rather pronounced. Table 2 presents characteristic sizes D_{mn} of agglomerates calculated in size range 120 μm - D_{max}. Mass size distribution functions for CCP and for unburnt *Al* in CCP do not essentially change in the pressure range 1-60 atm, and observed rise in D_{43} is mainly due to increase of number and mass of particles larger than 1000 μm. The porous structure of propellant E probably causes enhancement of agglomeration due to formation of *Al* particle clusters from neighbor "pockets" in the bulk of propellant. Completeness of *Al* combustion (Table 2, 2nd column) at low pressure is higher than at moderate pressures. One may suppose that presence (only in case of propellant E) of "matrix" agglomerates [4], the number of which diminishes at elevated pressures, is the cause of more effective combustion of metal at low pressures [1]. The structure of matrix agglomerate provides better opportunities for metal oxidation due to direct contact of oxidizer with neat metal at the surface of agglomerate. The observed trend in *Al* consumption completeness can be treated as indirect confirmation of hypothesis that variation of the structure of agglomerates can make an effect on completeness of metal combustion. Slight increase of metal combustion completeness at elevated pressures (22 and 62 atm) can be simple consequence of temperature increase at the burning surface and prolonged residence time for agglomerates in gaseous combustion products (due to reduction of velocity of gases issued from the burning surface with pressure).

Fine CCP particles, propellants I and E

The typical feature of mass size distribution of fine CCP for both propellants under study is the presence of local maximum (M-peak) in size range 2.4-5 μm at all tested combustion conditions. We calculated mass size distribution of oxide particles assuming that all virgin *Al* particles were converted into oxide ones with depositing 17% of theoretical available oxide back on the surface of *Al* particles. The results of these calculations show that the calculated peak for oxide particles practically coincides with main experimental peak in fine CCP distribution but its amplitude is much less than that of M-peak for CCP particles. Thus, it should be suggested some another (for example, condensation) mechanism for delivering large number of oxide particles into the M-peak.

At elevated pressures, an L-peak appears in the size range 0.5-1.2 μm with amplitude strengthening with pressure. The estimated residence time for fine particles increases with pressure and equals 6 ms at 22 atm and 10-12 ms at 62-64 atm for both propellants. At the same time, it is known that the longer residence time for smoke (including submicron) particles, the larger their size [5]. If one takes into account that sampling technique used permits to analyze particles exceeding 0.5 μm in size, the appearance of L-peak can be explained by enlargement of real submicron particles due to increase of their residence time in flame with pressure.

To conclude, the results of this study showed significant difference in metal combustion behavior for studied HMX-based propellants. Propellant with inert binder is characterized with relatively weak agglomeration and bad ignition of *Al* particles. Therefore the *Al* combustion incompleteness is rather high at low pressures but it is very small at elevated pressures (η=0.01 at 64 atm). In case of propellant with energetic binder the *Al* combustion incompleteness is relatively high (η=0.25-0.32) due to large size of agglomerates formed and ignited at the burning surface. Some better completeness of *Al* combustion at low pressures is probably caused by presence of "matrix" agglomerates with better access of oxidizer to the surface of neat *Al*. The causes of different combustion behavior of metalized propellants are still unknown.

Table 2.

Incompleteness of *Al* combustion η and mean diameters D_{mn} (μm) of coarse CCP

Propellant	P, atm	η	D_{10}	D_{20}	D_{30}	D_{21}	D_{32}	D_{43}	D_{53}
I	6	0.48	265	285	308	306	360	431	474
	22	0.04	196	202	210	209	228	267	308
	64	0.01	188	193	199	198	211	228	239
E	1	0.25	263	284	310	307	371	460	517
	6	0.26	270	291	317	313	378	477	547
	22	0.31	267	287	314	308	376	500	593
	62	0.29	260	280	310	302	377	529	654

1. Glotov, O. G., and Zyryanov, V. Ya. "The Effect of Pressure on Characteristics of Condensed Combustion Products of Aluminized Solid Propellant", *Archivum Combustionis*, 1991, Vol. 11, No. 3-4, pp. 251-262.

2. Glotov, O. G., and Zyryanov, V. Ya. "The Condensed Combustion Products of Aluminized Solid Propellants. I. The Method of Quenching at Various Distances from Burning Surface for Studying the Evolution of Particles", *Combustion, Explosion and Shock Waves*, 1995, Vol. 31, No.1

3. Sambamurthi, J. K., Price, E. W., and Sigman, R. K. "Aluminum Agglomeration in Solid Propellant Combustion", *AIAA Journal*, 1984, Vol. 22, No. 8, pp. 1132-1138.

4. Babuk, V. A., Belov, V. P., and Shelukhin, G. G. "Combustion of Aluminum Particles in Composite Condensed Systems Under Low and High Pressures", *Combustion, Explosion and Shock Waves*, 1981, Vol. 17, No. 3.

5. Bakhir, L. P., and Levashenko, G. I. "The Investigation of the Size of Alumina Drops Near the Burning Surface". *Combustion, Explosion and Shock Waves*, 1973, Vol. 9, No. 6.

STUDY OF DISPERSE PHASE OF HMX-BASED ALUMINIZED PROPELLANTS*. 2. TRANSIENT COMBUSTION CHARACTERISTICS

V. V. KARASEV, O. G. GLOTOV, A. B. KISKIN, V. N. SIMONENKO, A. G. SVIT, V. E. ZARKO

Institute of Chemical Kinetics and Combustion
Russian Academy of Sciences, Novosibirsk 630090, Russia

The objective of this study was receiving information on characteristics of transient combustion of HMX-based model aluminized propellants with inert (I) and energetic (E) binder. The experiments were performed on the measurement of recoil force and visualization of the flame zone via high speed photography.

The propellant characteristics and experimental data on particles sampled in course of stationary combustion are presented by Glotov O. G. and co-authors in companion paper in this proceedings.

In order to obtain data on transient burning rate response, the experiments were conducted for both propellants under action of sinusoidal radiant flux at atmospheric pressure. The set up [1] that included computer controlled laser (YAG, λ=1.06 μm, 120W) and microforce transducer for measuring recoil force of burning propellant sample was used. It was found that transient combustion behavior of studied propellants is quite different despite similar stationary burning rate laws under constant radiant flux. The following dependencies of burning rate r (mm/s) on radiant flux q (cal/(cm^2·s)) were obtained for radiation driven combustion:
r=1.44+3.77·10^{-2}·q-7.03·10^{-4}·q^2 for propellant I and r=1.93+4.23·10^{-2}·q-3.65·10^{-4}·q^2 for propellant E. Propellant I demonstrates remarkable response to perturbations of radiant flux with resonance frequency being equal about 2-3 Hz. For the propellant E, the recoil force signal has significant level of noise (intrinsic oscillations) that makes it difficult studying transient combustion response. It is assumed that in combustion behavior of propellant E the important role belongs to the presence of large agglomerate particles ignited at or close to the burning surface. Detachment of agglomerates from the surface may cause large scale perturbations of the signal of recoil force.

The experiments on visualization were performed only with propellant I at atmospheric pressure using shadow image high speed movie technique [2]. Combustion tests were made under action of constant and step-wise radiant flux with frequency close to the resonant for the burning rate response. The cylindrical propellant sample with diameter 7.5 and height 7-10 mm was tightly inserted into 15 mm long quartz tube. The propellant sample was mounted horizontally and visualized area located flush the edge of quartz tube and had the dimensions 6×4 mm^2. The flash illumination frequency was equal to 2 and 3.4 kHz, image magnification on the film amounted 2.5$^\times$ and 3$^\times$. In or-

*) The work has been sponsored in part by United States Air Force through its European Office of Aerospace Research and Development under Contract F61708-96-W0270.

der to obtain data on correlated with the phase of irradiation temporal particle characteristics special design time-marking system has been developed. The marks on the film made by emitting diode allow to bring in correspondence the sequence of the film frames and temporal phases of radiant intensity variation.

It should be noted that the possibilities of studying the characteristics of two phase flow in flame of propellant I are very restricted. The formed on the surface particles are the coral (grape) shape aggregates. Most of recorded on the films aggregates has characteristic size less than 100 μm and about 30% of their number have size less than 10-20 μm which is below resolving limit of high speed movie registration. The aggregates leave the burning surface non-ignited and they are ignited mainly at the distance 1-5 cm downstream in the flame. When constructing histograms, a diameter of aggregates was determined as diameter of the circle with the area equal to particle image area.

On the basis of film treatment the following parameters were determined:

n_f - averaged (mean) number of particles in a frame obtained during given time interval of histogram accumulation (40 ms in the case of constant flux; 25 ms or 1/8 of total period of pulsed irradiation in the case of step-wise radiant flux);

D_{10}, D_{20}, and D_{30} - mean particle diameters in size range 0-210 μm.

The value of relative error $\Delta n_f / n_f$ was estimated as ≤0.06 for experiments with constant radiant flux and as ≤0.02 for experiments with step-wise radiant flux. The error ΔD_{mn} of particle size determination was estimated as a half of the width of histogram size sub range and equals (30/2) μm.

The number of particles in the individual frame on the film is relatively high (about 15-25 on each frame) and the velocities of their motion are high enough (up to 7 m/s). Therefore there is impossible, as a rule, to identify just the same particle on neighbor frames. To ensure statistic validity of experimental data we treated not each frame but every 5th frame on the film. Thus, the data on particles concentration and size distribution obtained via high speed movie visualization in present work should be treated as ***local*** and ***instantaneous***, i. e. corresponding to the given visualized scene at given time interval.

The instantaneous histograms can be effectively used in evaluation of external radiation attenuation by flame and damping of acoustic (pressure) oscillations in rocket chamber. To construct histograms corresponding to volume flow rate of disperse phase in flame one should know the particle velocity field in the flame. The last histograms can be used in estimates for metal combustion completeness and for two phase losses of specific impulse.

The experiments with constant irradiation q=12 cal/(cm^2·s) showed substantial scatter in experimental data. However, only the variation of "instantaneous" value of n_f is larger than the estimated experimental error. The variations of n_f and D_{mn} can be caused by heterogeneous structure of propellant and relatively short time of accumulation of the data.

In experiments with step-wise oscillating radiant flux during first half (0.1 s) of period the burning surface is irradiated with flux 16 cal/(cm^2·s). During second half of the period irradiation intensity equals 8 cal/(cm^2·s). The films under treatment contained information about 6 whole periods. In course of treatment each half of the period was divided onto 4 equal portions and finally all histograms corresponding to appropriate (according to the current phase of irradiation) portions were summarized. This was done aiming to diminish "statistical" noise due to the effect of occasional micro non-uniformity of composition and structure of the propellant sample. The results for the combustion under step-wise oscillating irradiation are presented in Figure. To make it obvious every 8 points on the plots in Figure are repeated in a cyclic manner in accordance with the process repetition frequency 5 Hz. Each point on the plots is the result of treatment of 2100-2600 particle images that makes it possible to assume that the effect of micro compositional heterogeneity of the propellant sample can be neglected.

The results of this study have shown: a) There is distinguished response of disperse phase parameters to variations of the external radiant flux but temporal variations of the parameters exceed remarkably the experimental error only for n_f; b) Comparison of the n_f response with recoil force response at the same radiant flux oscillations allows to conclude that the value of n_f is proportional to the burning rate r if one assume that the recoil force $F \sim r^2$; c) The mean value of n_f under step-wise irradiation by 1.5 times higher then that under constant irradiation despite the same mean energy input to the burning surface. Study of this effect could be interesting and important from the point of view of suppression of acoustic pressure oscillations in rocket chamber.

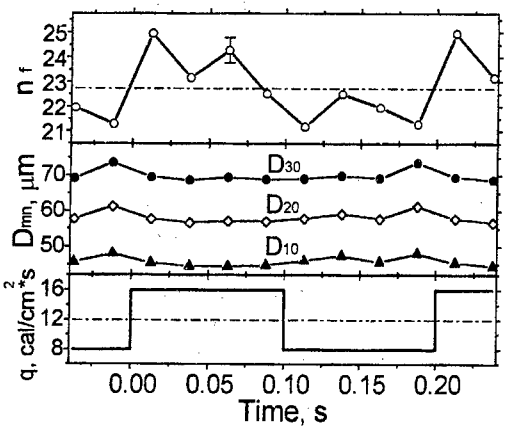

Figure. Temporal dependencies of particle characteristics in flame zone of propellant I combusted under step-wise radiant flux, pressure 1 atm.

1. Simonenko V N., Kiskin A. B., Fomenko V. M., and Svit A. G. "Study of Propellants Burning Rate Response to Periodical Laser Flux Irradiation", In: *Condensed Systems Combustion*, Chernogolovka, 1986, pp. 75-86 (in Russian).

2. Grigor'ev V. G., Zarko V. E., and Kutsenogii K. P. "Experimental Investigation of the Agglomeration of Aluminum Particles in Burning Condensed Systems", Combustion, Explosion and Shock Waves, 1981, Vol. 17, No. 3.

CLOSED VOLUME COMBUSTION OF EXPLOSIVE MATERIALS IGNITED BY COMBUSTION PRODUCTS OF GAS MIXTURES

B.A.VYSKUBENKO, V.F.GERASIMENKO, V.V.KOKSHAROV, L.E.KOLEGOV, V.A.MAZANOV, D.V.STRAKHOV, A.P.TOLOCHKO

(RFNC-VNIIEF, Sarov, Russia)

Now in different industry branches there are technological processes which at possible accidental regimes are followed by the fast energy release. It causes the overloading of the construction and under certain conditions actually destroys them [1]. Because these processes often realizes in large-scale or sometime even unique installations, the scale model experiments are used widely to estimate the strength of these objects. And the accidental energy releasing is simulated usually by the detonation of solid high explosives (HE) [1,2]. As shown [3], the accidental energy releasing simulation by solid HE detonation in the scale model experiments in many cases results some uncertainties and does not guarantee correct conservative evaluation of the adequate response of a full-scale objects to a disruptive accident. To increase the credibility to a strength prediction , the preliminary calculated accidental energy release must be reproduced experimentally with adequate parameters.

In this report, we briefly describe the results of experimental investigations of closed volume combustion of the condensed explosive materials (EM) ignited by the hot products of hydrogen-air mixtures combustion and show the possibility of developing the simulator which provides the monotone energy releasing with maximum combustion products pressure ranging to 100 MPa through the time of 20 to 400msec. These parameters exceed these ones of all known load simulators both in duration of process and in amplitude value [1,4].

The experiments were carried out in the cylindrical steel combustion chamber with inner volume of 0.012 m^3. The used explosive materials were the pyroxylin gun powder P15/1 and gelatin explosive (GE) based on finely divided penthrite. Powder charge was an assembly of tubular powder elements every of which was 0.35 m long. The mass of charge was varied from 0.15 kg to 0.5 kg. The GE charge was formed as a hollow cylinder, its mass of the same range was varied by the thickness of the explosive layer and the height of cylinder.

The EM charges were ignited by the hot products of combustion of 10% hydrogen-air mixture at initial pressure of 3 MPa. The technique of mixing the gases was the same which described elsewhere [5]. The mixture was fired in the center of the chamber by explosion of the thin Ni-Cr alloy wire by the capacitor discharging [6].

In experiments the pressure and the temperature of gas in combustion chamber and the heating of its wall were measured. From the pressure records the maximum combustion products pressure $\mathbf{P_K}$ and the time of EM charge combustion τ_f (equals t time of maximum pressure realizing, see Fig.1) were determined.

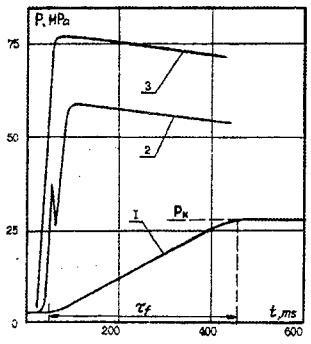

Fig.1.CP pressure **P(t)** for charging density variation
1- gelatine explosive, ρ=5kg/m^3
2- gun powder, ρ=25kg/m^3
3- gun powder, ρ=41.7kg/m^3

Experimental values of peak pressure $\mathbf{P_K}$ and temperature $\mathbf{T_K}$ were compared with the results of calculations of equilibrium parameters of combustion products for used EM. The possibility of 21 components presence in the combustion products has been taken into account. And it has been assumed that the explosive materials are in closed volume with heat insulated wall and the gas velocity equals zero in the chamber. The program of calculation includes the solution of simultaneous equations set, namely matter balance equation, heat balance equation, density constancy equation and equilibrium equation.

Charge EM combustion time (or in other words time of pressure increasing to maximum value) is determined by the type of EM and charging density, which defined as a charge mass referred to volume of combustion chamber. Increasing of charge density reduces the combustion time for both type of EM through the range investigated. Such reducing is caused by the increasing of normal combustion rate with pressure increasing [7].

As shown in Fig.3 in the equal conditions GE charge provides increasing of the combustion time because the normal combustion rate of gun powder is much higher than that of GE [7].

The parameter which defines the duration of combustion is the characteristic geometrical size of single powder element or the thickness of GE layer ***l***. Production process of gelatin explosives enables to product the plates with wide range of thickness. Thus the variations of combustion time from 40 ms to 400 ms are possible through the wide range of charging density using the GE charge.

The value of the peak combustion pressure is determined by the parameters of hydrogen-air mixture and the charging density. Using the 10% hydrogen-air mixture with initial pressure of 3 MPa the variations of charging density up to 65 kg/m allow to obtain the peak pressure in combustion chamber from 15 MPa to 100 MPa as for gun powder P15/1and GE (see Fig.2).

For powder charges through the whole parameters range investigated the differences between experimental and pre-calculated values of peak pressure are within error limits.

Thus the state of products of combustion of condensed EM ignited by the hydrogen-air mixture combustion products may be considered as the thermodynamic equilibrium state, and one can use the pre-calculated data to predict the impact load.

The level of peak pressure values realized both for gun powder charge and for GE charge is greater than the arithmetic sum of pressures caused by separate combustion of each components (see Fig.2). Considering the analysis of combustion

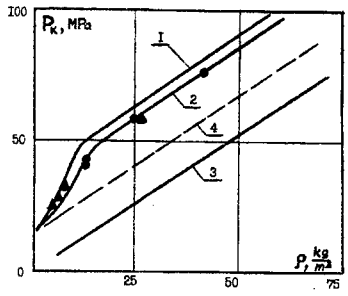

Fig.2.Maximum combustion products pressure P_K vs.charging density.
GE: 1- theory, ▲ - experiment
powder: 2-theory, ● - experiment
3- only powder combustion
4- arithmetic sum of pressures caused by separate combustion of gas and powder components.

products one can conclude that the noticed excess of pressure is caused by the after-burning of CO to CO_2 in the unusable oxygen in the chamber after the hydrogen-air combustion has been completed. For gun powder charge the after-burning contribution to increasing of pressure is greater as the charging density is higher up to 20 kg/m , and for GE charge - up to 12 kg/m .

Thus, the results presented show that the closed volume combustion of such explosive materials as gun powder and gelatin explosive ignited by the hot products of hydrogen-air mixture combustion is the stationary process in charging density range up to 65 kg/m . This energy source allows to produce the monotone increasing of load with predicted values of pressure in range from 15 to 100 MPa. And the time of realizing the peak pressure may be varied from 40 to 400 ms by monitoring both choosing the type of EM and the thickness of EM charge.

REFERENCES

1. V.N.Mineev, Yu.N.Tyunyaev, V.A.Ryzhansky, A.G.Ivanov. FGV, v.23, No.4, 1987, 104.
2. D.Cagliostro,A.Florence,G.Abrahamson. Nuclear Engineering and Design, v.27,1974, 94.
3. H.Holtbecker , Nuclear Engineering and Design, v.42,1977, 75.
4. G.Abrahamson,D.Cagliostro,F.Florence.Nuclear Engineering and Design, v.42,1977, 89.
5. B.Vyskubenko,V.Koksharov, L.Kolegov et al. Atomnaya energia, v.71, No.5, 1991, 402.
6. B.Vyskubenko, L.Kolegov et al. Patent RF №1807761 (16.04.90)
7. K.Andreev. Termicheskoe razlozhenie i gorenie vzryvchatych veshchestv, M., Nauka, 1966

INFLUENCE OF SOLID PROPELLANT STRUCTURE ON METAL AGGLOMERATION.

Babuk, V.A., Vasilyev, V.A., Sviridov, V.V
Baltic State Technical University
1st.Krasnoarmeyskaya str.,1, Saint Petersburg, 198005, RUSSIA

Metal agglomeration in solid propellant combustion is complex and multi-stage process. Agglomeration includes a number of phenomena. Necessary condition for the agglomeration is formation so-named "frame layer" of the propellant burning surface [1]. Frame layer is porous structure formed with metal, metal oxide, and carbon.

Structure of composite solid propellant has an sufficient influence on "frame layer" formation. Change of propellant structure leads to change in agglomeration and, consequently, in parameters of condensed phase combustion products (CPCP).

Propellant structure, can be characterized with the help of the terms "pocket" and "interpocket bridge". "Pocket" is a part of binder surrounded by oxidizer particles. "Interpocket bridge" is a part of binder located between two neighbouring oxidizer particles which take part in "pocket" formation.

"Frame layer" appears in "pocket" burning. Binder of "interpocket bridges" does not take part in "frame layer" formation. Hence, only metal of "pocket" is involved in agglomeration. So, characteristics of the "pockets" have strong influence on parameters of agglomerates [2]. To verify an influence of propellant structure on metal agglomeration, experimental investigation was carried out.

Particles of CPCP were quench-collected and analyzed. Also, experimental data were compared with results of numerical modeling of propellant structure. Computer calculations were made with the help of propellant structure model developed in [3]. For computer modeling, a method of "statistical tests" was used. Parameters of propellant structure were calculated on the base of information about distribution function for oxidizer particle centers in propellant and size distribution function for the oxidizer particles.

Propellants with isoprene rubber as binder and ammonium perchlorate (AP) as oxidizer were studied. Propellants were differed with oxidizer dispersity only. Mass content of components in the propellants is shown in Table 1. Propellants includes aluminum powder of up to 50 μm particle diameter. Four fraction of AP particles were used for propellant composition.

Fraction #1: particle size is of 1 μm.

Fraction #2: particle size is less than 50 μm.

Fraction #3: particle size is within 160-315 μm.

Fraction #4: particle size is within 400-600 μm.

Proportions of the AP fractions in the propellants are shown in Table 2.

Table 1

Components	Aluminum Al	Ammonium Perchlorate NH_4ClO_4	Isoprene Rubber $-CH_2-\underset{\underset{C}{|}}{C}=CH-$	Additives	Oil $C_{19}H_{35}$
Contain, %	24	64	2.6	0.4	9

Table 2

Propellant	#1	#2	#3	#4	#5
Proportion of AP fraction	Fr.#1-Fr.#2 50%-50%	Fr.#2 100%	Fr.#2-Fr.#3 40%-60%	Fr.#3 100%	Fr.#4 100%

Experiments consist in combustion of small propellant samples in constant volume bomb (CVB) filled with inert gas. Burning agglomerates were quenched and collected. Distribution functions and chemical compositions for samples of quench-collected agglomerates were determined.

Two main parameters characterize agglomeration process:

1. a part of metal taking part in agglomeration Z_m^a,
2. degree of integration of metal particles (increase of particle size due to agglomeration).

Particle integration degree can be characterized by mass-medium diameter D_{43} of agglomerates. Influence of propellant structure on agglomeration is well seen at low pressure (about 1 MPa). Increase of AP dispersity in propellant first (from Propellant #5 to Propellant #2) leads to decrease in Z_m^a and D_{43}, and then (from Propellant #2 to Propellant #1) these parameters increase. Nature of these dependencies is considered to connected with propellant structures. Decrease of oxidizer particle sizes causes increase in part of "interpocket bridges" in comparison with part of "pockets" in propellant. This lead to decrease of Z_m^a, when moving from Propellant #5 to Propellant #2 (Fig.1). In the case of Propellant #1, AP particles are supposed to be not able to form "pocket" due to their small sizes. So, structure of Propellant #1 is similar to homogeneous propellant structure. (Homogeneous propellant can be characterized as propellant consisted of one big "pocket"). That is why part of metal taking part in agglomeration (Z_m^e) for Propellant #1 at low pressure is more than the same for Propellant #2 (Fig.1).

Used model of propellant structure allows determine parameters and quantity of "pockets" in propellant. Pocket sizes have influence on agglomeratie sizes, but "pocket" model can be used for agglomerate size distribution calculations in the case of so-named "pocket mode" of agglomeration. Agglomerate dispersity depends also on propellant burning rate, "frame layer" features and others factors. As a result, agglomeration can go under so-named "interpocket" and "prepocket" regimes. However, parameters of "pockets" make it possible to evaluate agglomerate sizes.

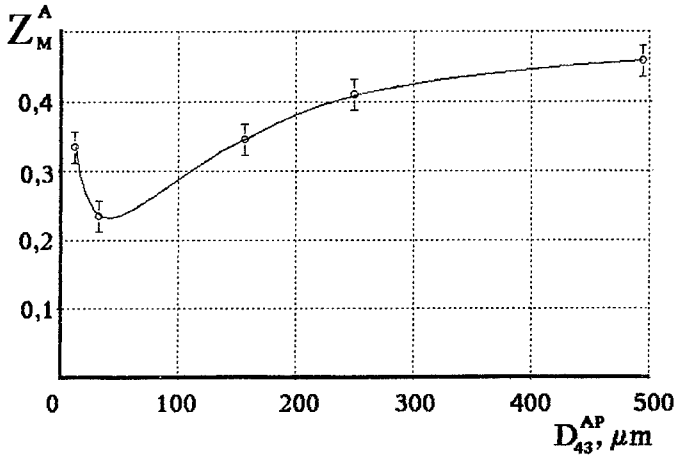

Figure1. Dependence of Z_m^a on mass-medium diameter of AP particles in propellants.

Table 3 shows parts of "pockets" in binder of propellants (g_p) calculated with the help of propellant structure model. These data confirm dependence of Z_m^a on propellant structure. Table 3 shows also mass-medium diameters for agglomerates D_{43}^a and for "pockets" in propellants D_{43}^p calculated with the help of propellant structure model. Both experimental investigation and calculations show that D_{43}^a decrease when moving from Propellant #5 to Propellant #2 and then D_{43}^a increase for Propellant #1 in comparison with Propellant #2.

Table 3

Parameters	Propellant #3	Propellant #4	Propellant #5
g_p	0,26	0,63	0,64
Z_m^a(1MPa)	0,35	0,409	0,452
D_{43}^k, μm	145	427	434
D_{43}^a(1MPa),μm	98	141	504

So, the result of this work allow to draw the conclusion that developed propellant structure model can be used for evaluation of agglomeration characteristics.

Experimental investigation was supported by United States Air Force European Office of Aerospace Research and Development (contract F61708-96-W0269)

References

1. Babuk,V.A., Belov,V.P., Khodosov,V.V., Shelukhin,G.G. Investigation of Agglomerate Structure in Aluminized Composite Condensed System Combustion. The Physics of Combustion and Explosion., 1988, N5, V.24, pp.52-57.
2. Babuk,V.A. Metal Fuel Combustion in the Rocket Propellant. (in Russian) Intra-Chamber Processes, Combustion and Gas Dynamics of Dispersed Systems., International Seminar., 1995, St.Petersburg, Book of Lectures, pp.74-84.
3. Babuk,V.A., Sviridov,V.V. Analysis and Synthesis of Models for CCP Formation Close to Burning Propellant Surface.,International Conference on Combustion, 1996, St.Petersburg.(in press)

MODEL OF ALUMINUM PARTICLE IGNITION IN SOLID ROCKET PROPELLANT COMBUSTION

Babuk V.A., Naslednikov P.A.
Baltic State Technical University
1st.Krasnoarmeyskaya str.,1, Saint Petersburg, 198005, RUSSIA

Use of Al as a metal fuel is characteristic for modern solid rocket propellants(SRP). Essential feature of aluminised SRP combustion is agglomeration (merging) of metal particles in surface layer of burning propellant that leads to a number of negative consequences. When modelling agglomeration phenomenon it is needed to consider various stages of metal fuel evolution in combustion process including ignition of Al particles in surface layer. Knowing domain of Al particles ignition it is possible to describe conditions in which heterogeneous combustion of particles takes place and hence, one can predict fraction of Al oxide in agglomerats being formed [2]. Model of ignition presented permits to take into account influence of composition and structure of SRP and also of pressure in combustion chamber of SPRE.

The basis for model developed is as follows.

When Al particle appears in surface layer, its oxide film gains some properties that remain invariable up to particle ignition. Initial oxide film has crystal structure and performs protective function (with respect to oxidation process). Because of high rate of heating it cracks under thermal stress. Oxidation of metal taking place around the cracks leads to formation of amorphous oxide. Such an oxide does not perform protective function and crumbles under the action of thermal stress.

All particles are equidistant from upper bound of "frame layer" [2]. They are subjected to identical conditions, i.e. heterogeneity of propellant structure and hence nonhomogeneity of surface layer hadn't been taken into account.

Consideration of all processes had been realized applying to "averaged cell" which is burning correspondingly to burning of the bulk of propellant [3].

When "averaged cell" burning variations of temperature and concentration of combustion products are assumed to be one-dimensional.

Properties of gaseous phase depend on point position respective to gasification surface of binder and oxidizer. The availability of relatively large heterogeneity's (such as dispersed oxidizer) in propellant structure leads to production of highly turbulized jets from binder and oxidizer. In the context of scheme assumed, concentration is linear with respect to coordinate and it can be determined by calculation of mixing interval length [1,5]. At the end of this interval gas composition is close to equilibrium which can be determined applying methods of equilibrium thermodynamics to mixture consisting of oxidizer and binder taken in ratio which is characteristic for the "pocket".

It is diffusion stage that limits oxidation rate of Al (but during model trials also different variants were considered [6]).

Analysis of ignition possibility is carried out having parameters of media and ones of particles fixed at levels corresponding to a certain position in a surface layer.

Temperature distribution in particle's cross section is absent.

Change of mass of metal owing to chemical interaction is not considered.

Convective heat exchange is determined by characteristics of "frame layer" as a porous structure and by Al particle's size [4].

The media's oxydizing components are : H_2O, CO_2.

The basis of the problem's mathematical description is heat balance equation. When surface temperature is T_S and media temperature is T_{BM} ignition condition is equality between feeding heat current (Q_+) and draining heat current (Q_-) and also excess of (Q_+) over (Q_-) in a given temperature vicinity.

For different SRP classes, ignition places in "frame layer" are different [2]. This is because of difference in ignition process conditions. Analysis of the model permits to determine ignition temperature values (in interval from 900K to 1400K) for a number of SRP compositions. These values are in reasonably good agreement with experimental data.

The model gives possibility to reconstruct a number of regularities that have been obtained experimentally. Analysis of T_{BM} dependence on a number of parameters was carried out for one particular SRP composition belonging to class B according to terminology of article [2] (fig.1). It can be seen that the difference $T_{BM}(P)-T_S(P)$ does not exceed 100K and in fact T_{BM} does not change when P>3MPa. Like in experiments, the place where ignition occurs coincides with surface of burning propellant (i.e. upper surface of "frame layer").

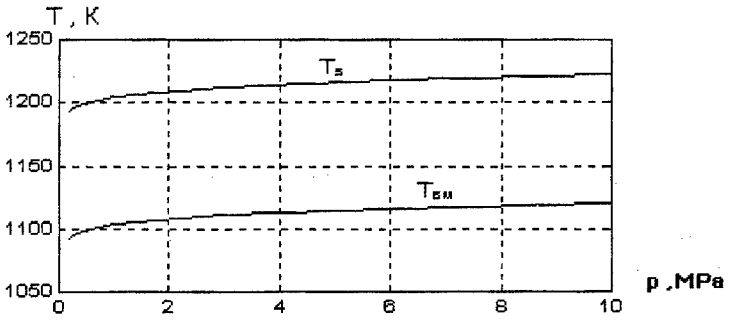

Fig.1 Temperature of particle T_S and that of media T_{BM} as functions of combustion chamber pressure P during ignition.

Usage of highly dispersed Al powder (d<1mkm) leads to fast decrease of $T_{вм}$ (fig.2).

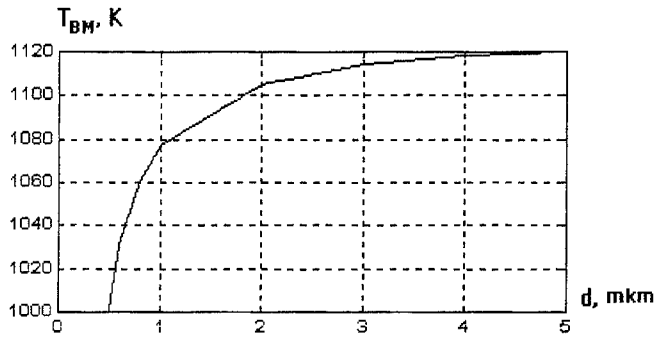

Fig.2 Temperature of media $T_{вм}$ as function of Al particle's diameter during ignition.

Thus the model of ignition developed meets experimental data in quantitative and qualitative sense.

The authors hope to apply the created model to method of prediction of agglomeration process characteristics for different SRP.

REFERENCES

1. Абрамович Г.Н. Прикладная газовая динамика. М., "Наука", 1991.
2. Бабук,В.А.,Белов В.П.,Ходосов В.В. и др. Исследование структуры агломератов при горении алюминизированных смесевых конденсированных систем. ФГВ, т.24, N5 , 1988 г., с.52-57
3. Бабук В.А. Горение металлического горючего в составе ракетных топлив. Внутрикамерные процессы, горение и газовая динамика дисперсных систем. Международная школа-семинар. Сб. лекций. СПб. 1996 г., с.74-84.
4. Галицкий Б.М., Ложкин А.Л. Исследование теплообмена в пористых структурах //труды Первой Российской национальной конференции по теплообмену, т.7, М.:МЭИ
5. Гусаченко Л.К. Об использовании решения Бурке-Шумана для диффузионного пламени при описании горения конденсированных веществ. ФГВ, N2 , 1985 г., с.41-45
6. Кофстад П. Высокотемпературное окисление металлов. М., "Мир" 1969.

STUDY OF HIGHLY DISPERSED OXIDE FORMATION IN ALUMINUM PARTICLE COMBUSTION

V.A.Babuk, M.S.Malakhov
Baltic State Technical University
1-st Krasnoarmeyskaya str., 1, Saint Petersburg, 198005, RUSSIA

As we know, aluminum powder is an organic part of many types of composite solid propellants. It is established that in the process of burning propellant agglomeration has been put into effect on its surface layer. Some particles of metal flow together into drops, exceeding by one order the size of initial particles. The rest of the particles are burnt down in the surface layer of burning propellant.

It is accepted to divide the particles of conditioning phase of products of combustion of aluminum into 2 fractions: the first one – agglomerates (particles with sizes more than 30-40 μm) and the second are the particles of Highly Dispersed Oxide (HDO) with sizes less than 30-40 μm.

Supposedly, the particles of three fractions will have to do with HDO, which differ from each other by way of formation. The first fraction is represented by the particles formed as a result of vapor-phase combustion of initial nonagglomerated particles. The second fraction – the particles of oxide as a result of initial burning of nonagglomerated particles in heterogeneous mode. The third is represented by particles which are the result of vapor-phase burning of agglomerates.

In this way, the preliminary analysis shows, that the function of size distribution of HDO will have complex polimodal character.

Authors of this paper created the method of research of HDO particles, the description of which is in the work [1]. The method described serves for direct determination of parameters of HDO particles and realizes with the help of contact research method. Due to this method some dispersible characteristics, chemical composition of HDO particles may be determined; it is possible to research selected particles with the use of a microscope.

With the help of this method an experimental investigation on determination of parameters of HDO particles near the surface of burning propellant has been held. The HDO particles of the third fraction are represented by less part (5 - 20%) from all HDO particles selected because the process of burning of agglomerates stopped near the surface of propellant burning (agglomerates were quenched with inert medium at the distance 6 mm from burning surface). So, the results of this work describe the process of HDO formation in the process of combustion nonagglomerated metal.

Several propellant compositions were studied which characterized by different oxidizer dispersion and, as a result, difference in agglomerate sizes and

agglomeration degree, that should lead to different correlation between HDO particles of three different fractions.

It is important to mention that HDO particles stick together actively after selection, forming coagulants. Their definition was realized by dispersion in a liquid with a help of ultrasound. We can not confirm, that all coagulation were destroyed and there were no repeated coagulation. Thus, in that way it is necessary to count that all got parameters of the particles can be raised to high.

Figure 1 shows distribution functions of HDO particles for different levels of pressure, built on the base of experimentally gotten histogrammes.

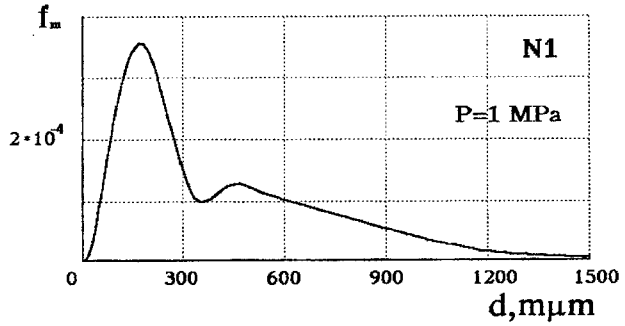

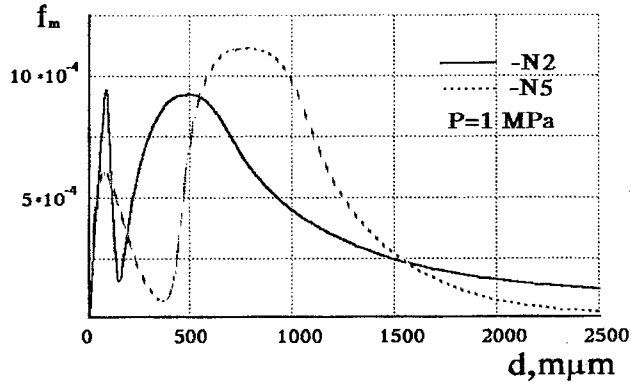

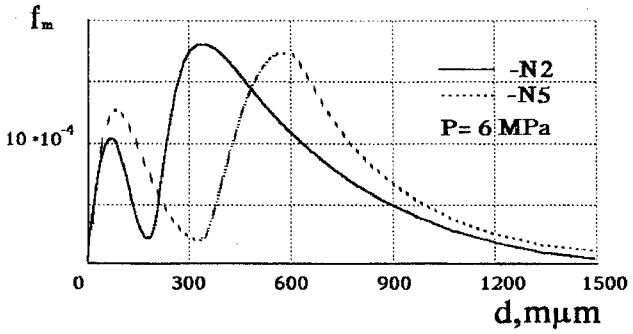

Fig.1. Functions of density of HDO particles distribution for the different compositions gotten in the conditions of different levels of pressure.

Composition N1 - oxidizer dispersity: 50% ~1 μm , 50% less than 50 μm
№2 - 100% less than 50 μm
№5 - 100% 400 - 600 мкм

As follows from all the results, there are two main fractions: in the intervals 20-200 mμm and 300-1000 mμm. Supposedly the first is represented by the particles of the lesser part fraction, formed as a result of vapor-phase burning of nonagglomerated particles. These particles – 10 % by mass from all selected HDO particles.

Graphically, the dependence of mass-medium diameter of HDO particles from the dispersion of oxidizer is represented in Figure 2.

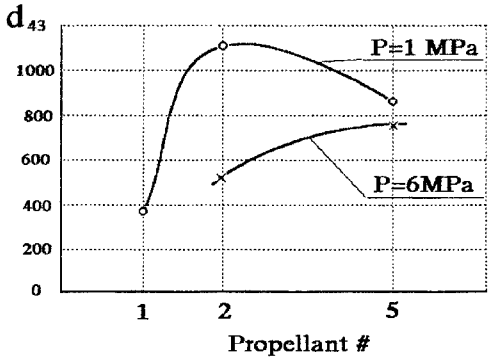

Fig 2. Dependence of mass-medium diameter of HDO particles on oxidizer dispersity.

It is necessary to notice that the particles of the first fraction will be the lesser parts (the smallest), because the size of the initial metal particles is much lesser than of agglomerates size. Supposedly their sizes are situated in interval 10-200 mμm.

Using this method, we can affirm that the losses of particles with sizes less than 300 mμm in size are very little. A number of experiments took place on determination of mass imposing of HDO particles selection for control compositions and it was established that 70-85% particles have been selected. In this case the losses of particles are more for the composition with less level of the agglomeration, thus is more the share of products of combustion of nonagglomerated particles. So, we can propose, that the part of submicron particles of HDO in size 10-200 mμm is more than it considered to be earlier and may consist of 20-50% from the mass of all HDO particles, forming in the process of combustion of nonagglomerated metal. Further investigation of conformities to natural laws foundation of HDO must be directed to verify the data proposal.

This investigation was supported by United States Air Force European Office of Aerospace Research and Development (contract F61708-96-W0269).

Литература

1. Babuk V.A. Malakhov M.S. The method of experimental research of formation highly dispersed oxide particles process in burning solid propellant., Combustion and Gas Dynamics of Dispersed System. International Seminar/ June 20-24 1995/ Saint-Petersburg., p.140.

AERODYNAMICS OF A CLOUD OF HOT SOLID AEROSOL PARTICLES

S.I.Igolkin

Baltic State Technical University

The physics model and the expressions are supposed for the parameters evaluation of anomalous motion of hot aerosol particles cloud in atmosphere and air flows. The equations are obtained related to the velocity of the cloud, geometry, concentration of the particles and their temperature.

Physics model and equation of motion

Let suppose the hot aerosol particles are confined in the sphere, having cross section S_0. The particles are faintly connected each other, for example, by the electrostatic forces. They have non-spherical shape and their concentration is not too high to suppose the cloud to be blow up by air jets and flows. The air penetrates through the front boundary of the cloud having V_0 velocity. It is heated by particles when moves inside the cloud, expands and leaves it at V_1.

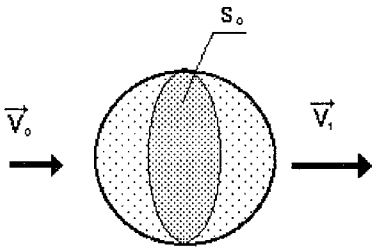

Follow equations are hold true in a frame of reference related to the cloud.

Flow continuity equation:

$$\rho_0 V_0 S_0 = \rho_1 V_1 S_0 = G . \qquad (1)$$

Equation of gas momentum:

$$G V_0 = - F_R + G V_1 . \qquad (2)$$

Equation of rectilinear motion for particles, being expressed by the balance of reactive driving force F_R and aerodynamic drug force F_{Cx}:

$$F_R = F_{C_X}, \tag{3}$$

or

$$\overline{\rho}\overline{V}S_0(V_1 - V_0) = C_X S_P \frac{\overline{\rho}\overline{V}^2}{2}. \tag{4}$$

Here

$$\overline{V} = (V_1 + V_o)/2, \tag{5}$$

C_X - average drug coefficient,
S_P - summary cross section of all particles.
At constant pressure flow continuity equation leads to follow relation:

$$V_1/V_0 = T_1/T_0 \quad . \tag{6}$$

Taking it into account and transformed (4) we get:

$$C_X = \frac{4S_0}{S_P}\frac{T_1 - T_0}{T_1 + T_0} \quad . \tag{7}$$

The relationship of the particles parameters and heated air temperature can be received from the heat transfer equations as well.

Let's introduce the follow meanings.

α – heat-transfer coefficient;

S_{PP} – summary surface of all particles;

T_P – surface temperature;

$\overline{T} = (T_1 + T_0)/2$ – average temperature of heated air.

In the assumption of constant temperature of the particles heat transfer equation is written as follow:

$$\alpha S_{PP}(T_P - \overline{T}) = (T_1 - T_0)\rho_0 V_0 S_0 C_P \quad , \tag{8}$$

or:

$$V_0 = \frac{\alpha}{C_P \rho_0}\frac{S_{PP}}{S_0}\frac{T_P - \overline{T}}{T_1 - T_0} \quad . \tag{9}$$

Excluding from (7) and (9) the unknown temperatures we get the follow expression for aerosol cloud motion through undisturbed air:

$$V_0 = \frac{2\alpha}{C_P \rho_0 C_X} \frac{S_{PP}}{S_P} \left[\frac{T_P}{T_0} (1 - C_X \frac{S_P}{4S_0}) - 1 \right]. \qquad (10)$$

The exit temperature of air is determined by (7) and the velocity of heated air passed through the cloud is given by (6). The real parameters of the particles C_X, S_p, S_{pp} have to be set or determined in a special investigation. All these parameters are completely dependent on the way of aerosol formation.

Thus, at some combinations of sizes, shapes, concentration and temperature of the dispersed particles the motion of aerosol cloud in undisturbed air, in the air flows and jets can take place. This result give us satisfy explanation of unpredictable behaviour of active, hot, for example condensing and relaxing, two-phases cloud formations.

The energy source for such motion is the temperature drop caused to the heating of the gas by hot particles. The nature of driving force affected on the aerosol cloud is the same as one to use in a classic ramjet engine.

References

1. Bartlma F. Gasdynamik Der Verbrennung. - Springer-Verlag /Wien. 1975.

2. Кошмаров Ю.А., Рыжов Ю.А. Прикладная динамика разреженного газа - М.: Машиностроение, 1977. - 184 с.

3. Аржаников Н.С., Мальцев В.Н. Аэродинамика - М.: Оборонгиз, 1956. - 483 с.

THE ROLE OF CONVECTION AND HEAT EXCHANGE BY RADIATION IN PROCESSES OF HETEROGENEOUS BURNING OF A PARTICLE

KALINCHAK V. V., ORLOVSKAYA S. G., PRUDNIKOVA J. V., LEKHNO D. A.

Odessa State University by I. I. Mechnikov

The burning of dispersible fuels in fire-chamber of torch type or with a circulating boiling layer occurs at intensive heat and mass exchange of particles with gas phase. The role of the exchange can change with changes of the diameter and the velocity of particles. An influence of natural and induced convection on steady (burning) and critical (ignition and extinction) hightemperature states of carbon particle taking into account its heat transfer by radiation to cold reaction chamber walls has been studied in the work.

Taking into account that the value of the Bio's criterion $Bi \ll 1$ the change of particle temperature in time is expressed by equation

$$\frac{1}{6}c_1\rho_1 d\frac{\partial T_1}{\partial t} = q_{ch} - q_{m.c} - q_r, \quad T_1(t=0) = T_{in}.$$

The density of chemical heat secretion q_{ch} is determined in the main by chemical reactions $C + O_2 \longrightarrow CO_2$ (I) and $2C + O_2 \longrightarrow 2CO$ (II)

$$q_{ch} = (k_1Q_1 + k_2Q_2)\,\rho_2 n_{ox}\left(\frac{k_1+k_2}{\beta}+1\right)^{-1},$$

$q_{m.c} = \alpha(T_1 - T_2)$ — is the density of the heat flow by molecular and convective mechanism,

$q_r = \varepsilon\sigma\left(T_1^4 - T_w^4\right)$ — is the density of the heat flow by radiation;

where $\alpha = \lambda_2 \cdot Nu/d, \quad \beta = D \cdot Nu/d, \quad D = \lambda_2/(c_2\rho_2),$

$$Nu = 2 + b\sqrt{Re}\cdot Pr^{1/3}, \quad b = 0.55, \quad Re = \frac{Ud}{\nu_2}, \quad \nu_2 = Pr \cdot D.$$

The increase of the particle diameter depends on the mass transfer coefficient β and constants of rates of chemical reactions (I) and (II) in the explicit form:

$$\frac{\partial(d)}{\partial t} = -\frac{2\rho_2}{\rho_1}(k_1\Omega_1 + k_2\Omega_2)\,n_{ox}\left(\frac{k_1+k_2}{\beta}+1\right)^{-1}, \quad d(t=0) = d_{in}.$$

The relative particle velocity U is obtained from the movement equation

$$\rho_1\frac{\partial U}{\partial t} = (\rho_1 - \rho_2)g - \frac{3}{4d}\psi\rho_2 U^2, \quad U(t=0) = U_{in},$$

where the coefficient of the particle head resistance depends on the Reynolds number and in the interval $1 < Re < 400$ it is determined by the formula Klyachko L.A.:

$$\psi = \frac{24}{Re} + \frac{4}{\sqrt[3]{Re}}.$$

A change of heat and mass transfer coefficients (α and β) in time is determined by dependences $T_1(t)$, $d(t)$ and $U(t)$. There exist critical values α and β characterizing transition from lowtemperature states into hightemperature ones and vice versa. The steady high- and lowtemperature states take place in the certain range of coefficients of heat and mass transfer. An operation of these coefficients is possible by giving the initial diameter and particle velocity. An investigation of stability of stationary regimes of heat and mass transfer ($dT_1/dt = 0$) gives a possibility to define critical values of particle velocities and diameters.

The dependence of coefficients α and β determining steady and critical states of the particle versus particle temperature is obtained from the condition of the stationary state $q_{ch} = q_{m.c} + q_r$ in the form:

$$\beta = \frac{\alpha}{c_2\rho_2} = \frac{(k_1Q_1 + k_2Q_2)\,\rho_2 n_{ox}\left(A \pm \sqrt{A^2 - B}\right)}{c_2\rho_2\,(T_1 - T_2)},$$

$$\text{where} \quad A = 0.5\,(1 - A_1 - A_2), \quad B = A_1A_2;$$

$$A_1 = \frac{c_2\,(T_1 - T_2)\,(k_1 + k_2)}{(k_1Q_1 + k_2Q_2)\,n_{ox}}, \quad A_2 = \frac{\varepsilon\sigma\left(T_1^4 - T_w^4\right)}{(k_1Q_1 + k_2Q_2)\,\rho_2 n_{ox}}.$$

Introducing the complex $f = 2d/Nu$ we can write the stationary state condition in the form:

$$f = \frac{2d}{Nu} = \frac{2\lambda_2\,(T_1 - T_2)}{(k_1Q_1 + k_2Q_2)\,\rho_2 n_{ox}\left(A \pm \sqrt{A^2 - B}\right)}.$$

How it follows from this equality, for $T_1 \longrightarrow T_2$ the $f \longrightarrow 0$, and $f \longrightarrow \infty$ for $T_1 \longrightarrow T_w$. Here the chemical heat secretion power becomes negligible as compared with $q_{m.c}$ in the first case and with q_r in the second one.

The complex f makes it possible to take into account a change both the particle diameter and the particle velocity. Therefore the results of investigations of dependences $d(T_1)$ and $U(T_1)$ we can represent as one generalized dependence $f(T_1)$. It is illustrated by figure in which the results of calculations on the stationary model (dashed lines) and the non-stationary one are represented. In fig. a is shown the behaviour of the complex $2d/Nu$ which has been calculated on the non-stationary model taking into account the natural convection and without it. The relative gas velocity at the natural

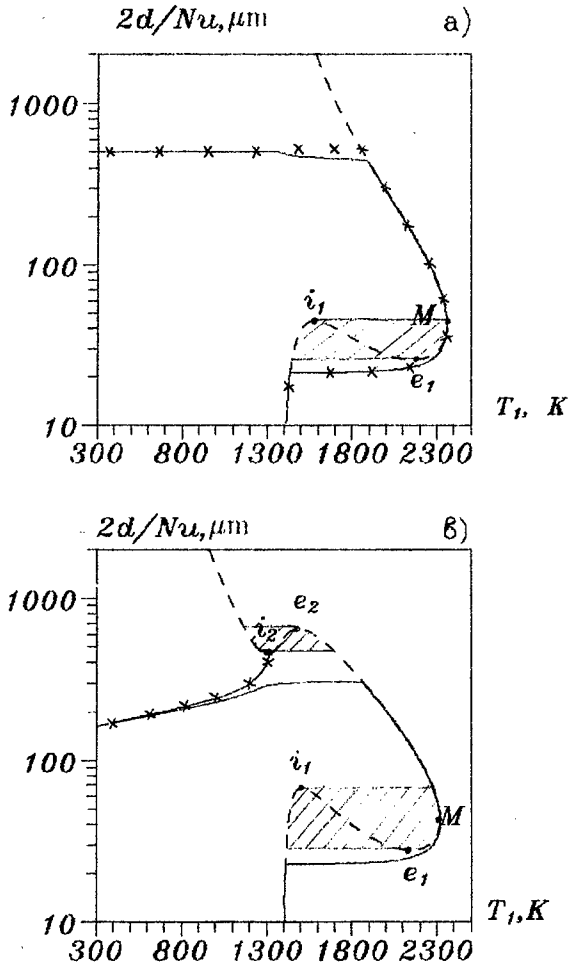

Fig. Dependences of the value $f = 2d/Nu$ on stationary particle temperature at $T_2 = 1400$ K. a) $T_w = 1400$ K; —— – taking into account, × × × – without taking into account of the natural convection; b) $T_w = 500$ K, — · · · $F_y \neq 0$, –×–×–×– $F_y = 0$. – – – – the calculation according to the stationary model, ——, –×–×–×–, × × × – the calculation according to the non-stationary model, $d_{in} = 505$ μm.

convection was obtained by the Grashof criterion Gr in the form

$$U_{n.c} = \frac{\nu_2}{d}\sqrt{0.5Gr}, \quad Gr = \frac{gd^3(T_1 - T_2)}{273 \cdot \nu_2^2}.$$

The natural convection enlarges the criterion Nu what leads to some decreasing of the complex f. The effective air velocity during the natural convection induces the increase of mass transfer what leads to the growth of the burning rate, consequently, to the decrease of particle burning time t_{burn}. On the induction period t_{ind} and the critical diameter d_e (the diameter at which the particle extinction takes place) the natural convection does not influence, since the chemical reactions occur in the kinetic range (see Table). The influence of the natural convection more strongly tells at large initial diameters of the particle.

Table

The influence of the natural convection on the burning characteristics of carbon particles at $T_2 = T_w = 1400$ K.

d_{beg}, μm	taking into account (+), without taking into account (–) of the natural convection	t_{ind}, s	t_{burn}, s	d_e, μm
100	–	0.069	0.17	21.3
	+	0.067	0.16	21.5
505	–	0.54	4.74	21.3
	+	0.53	4.40	21.5
800	–	0.99	12.23	21.4
	+	0.83	11.58	21.5

In the fig. b are represented the results of calculations according to the non-stationary model for two cases: i) the forces of gravitation and friction act on the particle, ii) only the friction force acts on the particle. In the first case ($F_g \neq 0$) the particle ignition takes place as a result of heating of the particle by the convective heat and mass transfer. In the second case ($F_g = 0$) heat losses by radiation at weak heating by heat conductivity do not make it possible the particle to ignite.

The extremums on curves $2d/Nu(T_1)$ define unsteady particle states: points i_1 and i_2 correspond to ignition, points e_1 and e_2 — to extinction of the particle. They are characterized by the condition of the loss of the stability of stationary regimes of heat and mass transfer $\partial d/\partial T_1 = 0$, that is equivalent to the second Semenov condition

$$\frac{\partial q_{ch}}{\partial T_1} = \frac{\partial (q_{m.c} + q_r)}{\partial T_1}$$

or to the contact of the curves $q_{ch}(T_1)$ and $q_{m.c} + q_r(T_1)$.

Branches connecting points i_1 and e_1, i_2 and e_2 describe the influence of the initial particle temperature on the critical particle diameter and velocity which characterize the ignition. In this range (it is shaded in the figure) the hysteresis character is realized: two possible steady stationary states of the particle correspond to one value of $2d/Nu$ — the high- and lowtemperature states. The hightemperature regime of heat and mass transfer is realized only in the case when the initial particle temperature at the fixed value of the complex $2d/Nu$ exceeds the temperature value that lies on the curve connecting points i и e.

For $T_w < T_2$ at the increase of gas temperature the critical values of the complex f (and so for d and U) corresponding to ignition and extinction come close and at some gas temperature value $T_2 = T_{2\gamma}$ the degeneracy of critical conditions takes place (here $\partial^2 d/\partial T_1^2 = 0$), that is for $T_2 > T_{2\gamma}$ the crisis-free transition from one stationary state into another and vice versa is realized. Points i and e degenerate into the inflection point γ (γ_1 for i_1 and e_1, and γ_2 for i_2 and e_2).

Parameters of the degeneracy of critical conditions of heterogeneous ignition and extinction of the particle $(2d/Nu)_{\gamma_1}$ and $(2d/Nu)_{\gamma_2}$ are obtained from the solving of the system of equations:

$$q_{ch} = q_{m.c} + q_r,$$

$$\frac{\partial q_{ch}}{\partial T_1} = \frac{\partial (q_{m.c} + q_r)}{\partial T_1},$$

$$\frac{\partial^2 q_{ch}}{\partial T_1^2} = \frac{\partial^2 (q_{m.c} + q_r)}{\partial T_1^2}.$$

The solution of this system shows that in the range of large particles the value of $(2d/Nu)_\gamma$ grows when the oxidizer concentration increases. The decrease of wall temperature enlarges $(2d/Nu)_{\gamma_2}$, since the existence of the hysteresis loop in the range of large diameters and small velocities (points i_2 and e_2) is connected with heat exchange of the particle by radiation [1]. Here $(2d/Nu)_{\gamma_1}$ practically does not change that is connected with prevailing of heat exchange by heat conductivity.

Literature

1. Kalinchak V.V., Orlovskaya S.G., Kalinchak A.I. Heterogeneous ignition and extinction of a particle taking into account heat exchange by radiation // Inzh.Fiz.Zh. 1992. V.62, N3. P. 436-442.[in Russian]

Section 5
ECOLOGICAL PROBLEMS

112

ATMOSPHERIC POLLUTION RESULTING FROM FIELD TESTS AND LAUNCHING OF SOLID-FUEL PROPULSION SYSTEMS

MATVIENKO O.V., VOROZHTSOV A.B.

Research Institute of Applied Mathematics and Mechanics, Tomsk

During full-scale evalution of propulsion systems using an open engine test bed a considerable amount of harmful gaseous and condensed species is releaseed into atmosphere.

The calculation of adiabatic temperature and equilibrium composition of combustion products given shows that combustion products contain considerable amounts of ecologically harmful substances: HCl, Cl, CO. A series of calculations was carried out for determining the effect of cooling on combustion products. On the basis of these calculations one can draw conclusion that in cooling up to $300K$ such impurities as CO, Cl, disappear in gaseous products, but then the concentration of hydrochloride which appears in considerable amounts increases. Therefore a question on neutralization of ecologically harmful gases released in atmosphere in testing solid-fuel charges mainly comes to the question on neutralization of HCl or muriatic solution.

Consumption of water solution of alkali with respect to the weight of dry composition is 100 %. The results of calculation show that neutralization of products by water solution of sodium hydrate leads to a sharp decrease of concentration of hydrogen chloride. At the same time sodium chloride appears in products, it being in gaseous state at temperature $1000K$ and at lower temperatures in condensed state. In cooling products lower $1500K$ the content of hydrogen chloride in gases does not depend on temperature. The concentration of HCl in exhaust gases is the same for 300 and $1200K$. At temperature higher than $1500K$ equilibrium content of hydrogen chloride somewhat rises and action of concentration solutions of alkali it becomes higher than for less alkali solutions. It is explained by the fact that at higher temperatures thermal dissociations $NaOH$ increases and in gases at temperatures higher than $1500K$ sodium vaporous are present and content of water stream increases due to radicals OH.

Summing the results of thermodynamic analysis a conclusion may be drawn that application of alkali solutions for neutralization of gases forming in combustion of solid propellant can reduce to minimum content of ecologically harmful impurities in combustion products.

Mathematical modelling is to help indentify constituent components of the gas-particle cloud at all the pollution stages including the formation of the impurity cloud in the ground layer and its uplift and spreading in the atmosphere. Each stage, however, is characterized by a time-space scale which differs greatly from those of other stages. Therefore, to improve the efficiency of computational procedure it appears expedient to do a step-by-step investigation of impurity spreading. This approach makes it possible to use output data for each stage as input for the subsequent stages. Tnis paper presents

numerical simulations of the overheated impurity uplift and propagation in the atmosphere. The latter is a three-dimensional process whose simulation turns out to be complicated and costly. To avoid these difficultes we used a combined model where the vertical impurity dispersial was calculated by means of a set of differential equations, such as equations of motion, turbulent diffusion and heat conduction, while the horizontal dispersal was computed by a Gaussian model. The proposed model is complemented with assigned semi-empirical dependences for altitude variations of wind velocity, turbulent exchange coefficient, atmospheric temperature and turbulence statistics. The initial conditions for the impurity uplift calculations (cloud size, temperature and composition) were determined from thermodynamic computations of combustion products in a solid-rocket engine.

The overheated exhaust gases appear to be lighter than the ambient air. They move upwards in the gravity field entraining gas-particle species to give a free convection flow in the form of a cloud. The most critical parameters for the impurity uplift and transport processes are wind velocity, atmospheric turbulence intensity and temperature distribution.

Stable stratification was found to cause a faster decrease in the buoyancy force in the upward direction than in the isothermal atmosphere and hence a decrease in the uplift velocity. In the external part of the flow there forms a temperature defect which tends to increase with altitude and with the increase in the stratification parameter. The buoyancy force eventually goes to zero and then assumes a negative value which gives rise to a maximum of the uplift height and the reversed movement of the cloud. The cloud does not rise higher than a certain penetration altitude. The trajectory of the center-of-gravity of the cloud varies smoothly, first ascending, then descending under the action of the vertical density gradient.

The absence of wind (calm) coupled with the temperature inversion is the most unfavorable factor for the estimation of the atmospheric pollution. If the height of the boundary of the inversion layer is fairly low, then for light winds the impurity cloud seems to hover over the pollution source and the impurity concentration increases considerably. For example, as the wind velocity decreases from 1 m/s to zero, the maximum impurity concentration near the Earth's surface may increase approximately by an order of magnitude.

Our calculations show that above 30 km nitrogen oxides generally thought to be the major ozone destructors are virtually missing from the exhaust products and ozone may decay basically via the following chlorine cycle.

For the solid rocket propellant formulation in question the content of nitrogen oxides above 30 km is much lower than that of chlorine-bearing compounds. Therefore, at $z > 30$ km the major mechanism of ozone depletion is associated with chlorine cycle. However, in the tropopause and lower stratosphere the impact of nitrogen oxides found in exhaust products is fairly significant and neglect of nitrogen contribution to ozone depletion may introduce large errors. Characteristic distributions of

As a result of the interaction of the SPC products with atmospheric ozone there develops a region in the stratosphere wherefrom O_3 is either missing or its concentration is negligible as compared to natural ozone (what is known as the ozone hole). As time elapses, the hole starts moving relative to the Earth's surface together with the atmospheric motion of masses, and its size and shape undergo essential changes.

On the basis of the analysis of the time history we recognize two stages in the ozone hole life time. In the first stage there occurs mixing and chemical interaction of exhaust products with atmospheric ozone to destroy the ozonosphere, causing the area of the ozone hole to expand. In the second stage, when ozone destructors from exhaust products have reacted with ozone masses surrounding the trace combustion species and chemical reactions terminated, the gas content in the trace exhaust products is determined solely by diffusion processes which act to supply ozone from fairly distant regions to the neighborhood of the ozone hole. As a result the area of the ozone hole is decreased and the original atmospheric condition regained.

The area of the ozone hole is at its maximum (approximately $5 * 10^3\ m^2$) within 4 hours after the launch. Notably, due to advective processes the center of the ozone hole is shifted with the wind by 40-50 km from the launch pad. Thus the 40-50 km area in the vicinity of the launch pad is a potentially hazardous zone because it is in this area that most of the ozone destruction occurs and ultraviolet and hard cosmic radiation is enhanced.

The calculations done allowed us to estimate the pollution level for different meteorological conditions and pollution sources and provide recommendations as to how to reduce its disastrous effect on the environment.

CONTENTS

Section 3
TWO-PHASE FLOWS

Section 4
COMBUSTION OF DISPERSED SYSTEMS

Section 5
ECOLOGICAL PROBLEMS

Ответственные за выпуск: В.А.Васильев, М.С.Малахов

Подписано в печать 07.04.1997. Формат 60*84/16
Бумага документная. Печать трафаретная.
Уч.-изд.л. 7,5. Тираж 120 экз. Заказ N 30.
Балтийский государственный технический университет
Типография БГТУ
Адрес университета и полиграфпредприятия:
198005, Санкт-Петербург, 1-я Красноармейская ул., д.1